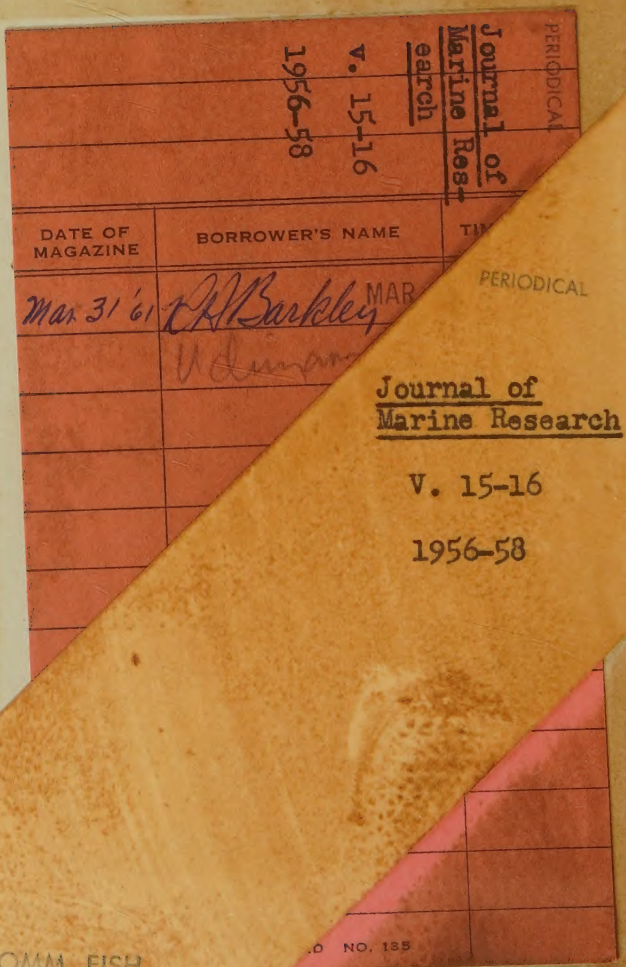
Journal of Marine Research
v. 15-16
1956-58
PERIODICAL
DATE OF MAGAZINE
BORROWER'S NAME
Mar 31 '61
C.H. Barkley
MAR
PERIODICAL
Journal of Marine Research
V. 15-16
1956-58
LIBRARY
BUR. OF COMM. FISH.
HON. BIOL. LAB.
NO. 185

2574 61
Journal of Marine Research
V. 15-16
1956-58

15

SEARS FOUNDATION FOR MARINE RESEARCH
BINGHAM OCEANOGRAPHIC LABORATORY, YALE UNIVERSITY

JOURNAL OF MARINE RESEARCH

VOLUME 15, 1956

NUMBER 1

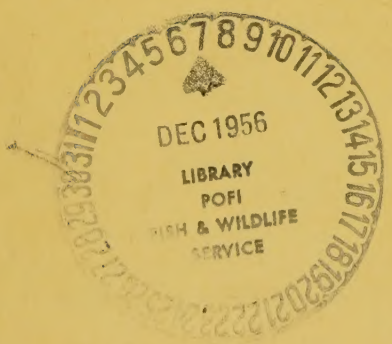

ISSUED OCTOBER 15, 1956, NEW HAVEN CONN., U. S. A.

JOURNAL OF MARINE RESEARCH

PUBLISHED BY

SEARS FOUNDATION FOR MARINE RESEARCH

BINGHAM OCEANOGRAPHIC LABORATORY, YALE UNIVERSITY

BOARD OF EDITORS

COLUMBUS O'D. ISELIN
Woods Hole Oceanographic Institution
Woods Hole, Mass.

Chairman: A. E. PARR
American Museum of Natural History
New York, N. Y.

ROGER REVELLE
Scripps Institution of Oceanography
La Jolla, Calif.

DALE F. LEIPPER
A. and M. College of Texas
College Station, Texas

WALTER H. MUNK
Scripps Institution of Oceanography
La Jolla, Calif.

C. G. ROSSBY
Institut für Meteorologi
Stockholm, Sweden

DANIEL MERRIMAN
Bingham Oceanographic Laboratory
New Haven, Conn.

DONALD W. PRITCHARD
Chesapeake Bay Institute
Annapolis, Maryland

HARALD U. SVERDRUP
Norsk Polorinstitutt
Oslo, Norway

THOMAS G. THOMPSON
Oceanographic Laboratories
University of Washington
Seattle, Wash.

MANAGING EDITOR

YNGVE H. OLSEN
Bingham Oceanographic Laboratory
Yale University
New Haven, Conn.

The Journal is normally issued in three numbers per year constituting one volume. All income derived from subscriptions is used solely to increase the volume and improve the quality of the Journal for the benefit of its readers.

Subscription price for volumes 1 through 12, $3.00 per volume or $1.50 per number. Subscription price for volume 13 (1954) and subsequent volumes, $5.00 per volume or $2.00 per number. Address all communications to the Managing Editor. See inside cover for Note to Authors.

15(1)

TABLE OF CONTENTS

Page

1. **D. H. Cushing, A. J. Lee and I. D. Richardson:** Echo traces associated with thermoclines 1
2. **Nelson Marshall:** Chlorophyll *a* in the phytoplankton in coastal waters of the eastern Gulf of Mexico 14
3. **D. W. Pritchard:** The dynamic structure of a coastal plain estuary. 33
4. **G. Veronis and Henry Stommel:** The action of variable wind stresses on a stratified ocean 43
5. **W. V. Burt:** A light-scattering diagram 76
6. **D. W. Pritchard and R. E. Kent:** A method for determining mean longitudinal velocities in a coastal plain estuary 81
7. **A. C. Duxbury and C. S. Yentsch:** Plankton pigment nomographs. 92

NOTE TO SUBSCRIBERS

All back issues of the Journal of Marine Research are available at the following prices:

Volumes 1 to 12. $3.00 per volume, $1.50 per number.
Volumes 13 through 15. $5.00 per volume, $2.00 per number

NOTE TO AUTHORS

The pages of this Journal are open to all contributors, and manuscripts may be submitted to any member of the Board of Editors or to the Managing Editor. Publication will be made only in the English language, but copy may be submitted for consideration in other languages. Aid in translation of accepted manuscripts will be given when possible.

All manuscripts should be typewritten with double space, carefully corrected, with footnotes continuously numbered and set off in the body of the text. If an article is to appear as a contribution from another institution, it should be approved by that institution before submission; contribution numbers of such institutions are submitted with the return of galley proofs.

The author (or authors) of each article will receive a total of 50 free reprints (with covers). Additional reprints with or without covers may be ordered by authors or institutions at the cost of printing. Orders for reprints are given when galley proofs are returned.

Both galley and page proofs are submitted to the senior author of each article.

Tables should be prepared for clarity and as near as practicable to Journal pattern, without ruled lines if possible. Table footnotes should appear at the base of each Table.

Figures are required for consideration simultaneously with the manuscript. Original figures of inconvenient size for forwarding may be represented by photographs on first submission of a manuscript; originals are required for line cuts. Illustrations requiring half-tone reproduction should be avoided so far as possible, but they will be accepted when necessary. *It is very important that the proper size of characters and symbols should be used for the lettering of illustrations.* A diagram for determining suitable heights of letters for original drawings that will be reduced, together with an explanatory note, has been published in this Journal, Vol. III, No. 1: 89–91; reprints will be submitted to authors on request. Mechanical lettering is recommended. If facilities for lettering are not available to the author, it is preferable to receive illustrations with lettering indicated in pencil only, to be finished in ink in the editorial office. All illustrations will be subject to at least a minimum reduction at the rate of 1 : 1.2. Drawings which have been heavily patched and pasted must *not be rolled* for mailing. The legends for the figures, identified by corresponding figure numbers on the illustrations also, should be typed in sequence at the end of the manuscript.

A complete and *accurate list of references* in alphabetical order at the end of each article is essential. References may be indicated in the text by author's name (or names) and *year of publication*, or by italicized numbers which correspond to the numbers given in sequence in the list of references. Each reference should include the last name followed by at least two initials or first name; co-authors should be listed with the initials or first name preceding the last name. The date should be indented on the line below, followed by a complete title *verbatim* in lower case except for the first word. Publisher, city and pagination should be indicated for books, for periodicals (abbreviations from "World List of Scientific Periodicals," Oxford; so far as possible), the volume (italicized), number and pagination should be given.

Additional information regarding the preparation of manuscripts will be furnished by the Managing Editor.

1572

TABLE OF CONTENTS

Page

1. **J. B. Mullin and J. P. Riley:** The occurrence of cadmium in seawater and in marine organisms and sediments 103

2. **F. T. Walker and W. D. Richardson:** The Laminariaceae off North Shapinsay, Orkney Islands; changes from 1947 to 1955 ... 123

3. **R. J. Urick:** The processes of sound scattering at the ocean surface and bottom 134

4. **T. H. Waterman and W. E. Westell:** Quantitative effect of the sun's position on submarine light polarization 149

5. **R. E. Jentoft and R. J. Robinson:** The potassium-chlorinity ratio of ocean water 170

NOTE TO SUBSCRIBERS

All back issues of the Journal of Marine Research are available at the following prices:

Volumes 1 to 12. $3.00 per volume, $1.50 per number.
Volumes 13 through 15. $5.00 per volume, $2.00 per number

NOTE TO AUTHORS

The pages of this Journal are open to all contributors, and manuscripts may be submitted to any member of the Board of Editors or to the Managing Editor. Publication will be made only in the English language, but copy may be submitted for consideration in other languages. Aid in translation of accepted manuscripts will be given when possible.

All manuscripts should be typewritten with double space, carefully corrected, with footnotes continuously numbered and set off in the body of the text. If an article is to appear as a contribution from another institution, it should be approved by that institution before submission; contribution numbers of such institutions are submitted with the return of galley proofs.

The author (or authors) of each article will receive a total of 50 free reprints (with covers). Additional reprints with or without covers may be ordered by authors or institutions at the cost of printing. Orders for reprints are given when galley proofs are returned.

Both galley and page proofs are submitted to the senior author of each article.

Tables should be prepared for clarity and as near as practicable to Journal pattern, without ruled lines if possible. Table footnotes should appear at the base of each Table.

Figures are required for consideration simultaneously with the manuscript. Original figures of inconvenient size for forwarding may be represented by photographs on first submission of a manuscript; originals are required for line cuts. Illustrations requiring half-tone reproduction should be avoided so far as possible, but they will be accepted when necessary. *It is very important that the proper size of characters and symbols should be used for the lettering of illustrations.* A diagram for determining suitable heights of letters for original drawings that will be reduced, together with an explanatory note, has been published in this Journal, Vol. III, No. 1: 89–91; reprints will be submitted to authors on request. Mechanical lettering is recommended. If facilities for lettering are not available to the author, it is preferable to receive illustrations with lettering indicated in pencil only, to be finished in ink in the editorial office. All illustrations will be subject to at least a minimum reduction at the rate of 1 : 1.2. Drawings which have been heavily patched and pasted must *not be rolled* for mailing. The legends for the figures, identified by corresponding figure numbers on the illustrations also, should be typed in sequence at the end of the manuscript.

A complete and *accurate list of references* in alphabetical order at the end of each article is essential. References may be indicated in the text by author's name (or names) and *year of publication*, or by italicized numbers which correspond to the numbers given in sequence in the list of references. Each reference should include the last name followed by at least two initials or first name; co-authors should be listed with the initials or first name preceding the last name. The date should be indented on the line below, followed by a complete title *verbatim* in lower case except for the first word. Publisher, city and pagination should be indicated for books, for periodicals (abbreviations from "World List of Scientific Periodicals," Oxford; so far as possible), the volume (italicized), number and pagination should be given.

Additional information regarding the preparation of manuscripts will be furnished by the Managing Editor.

TABLE OF CONTENTS

Page

1. **E. M. Hulburt:** Distribution of phosphorus in Great Pond, Massachusetts 181
2. **J. P. Barlow:** Effect of wind on salinity distribution in an estuary .. 193
3. **J. Neumann:** On the range of variation in sea level 204
4. **W. R. Coe:** Fluctuations in populations of littoral marine invertebrates 212

NOTE TO SUBSCRIBERS

All back issues of the Journal of Marine Research are available at the following prices:

Volumes 1 to 12. $3.00 per volume, $1.50 per number.
Volumes 13 through 15. $5.00 per volume, $2.00 per number

NOTE TO AUTHORS

The pages of this Journal are open to all contributors, and manuscripts may be submitted to any member of the Board of Editors or to the Managing Editor. Publication will be made only in the English language, but copy may be submitted for consideration in other languages. Aid in translation of accepted manuscripts will be given when possible.

All manuscripts should be typewritten with double space, carefully corrected, with footnotes continuously numbered and set off in the body of the text. If an article is to appear as a contribution from another institution, it should be approved by that institution before submission; contribution numbers of such institutions are submitted with the return of galley proofs.

The author (or authors) of each article will receive a total of 50 free reprints (with covers). Additional reprints with or without covers may be ordered by authors or institutions at the cost of printing. Orders for reprints are given when galley proofs are returned.

Both galley and page proofs are submitted to the senior author of each article.

Tables should be prepared for clarity and as near as practicable to Journal pattern, without ruled lines if possible. Table footnotes should appear at the base of each Table.

Figures are required for consideration simultaneously with the manuscript. Original figures of inconvenient size for forwarding may be represented by photographs on first submission of a manuscript; originals are required for line cuts. Illustrations requiring half-tone reproduction should be avoided so far as possible, but they will be accepted when necessary. *It is very important that the proper size of characters and symbols should be used for the lettering of illustrations.* A diagram for determining suitable heights of letters for original drawings that will be reduced, together with an explanatory note, has been published in this Journal, Vol. III, No. 1: 89–91; reprints will be submitted to authors on request. Mechanical lettering is recommended. If facilities for lettering are not available to the author, it is preferable to receive illustrations with lettering indicated in pencil only, to be finished in ink in the editorial office. All illustrations will be subject to at least a minimum reduction at the rate of 1 : 1.2. Drawings which have been heavily patched and pasted must *not be rolled* for mailing. The legends for the figures, identified by corresponding figure numbers on the illustrations also, should be typed in sequence at the end of the manuscript.

A complete and *accurate list of references* in alphabetical order at the end of each article is essential. References may be indicated in the text by author's name (or names) and *year of publication*, or by italicized numbers which correspond to the numbers given in sequence in the list of references. Each reference should include the last name followed by at least two initials or first name; co-authors should be listed with the initials or first name preceding the last name. The date should be indented on the line below, followed by a complete title *verbatim* in lower case except for the first word. Publisher, city and pagination should be indicated for books, for periodicals (abbreviations from "World List of Scientific Periodicals," Oxford; so far as possible), the volume (italicized), number and pagination should be given.

Additional information regarding the preparation of manuscripts will be furnished by the Managing Editor.

V.16(1)

TABLE OF CONTENTS

Page

1. **C. B. Taylor:** Extreme sea water temperatures and densities along the North Atlantic States during summer 1955 1

2. **G. W. Groves and Townsend Cromwell:** Experimental investigation of the effect of "secondary instability" on mixing processes.. 8

3. **J. C. Freeman, jr., Ledolph Baer, and G. H. Jung:** The bathystrophic storm tide 12

4. **F. N. Spiess:** Acceleration measurements in the deep ocean 23

5. **R. W. Stewart:** A note on the dynamic balance in estuarine circulation.
D. W. Pritchard: Comment 34

6. **Kozo Yoshida and Han-Lee Mao:** A theory of upwelling of large horizontal extent 40

7. **William H. Glezen:** An external core catcher for oceanographic work 55

NOTE TO SUBSCRIBERS

All back issues of the Journal of Marine Research are available at the following prices:

Volumes 1 to 12. $3.00 per volume, $1.50 per number.
Volumes 13 through 15. $5.00 per volume, $2.00 per number

Reprints of individual articles are available in the United States at 50¢ each; in foreign countries at 75¢ each.

NOTE TO AUTHORS

The pages of this Journal are open to all contributors, and manuscripts may be submitted to any member of the Board of Editors or to the Managing Editor. Publication will be made only in the English language, but copy may be submitted for consideration in other languages. Aid in translation of accepted manuscripts will be given when possible.

All manuscripts should be typewritten with double space, carefully corrected, with footnotes continuously numbered and set off in the body of the text. If an article is to appear as a contribution from another institution, it should be approved by that institution before submission; contribution numbers of such institutions are submitted with the return of galley proofs.

The author (or authors) of each article will receive a total of 50 free reprints (with covers). Additional reprints with or without covers may be ordered by authors or institutions at the cost of printing. Orders for reprints are given when galley proofs are returned.

Both galley and page proofs are submitted to the senior author of each article.

Tables should be prepared for clarity and as near as practicable to Journal pattern, without ruled lines if possible. Table footnotes should appear at the base of each Table.

Figures are required for consideration simultaneously with the manuscript. Original figures of inconvenient size for forwarding may be represented by photographs on first submission of a manuscript; originals are required for line cuts. Illustrations requiring half-tone reproduction should be avoided so far as possible, but they will be accepted when necessary. *It is very important that the proper size of characters and symbols should be used for the lettering of illustrations.* A diagram for determining suitable heights of letters for original drawings that will be reduced, together with an explanatory note, has been published in this Journal, Vol. III, No. 1: 89–91; reprints will be submitted to authors on request. Mechanical lettering is recommended. If facilities for lettering are not available to the author, it is preferable to receive illustrations with lettering indicated in pencil only, to be finished in ink in the editorial office. All illustrations will be subject to at least a minimum reduction at the rate of 1 : 1.2. Drawings which have been heavily patched and pasted must *not be rolled* for mailing. The legends for the figures, identified by corresponding figure numbers on the illustrations also, should be typed in sequence at the end of the manuscript.

A complete and *accurate list of references* in alphabetical order at the end of each article is essential. References may be indicated in the text by author's name (or names) and *year of publication*, or by italicized numbers which correspond to the numbers given in sequence in the list of references. Each reference should include the last name followed by at least two initials or first name; co-authors should be listed with the initials or first name preceding the last name. The date should be indented on the line below, followed by a complete title *verbatim* in lower case except for the first word. Publisher, city and pagination should be indicated for books, for periodicals (abbreviations from "World List of Scientific Periodicals," Oxford; so far as possible), the volume (italicized), number and pagination should be given.

Additional information regarding the preparation of manuscripts will be furnished by the Managing Editor.

16(2)

TABLE OF CONTENTS

Page

1. **H. G. Gade:** Effects of a nonrigid, impermeable bottom on plane surface waves in shallow water 61

2. **B. V. Hamon:** The effect of pressure on the electrical conductivity of sea-water 83

3. **G. I. Roden:** Spectral analysis of a sea-surface temperature and atmospheric pressure record off southern California 90

4. **J. E. Tyler:** Comparison of light distribution above and below water 96

5. **A. H. Schooley:** Profiles of wind-created water waves in the capillary-gravity transition region 100

6. **R. O. Reid:** Effect of Coriolis force on edge waves (I) Investigation of the normal modes 109

7. **Kinjiro Kajiura:** Effect of Coriolis force on edge waves (II) Specific examples of free and forced waves 145

8. **William Aron:** The use of a large capacity portable pump for plankton sampling, with notes on plankton patchiness 158

NOTE TO SUBSCRIBERS

All back issues of the Journal of Marine Research are available at the following prices:

Volumes 1 to 12. $3.00 per volume, $1.50 per number.
Volumes 13 through 15. $5.00 per volume, $2.00 per number

NOTE TO AUTHORS

The pages of this Journal are open to all contributors, and manuscripts may be submitted to any member of the Board of Editors or to the Managing Editor. Publication will be made only in the English language, but copy may be submitted for consideration in other languages. Aid in translation of accepted manuscripts will be given when possible.

All manuscripts should be typewritten with double space, carefully corrected, with footnotes continuously numbered and set off in the body of the text. If an article is to appear as a contribution from another institution, it should be approved by that institution before submission; contribution numbers of such institutions are submitted with the return of galley proofs.

The author (or authors) of each article will receive a total of 50 free reprints (with covers). Additional reprints with or without covers may be ordered by authors or institutions at the cost of printing. Orders for reprints are given when galley proofs are returned.

Both galley and page proofs are submitted to the senior author of each article.

Tables should be prepared for clarity and as near as practicable to Journal pattern, without ruled lines if possible. Table footnotes should appear at the base of each Table.

Figures are required for consideration simultaneously with the manuscript. Original figures of inconvenient size for forwarding may be represented by photographs on first submission of a manuscript; originals are required for line cuts. Illustrations requiring half-tone reproduction should be avoided so far as possible, but they will be accepted when necessary. *It is very important that the proper size of characters and symbols should be used for the lettering of illustrations.* A diagram for determining suitable heights of letters for original drawings that will be reduced, together with an explanatory note, has been published in this Journal, Vol. III, No. 1: 89–91; reprints will be submitted to authors on request. Mechanical lettering is recommended. If facilities for lettering are not available to the author, it is preferable to receive illustrations with lettering indicated in pencil only, to be finished in ink in the editorial office. All illustrations will be subject to at least a minimum reduction at the rate of 1 : 1.2. Drawings which have been heavily patched and pasted must *not be rolled* for mailing. The legends for the figures, identified by corresponding figure numbers on the illustrations also, should be typed in sequence at the end of the manuscript.

A complete and *accurate list of references* in alphabetical order at the end of each article is essential. References may be indicated in the text by author's name (or names) and *year of publication*, or by italicized numbers which correspond to the numbers given in sequence in the list of references. Each reference should include the last name followed by at least two initials or first name; co-authors should be listed with the initials or first name preceding the last name. The date should be indented on the line below, followed by a complete title *verbatim* in lower case except for the first word. Publisher, city and pagination should be indicated for books, for periodicals (abbreviations from "World List of Scientific Periodicals," Oxford; so far as possible), the volume (italicized), number and pagination should be given.

Additional information regarding the preparation of manuscripts will be furnished by the Managing Editor.

SEARS FOUNDATION FOR MARINE RESEARCH
BINGHAM OCEANOGRAPHIC LABORATORY, YALE UNIVERSITY

JOURNAL OF
MARINE RESEARCH

VOLUME 15 1956 NUMBER 1

ECHO TRACES ASSOCIATED WITH THERMOCLINES[1, 2]

By

D. H. CUSHING, A. J. LEE AND I. D. RICHARDSON

Fisheries Laboratory, Lowestoft

ABSTRACT

Echoes received from the depth of the thermocline in Windermere, the North Sea, the Barents Sea and off Spitsbergen have been associated with aggregations of plankton organisms: zooplankton at a density of 25/litre in Windermere and phytoplankton at a density of 100,000 cells/litre (*Thalassiosira gravida* and *Chaetoceros* sp.) in the Barents Sea.

INTRODUCTION

With commercial sounders, signals have been recorded from sharp temperature discontinuities in the sea or from "scatterers" associated with them (Schubert, 1950 a, b; Schüler and Krefft, 1951 a, b; Krefft and Schüler, 1951; Tucker, 1951; Schüler, 1952; Trout, *et al.*, 1952; Herdman, 1953). Such traces are characterized by vertical thinness (about one pulse length) and horizontal extensiveness, thereby indicating that signals are being received from the axis of the sound beam only. It is unlikely, therefore, that such signals are received

[1] Since writing this paper, we have read "Visual detection of temperature-density discontinuities in water by diving" by Limbaugh and Rechnitzer (Science, *121:* 395; 1955). Our results differ from theirs in that our echo record is not diffuse; nor did Lt.-Cdr. Hodges see any aggregation of material at the thermocline. This suggests that the aggregation described in Limbaugh and Rechnitzer's paper was denser than ours; consequently it is possible that echoes were received from angles away from the axis, thus making a diffuse trace, which was presumably more extensive in depth than ours.

[2] Submitted for publication 3 September 1954.

from fish, since fish traces are fairly thick vertically and comparatively narrow horizontally, the signals being received from any part of the sound cone. They might be received from three possible sources: (a) the physical discontinuity itself; with oscillators fairly distant from the reflecting surface and with a discontinuity giving a temperature change from 16° to 10° C, within one wavelength, the relative impedance is 0.005% (speeds of sound in fresh water at 16° and 10° C are taken from Matthews, 1939); most discontinuities, however, are not flat surfaces of zero thickness but show a graded distribution of temperature and density with depth; (b) a layer of turbid sediment at the discontinuity; (c) plankton organisms at or near the discontinuity.

In July 1952, observations were made on a fairly sharp thermocline in Windermere in order to try to separate three possible sources all effective in producing echoes. Also, a thermocline obtained in the North Sea in July 1952 was examined, and discontinuities in the Barents Sea and off southern Greenland in the summers of 1951 and 1952 respectively have been considered.

I. OBSERVATIONS IN WINDERMERE

Method. The echo sounder was a special triple-frequency sounder (see Cushing and Richardson, 1955), of which only the 30 kc/s oscillator (pulse length 1 ms or millisecond) was used; the transmitter was activated by an 800v. inductive charger. The machine was mounted in the Freshwater Biological Association's vessel Mysis, with the oscillators lashed outboard on either side.

Temperature measurements were made with a thermistor and with a bathythermograph. Plankton and sediments were sampled at different depths with water bottles; the 5-litre Rodhe bottle attached to a wire was used to catch plankton animals; diatoms and sediments were sampled with an Ekman reversing bottle which, when lowered on its side on a wire to the required depth, was closed by a frogman, who also observed the visible nature of the thermocline.

Stations were made at four locations: at the Centre Buoy in the North Basin, off Slape Scar, at Rough Nab Buoy (RNB), and off Windermere Sewage outfall (WS).

Echo Records. An echo from the thermocline was certainly recorded on one day (RNB 1 and 2). Plate 1a, illustrating a trial run at RNB 1, shows a clear record of three echoes in order of depth: from the thermocline, from the depth marker at 10 m on the frogman's rope, and from the weight on the rope. The strong echo is from the frogman; he found the thermocline quickly, went beneath it, above it, returned to it, and then surfaced.

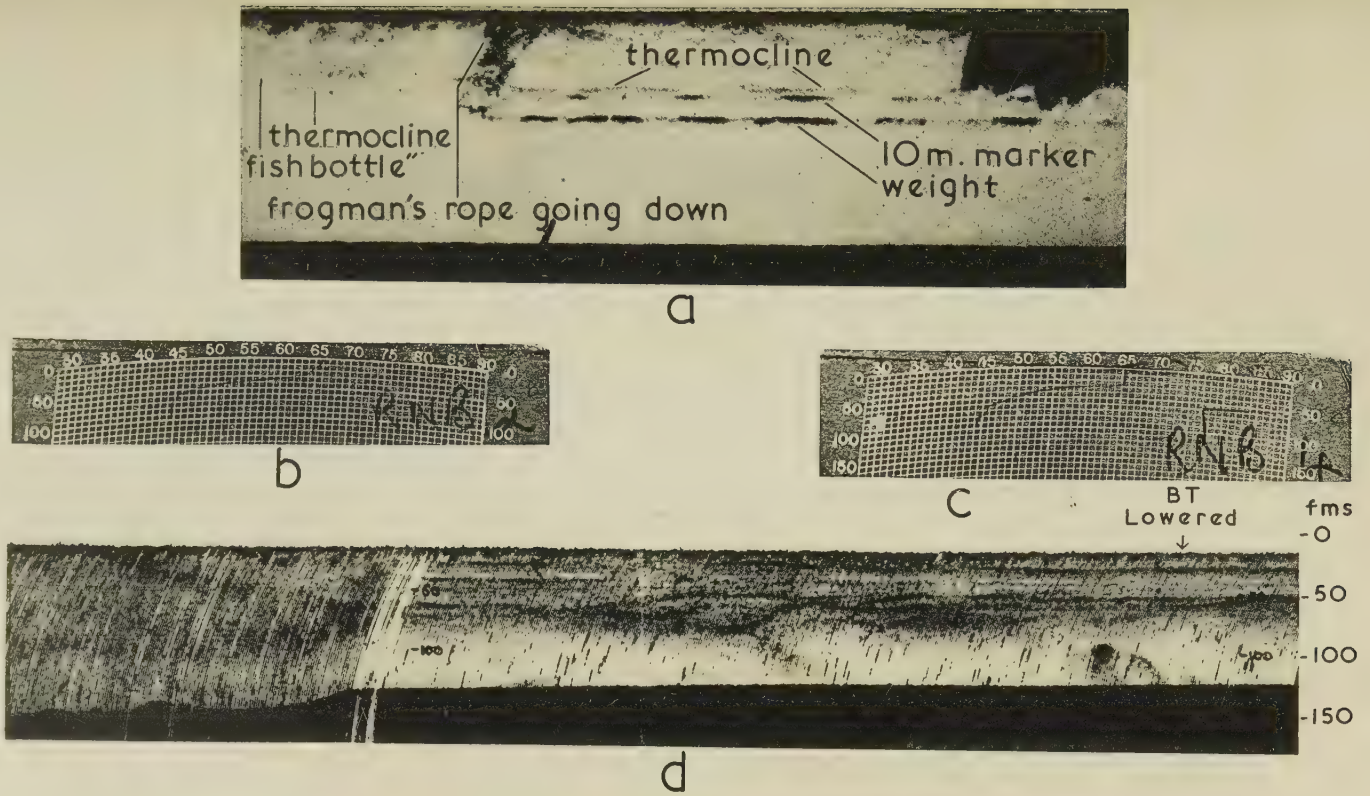

Plate I. **a.** An echo trace of the thermocline in Windermere. The large dark patch on the right is the echo from the frogman, his breathing set, and his air bubbles. The marker rope was suspended from the Mysis and the fish bottle was hanging from the buoy to which Mysis was moored. **b, c.** Bathythermograph records showing a sharp "knee" at RNB 4 (temp. corr. - 0.2°F) where no echo was recorded, and a less sharp one at RNB 2 (temp. corr. - 0.3°F) where an echo was recorded. **d.** Echo trace taken approaching St. 82, Cruise V, Ernest Holt, 1952 SW of Cape Farewell at 59° 31'N, 44° 29'W. The horizontal temperature profile in Fig 3(a) corresponds to the noisy part of the record when the ship was approaching the station. When the ship had stopped and was occupying the station, the record was clearer. The bathythermogram is shown in Fig. 3(b).

Records of thermoclines were possibly obtained on our preliminary survey off Slape Scar, since our echo records show marks at the depth of the thermocline as determined from thermistor observations. However, no further records of the thermocline were obtained, but failure was apparently not due to our sounder since it continued to give signals from the Ekman bottle as strongly as before.

Temperature Records. Examination of the individual bathythermograph records (Plate 1b, 1c) show that there are marked differences between them at or near 30 feet (about 9 m), which is where the frogman found the thermocline independently. At RNB 3, 4, 5 and WS there is a sharp "knee" at about 30 feet whereas at RNB 2 there is none. Obviously it is difficult to define the temperature gradient exactly with such a small scaled instrument, but a close approximation for RNB 2 would be of the order of 2.7° F in three feet (1½° C in 1 m) and for RNB 3, 4, 5, and WS it would be 6.6° F in three feet (3½° C in 1 m); the temperature difference at RNB 3 is probably considerably sharper.

Plankton Results. The animals in plankton samples from RNB 2, 3, 4 and WS, north of the Centre Buoy, and off Slape Scar were identified as *Diaptomus gracilis* Sars and *Daphnia hyalina* Leydig. Numbers per litre of each species at each level are given in Table I. Phytoplankton sampled at RNB 2, 3 and 4 were identified as *Asterionella formosa* Hass and *Staurastrum* sp.

Since counts were made by the sedimentation technique, it should have been possible to estimate the numbers of particles of detritus. However, since no particles were observed in sufficient quantity to merit counting, no estimate was made of numbers of particles as estimated by Jerlov (1953) or of turbidity by Joseph (1949).

In Table I it is clear that, at the thermocline, there are no differences of significance in plant numbers at the stations sampled (RNB 2, 3 and 4). In animal numbers, however, there *are* marked differences at the thermocline, there being many at RNB 2 and at Slape Scar, but few at RNB 3, 4, 5 and at Centre Buoy.

Frogman's Report. The late Lt.-Cdr. H. J. Hodges, R.N.V.(S) R., who was employed primarily to close the water bottles, made valuable observations which he described immediately on surfacing at each station. The report which appears as an Appendix (p. 12) has been condensed from notes taken at the time of interrogation.

According to Lt.-Cdr. Hodges, the thermocline appears to be defined by a visible edge, hence the assumption that the discontinuity took place within one wavelength was probably not unreasonable. Furthermore, the plankton organisms appeared to drift in a mass,

TABLE I. Estimation of Zooplankton and Phytoplankton (Numbers/litre) at Certain Depths

Station; Depth of Thermocline	*Depth Metres*	*Diaptomus gracilis*	*Daphnia hyalina*	*Asterionella formosa*	*Staurastrum* sp.
RNB 2	5	9	40	3,800	7,200
	11	135	5	13,900	6,700
11–13.7 m	13.7	—	—	3,800	6,100
	15	63	0	—	—
	18.3	—	—	18,000	3,800
RNB 3	5	3	0	2,800	16,200
	8	6	11	—	—
9 m	8.5	—	—	16,700	3,300
	9	5	3	7,500	24,400
	9.5	—	—	3,600	7,000
	10	8	3	21,400	15,800
	12	—	—	7,400	11,200
	15	27	0	—	—
RNB 4	5	2	28	—	—
	8	16	55	—	—
9 m	above	—	—	15,000	30,700
	9	5	5	6,700	14,300
	below	—	—	4,400	6,600
	10	18	2	—	—
	15	70	—	—	—
RNB 5	0	1	131		
	5	21	47		
8 m	12	2	31	No Samples	
	16	1	6		
	25	0	0		
Centre Buoy	8	10	3		
	11	2	0	No Samples	
11 m	14	31	0		
Slape Scar	8	6	0		
	12	88	0	No Samples	
12 m	15	63	0		

with individuals hopping randomly in any direction. The rate of drift of air bubbles from his diving apparatus was least at RNB 1 and greatest at RNB 2; this increase resulted from a southeast wind that sprang up in the afternoon of the first day of observations during the interval between RNB 1 and RNB 2. Assuming that large air bubbles rise at about 15 cm/sec, the midlayers were probably moving at about 1.3 cm/sec while the epilimnion was moving at 7 cm/sec. These velocities are not inconsistent with the theoretical estimates made by Mortimer (1952) for a three-layer model in Windermere.

II. OBSERVATIONS IN THE NORTH SEA. CRUISE XIV 1952 SIR LANCELOT

In 1952, a thermocline was found off the northeast coast of England, and observations were made on the depth distribution of temperature, plants, detritus, and animals. The animals were sampled at 5-fathom depth intervals with a coarse net (60 meshes to the linear inch)

TABLE II. Numbers of Algae at Different Depths in Association with Echo Records

	Station 1 No echo layer			*Station 2 Echo layer at 24.5 m*			*Station 4 Echo layer at 24 m*		
Depth (m)	*Dino-flagellates*	*Detritus*	*Green lumps*	*Dino-flagellates*	*Detritus*	*Green lumps*	*Dino-flagellates*	*Detritus*	*Green lumps*
18	16	210	40	—	—	—	1	231	1
19	10	777	0	—	—	—	—	—	—
20	122	735	50	1	210	6	2	420	25
21	120	1470	73	0	315	75	—	—	—
22	—	—	—	9	0	40	4	189	25
23	80	735	125	6	105	15	—	—	—
24	9	525	100	10	1995	15	3	210	10
25	—	—	—	—	—	—	—	—	—
26	—	—	—	—	—	—	—	40	15
27	—	—	—	—	—	—	—	—	—
28	—	—	—	—	—	—	—	5	3

towed horizontally. A Nansen-Pettersson water bottle was used to obtain temperatures as well as plants and detritus, the latter two being estimated by the sedimentation technique. Counts were made of dinoflagellates, detritus and "green lumps" and the numbers are given in Table II; it is probable that the lumps were *Phaeocystis*, but after prolonged preservation *Phaeocystis* becomes difficult to identify. The term "detritus" includes any dark irregular particle that was not referrable to the above categories.

The zooplankton samples, taken at depths of 7 and 15 fathoms, were obviously too far apart in depth for our purpose. However, at night the numbers of plankton animals at these depths increased by four to six times, and at the same time the signals from the echo sounder increased by four to nine times. Signals were measured on a C.R.T. by matching them with known voltages from a signal injector. Although the evidence is by no means positive, we think it possible that the recorded echoes in the North Sea were associated with layers of plankton animals.

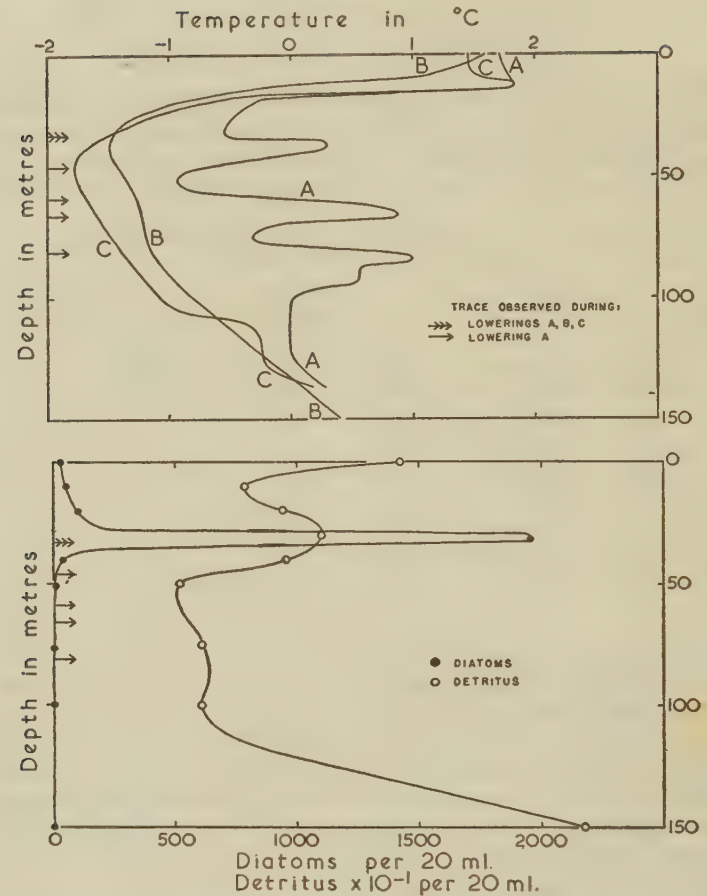

Figure 1. *a* (top), temperature gradients at St. 32, near Hope Island on 26 August 1951. A: BT lowering at 1335 hours. B: Water bottle lowering at 1408–1434 hours. C: BT lowering at 1440 hours. *b* (bottom), distribution of diatoms and detritus at the same station.

III. OBSERVATIONS IN THE BARENTS SEA AND OFF SPITSBERGEN

While investigating possible relationships of echo traces and sharp temperature discontinuities near Hope Island in the Barents Sea in August 1951, water samples were taken with Nansen reversing bottles at St. 32 in order to estimate the quantity of plants and detritus by the sedimentation technique. Discontinuity traces were observed on the 10 and 30 kc/s sounders, and a BT lowering was made at 1335

hours with the ship stopped. The resulting profile is shown in Fig. 1a together with depths at which traces were observed. No trace could be observed in the upper 18 m because of a strong echo produced by a trawl over the ship's side; however, at depths greater than that of the trawl a clear association between temperature discontinuities and traces was observed. The temperature profile obtained concurrently with the lowering of water bottles between 1408 and 1434 hours, together with a profile obtained by another BT lowering at 1440 hours, are also shown in Fig. 1a.

These latter profiles show only the uppermost of the discontinuities recorded by the first BT lowering; the ship probably did not move far off station in the interval since there was no wind. After the first BT lowering at 1335 hours the echo-sounder records often became masked by large echoes, but so far as we can tell all the discontinuity traces disappeared except that at 33 m, although that too became weaker than before. Only the two most shallow traces were recorded on the 30 kc/s sounder, and these had, in fact, disappeared on this sounder even before the first BT lowering was made.

The results of the plant and detritus counts are given in Fig. 1b. There was a pronounced maximum in the diatom distribution at 30 m, the main species being *Thalassiosira gravida* Cleve and *Chaetoceros* sp. There was also a less pronounced maximum in the detritus distribution at the same depth.

From these observations we conclude first that, whatever causes the echo, the structure considered as a whole changes its character rapidly, and second that the first and sharpest echo is associated with a layer of detritus and a pronounced layer of diatoms.

Data from a later observation indicate that these traces were not caused by the physical discontinuities themselves. On 11 September 1951 an echo was obtained at night on a 30 kc/s machine at St. 113 about 22 miles southwest of Sörkapp, Spitsbergen. The temperature profile from a BT lowering at 2305 hours is shown in Fig. 2. Since a strong signal was associated with the steep temperature gradient between 29 and 35 fathoms while no signal of similar strength was associated with the shallower and even steeper temperature gradient between 16 and 19 fathoms, it seems plausible to rule out temperature discontinuities themselves as the cause of echoes.

Both Sts. 32 and 113 were close to fronts where relatively warm Atlantic and cold Arctic water meet. Since eddies are common in these areas, the temperature profile obtained at St. 32 is probably due to vorticity; indeed it is difficult to understand how such a distribution arose in any other way if we assume that each echo was associated with a diatom layer. Herdman (1953) has noted that traces

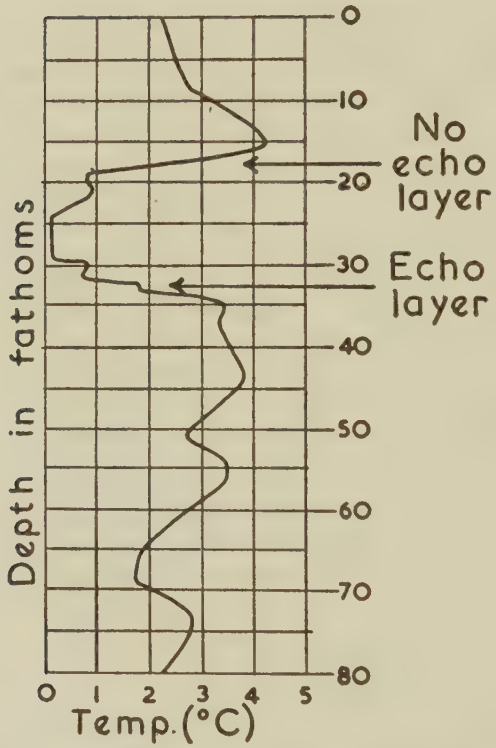

Figure 2. Vertical temperature profile and depth of the echo layer from a BT lowering at St. 113, Cruise V, Ernest Holt, 1951.

similar to those observed in the Barents Sea have been recorded at the Antarctic Convergence where water also sinks.

On 14 September 1952 further evidence of such sinking was obtained with a 10 kc/s machine in the South Greenland area at St. 82, 24 miles southwest of Cape Farewell. A surface temperature survey with a thermograph showed the presence of a clockwise eddy on the boundary between the warm Irminger and the cold East Greenland components of the West Greenland Current. The temperature profile obtained from a BT lowering near the end of the station is shown in Fig. 3b. Strong "discontinuity traces" observed on the echo sounder (Plate 1d) can be associated with the different gradients on the vertical temperature profile.

The surface temperature profile recorded by the thermograph when the station was approached is shown in Fig. 3a. Traces descended from the surface at the front between the two water masses:

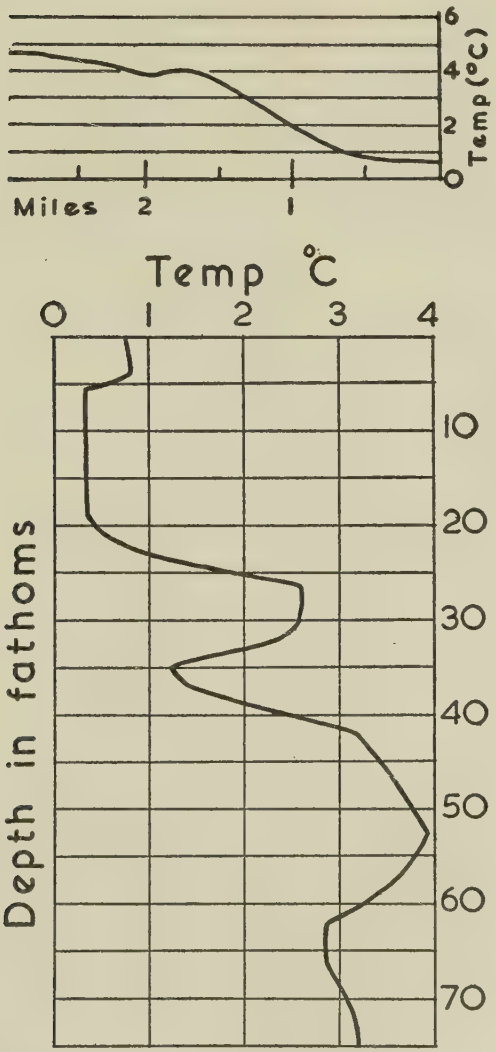

Figure 3. *a* (top), surface thermograph record preceding St. 82, Cruise V, Ernest Holt, 1952. The distance in miles corresponds to the duration of the noisy part of the record shown in Plate I *d*. *b* (bottom), bathythermogram at St. 82, Cruise V, Ernest Holt, 1952.

those below 50 fathoms in water between 3° and 4° C at St. 82 left the surface where the temperature was just over 4° C, whilst those above 50 fathoms in water slightly more than 2° C left the surface in water of 2° C. The echo which was at a depth of 100 fa. just as we approached St. 82 started to descend from the surface at a point nine miles from that station where the temperature fell sharply from 6° C. The association between the traces and the temperature profiles may well be explained by assuming that organisms carried downwards in the eddy caused the echoes.

TABLE III. Comparison of the Sharpness of the Thermocline with the Presence or Absence of Echo Records Associated with It

Station	*Thermocline*	*Echo record*
RNB 2	1½°C in 1 m	Yes
RNB 3	3°C in 1 m	No
RNB 4	3°C in 1 m	No
Centre Buoy	1–1½°C in 1 m	No
Slape Scar	2°C in 1 m	Possibly

TABLE IV. Comparison of the Numbers of Plankton Organisms per Litre with the Presence or Absence of an Echo Record from the Thermocline

Station	*Zooplankton organisms*	*Phytoplankton organisms*	*Echo record*
RNB 2	28	20,600	Yes
RNB 3	1.6	31,900	No
RNB 4	2	21,000	No
Centre Buoy	0.4	Not sampled	No
Slape Scar	17.6	Not sampled	Possibly

DISCUSSION

Earlier we mentioned three possibilities that might account for the rather considerable signals that are sometimes received by echo sounders from the region of a thermocline: the physical discontinuity itself, the plankton organisms, and suspended particles.

The first factor is dealt with in Table III, which compares the sharpness of the Windermere thermocline with the presence of echo records. This table shows that it is unlikely that the presence of an echo from the thermocline is associated with the sharpness of the discontinuity; confirmation is found in the BT record taken off Sörkapp (Fig. 2). There are two possibilities not covered by this simple treatment. First, perhaps the surface of the whole gradient and not just its sharpest boundary should be considered; hence one would expect signals extensive in time, which are not found. Second, small changes in the micro structure of the discontinuity might scatter sound back to the receiver, but this is unlikely to be of importance when the discontinuity is normal to the axis of the sound beam.

The effect of the second factor is set out in Table IV, from which it seems possible that the echo record is associated with the presence of plankton animals. Trout, *et al.* (1952) describe a thermocline echo obtained off Whitby by the M. V. Platessa, and it is worth noting here that this trace was distinctly patchy in its occurrence, being sometimes completely absent, whilst the thermocline persisted. The observations presented in Table IV do not constitute conclusive evidence that plankton animals produce the echo, but negative evidence from the numbers of phytoplankton and from temperature structure do reinforce such an hypothesis.

The evidence given in Fig. 1b shows an association between a marked echo trace and a thin but concentrated diatom layer. In Windermere there were about 25,000 cells/l, whereas off Hope Island in the Barents Sea there were 100,000, or about four times as many. Furthermore, the diatoms found off Hope Island were between 50 and 200 times larger than those found in Windermere, and the two species found in the Barents Sea layer form long chains; it is possible that the diatom layer off Hope Island was much thicker and more concentrated than that in Windermere.

The third possible factor is the presence of a layer of detritus. Counts of the North Sea samples by the sedimentation technique revealed numbers of particles up to 2,000,000/litre. At Windermere, however, numbers approaching such a level were not observed. This evidence, combined with the results from the North Sea, leads us to believe that sedimented particles do not always contribute to the echoes associated with thermoclines.

From examination of the evidence collected for the three possibilities, it seems that the echo associated with the thermocline was returned from a very definite layer of plankton organisms. Sometimes the layer may continue in the same form for many miles and sometimes, possibly in association with sinking vortices, layering becomes complex. It appears that both diatoms and animals, and in one case, detritus, if concentrated sufficiently at the thermocline, may scatter enough energy back to the receiver to record consistent signals.

BIBLIOGRAPHY

Cushing, D. H. and I. D. Richardson
1955. A triple frequency echo sounder. Fish. Invest. Lond., (II) *20* (1).

Herdman, H. F. P.
1953. The deep scattering layer in the sea: association with density layering. Nature, London, *172*: 275.

Jerlov, N. G.
1953. Influence of suspended and dissolved matter on the transparency of sea water. Tellus, *5* (1): 59.

Joseph, J.
1949. Durchsichtigkeitsmessungen im Meere im ultravioletten Spektralbereich. Dtsch. Hydrogr. Z., *2* (5): 212.
Krefft, G. and F. Schüler
1951. Fischzeichen-Häufigkeit und Heringsfangergebnisse in der nördlichen und westlichen Nordsee im August 1950. Fischereiwelt, *3* (2): 27.
Limbaugh, C. and A. B. Rechnitzer
1955. Visual detection of temperature-density discontinuities in water by diving. Science, 121: 395.
Matthews, D. J.
1939. Tables of the velocity of sound in pure water and in sea water for use in echo sounding and sound ranging. Hydrog. Dept., Admiralty, London.
Mortimer, C. H.
1952. Water movements in lakes during summer stratification; evidence from the distribution of temperature in Windermere. Phil. Trans., B, *236*: 355.
Schubert, K.
1950a. Der Heringsfang im Juni in der nördlichen Nordsee. Fischereiwelt, *2* (8): 118.
1950b. Einige Bemerkungen über den Gebrauch der Fischortungsgeräte. Fischereiwelt, *2* (8): 119.
Schüler, F.
1952. Über das Lesen von Echogrammen. Fischereiwelt, *4* (1): 7.
Schüler, F. and G. Krefft
1951a. Zur Frage der Verwendung des Echographen in der Loggerfischerei. Fischereiwelt, *3* (4): 63.
1951b. Versuche zur Beeinflussung von Meeresfischen durch Schalldruckwellen und künstliches Licht. Fischereiwelt, *3* (1): 8.
Trout, G. C., A. J. Lee, I. D. Richardson, and F. R. Harden Jones
1952. Recent echo sounder studies. Nature, London, *170:* 71.
Tucker, G. H.
1951. Relation of fishes and other organisms to the scattering of underwater sound. J. Mar. Res., *10* (2): 215.

APPENDIX

Report of Observations by Lt.-Cdr. H. J. Hodges

RNB 1. Midday. Sun, white clouds and clear water (Trial dive). At a depth of 10 m I could see 19 feet in green water. The sun was constantly visible as a dull white area. I could distinguish between "hoppers" (zooplankton) and "sedimentation" (phytoplankton); as I looked upward, the plankton was brown against a pale green background, on looking horizontally it was white against a green background, and on looking down, nothing was seen. There was a general slow northerly drift of plankton in the upper layer (epilimnion); this was gauged by watching individuals moving across the field of view. Individual plankton animals made sudden hops in any direction

and there appeared to be little difference in numbers either vertically or horizontally.

RNB 2. Afternoon. Heavy rain and dark clouds; wind from the SE. Visibility was reduced to the width of the boat. The thermocline was perceptible in a layer of approximately 8–10 inches thick; I found it easy to break the thermocline by forcing cold water up into the warm water and by forcing warm down into the cold. At RNB 1, by hanging onto my measured rope, I observed a positive drift of organisms to the north above the thermocline, but I noticed no such drift below it. At RNB 2, however, I did observe plankton organisms moving north beneath the thermocline, but those above it were moving much more rapidly.

RNB 3. Clouds with some sunshine. The thermocline was exactly at 9 m by my measured rope (suspended from the anchored ship). The boundary between warm and cold water appeared to lie within a 7 inch layer; it was possible to have three inches above the horizontal Ekman bottle, in warm water, and four inches below it, in cold water. At 9.5 m the water was much colder than at 9 m and it seemed that the boundary was actually limited to about 3 or 4 inches. The light, when I descended, changed from pale green above to a darker green across the boundary. When I looked horizontally below the boundary, visibility again increased markedly. Whether I was above or below, the boundary appeared as a line. The boundary is a visible line; from above it is rather like looking over the tops of clouds and from below it is rather like a cloud base. Above the thermocline, the plankton consisted of sedimentation (small brown or dark brown objects rather like cigarette ash) with a certain number of "hoppers" dispersed amongst it, the latter appearing black. Below the thermocline, only "hoppers" occurred. I estimated the drift in two ways: (a) by observing the plankton directly; all of them were moving in one direction, with the movement above the thermocline twice as fast as that below; (b) by using the air bubbles from my breathing set; below the boundary the air bubbles went up nearly vertically (5° from the vertical), but at the boundary they bent off sharply at an angle of 30° from the vertical.

RNB 4. Clouds with some sunshine. Above the boundary the bubbles went up at 25–30° from the vertical, below it at 5–10° from the vertical. I could now locate the thermocline by watching the rising bubbles alter course. Again there was a faster northward drift above the thermocline than below.

Hoppers (i.e., plankton animals) make no 'up and down' movement but usually make tight spiral or circular movements in any direction.

CHLOROPHYLL *a* IN THE PHYTOPLANKTON IN COASTAL WATERS OF THE EASTERN GULF OF MEXICO[1]

By

NELSON MARSHALL[2]

ABSTRACT

Chlorophyll *a* was measured about twice a month for one year at three surface stations along the axis of Alligator Harbor, Florida; additional observations were made at stations along Tampa Bay and elsewhere in the coastal waters of the eastern Gulf of Mexico. The greatest concentrations, toward the head of the estuaries studied, were probably associated with low dispersal rates and with mixing of benthic forms into the plankton of shallow water. Except for red tide waters, which yielded values approximating spring flowering in Long Island Sound, the chlorophyll concentrations offshore were low. Comparison with chlorophyll observations from other regions suggests that phytoplankton crops from the Florida west coast approximate those of similar waters elsewhere.

In addition, experiments were conducted to ascertain the chlorophyll histories of water samples held in light and dark bottles at different depths. Light bottles exposed to surface or near-surface light intensities commonly exhibited chlorophyll decline even when the phytoplankters were multiplying. This decline diminished rapidly with depth. Though surface light may be too intense for some phytoplankters, such fading is not to be regarded as a serious deterrent to the use of chlorophyll values as an index of phytoplankton mass where the plankton is free to mix vertically.

INTRODUCTION AND METHODS

As one index of basic production in water, the chlorophyll *a* content was measured in samples taken at the surface along the west coast of Florida. Seasonal measurements were made for Tampa Bay, and more intensive sampling for one year was carried out for Alligator Harbor. For the rest of the coastal area the sampling was sporadic. In Alligator Harbor, experiments were also conducted which showed relationships of depth with the chlorophyll *a* content of phytoplankton.

The measurements reported are for chlorophyll extracts of phytoplankton that was concentrated from water samples in three ways: with Whatman No. 42 paper coated with barium sulfate, with a Foerst centrifuge, or with an AA millipore filter. For the samples

[1] Contribution No. 29, Oceanographic Institute, Florida State University.

[2] Present address: Alfred University, Alfred, New York.

processed in 1952, extraction was in 90% methyl alcohol; the later samples were extracted in 90% reagent grade acetone.

Early in these studies, extracting was done at room temperature for about 20 hours; later it was done for only ten minutes (30 min. with a millipore filter) at temperatures slightly above 40° C with repeated stirring. Before the reading was taken, the undissolved matter was settled out of the extracts, usually by centrifuging. Note, however, that millipore filters dissolved in the acetone and altered the transparency, thus necessitating application of a correction factor (discussed under conversions) to the light transmission readings.

Extracts were read on a Klett Summerson photoelectric colorimeter by using a sharp cut-off Corning filter (No. 2404[3]) with maximum transmission starting at 667 mμ and extending above that wave length. Occasional comparative readings were made on a Beckman DU Spectrophotometer, and from these the formula of Richards with Thompson (1952) was used to determine the chlorophyll *a* and to work out the conversion factor for the Klett readings. The conversion[4] applied was as follows: Klett units of extract in 90% acetone × .034 = mg chlorophyll *a*/L. (This conversion was used also for the few methanol extracts obtained. From comparison it is known that this is not accurate, but the error is small.) As applied to the determinations made, the conversion is:

$$\frac{\text{Klett readings} \times \text{volume of extract in ml}}{\text{vol. of sample in liters}} \times .034 = \text{mg chlorophyll } a/\text{m}^3.$$

ALLIGATOR HARBOR

Fig. 1 presents chlorophyll *a* measurements from the three stations in Alligator Harbor for an entire year. This indicates a trend to higher chlorophyll *a* levels toward the head of the Harbor, especially in summer. Assuming a fair correlation between the quantity of chlorophyll and the phytoplankton mass (as established by Graham [1943] and others), this also indicates a greater phytoplankton population toward the head waters.

[3] Several workers have been using a Klett 66 filter for this. Six chlorophyll extracts, read almost simultaneously on both filters, indicate that a reading on the Corning 2404 × 1.03 = reading on the Klett 66 filter.

[4] When a millipore filter was used, 1.5 was subtracted from the original Klett readings before making this conversion. As determined by blank runs, this correction applies when the extraction procedure is conducted as follows: The exposed portion of a 47 mm diameter AA millipore filter is dissolved as much as possible in 3.5 ml of 90% acetone. After centrifuging, the upper 3 ml of acetone is decanted off and 2 ml additional acetone is added to the decanted extract to clear it further. The 5 ml of extract obtained is equivalent to extracting originally in 5.8 ml.

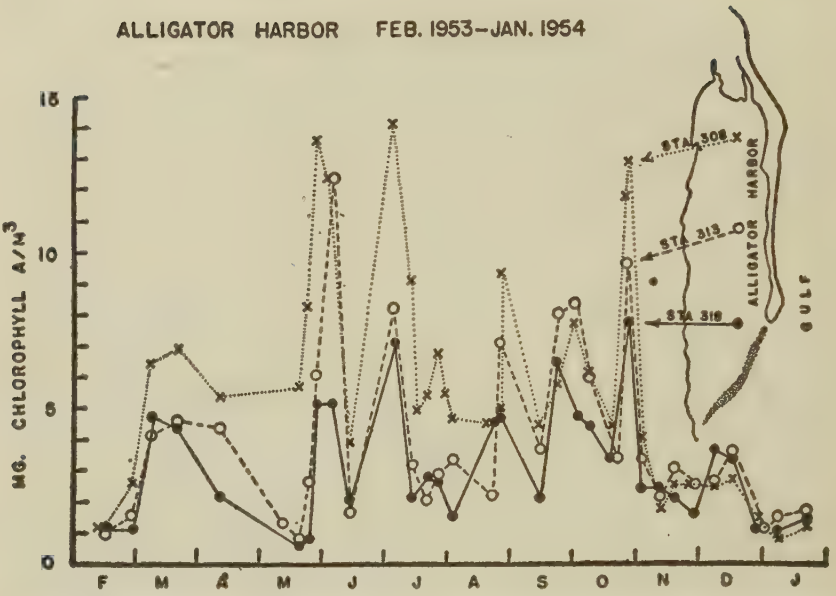

Figure 1. Measurements of chlorophyll *a* at three stations along the length of Alligator Harbor, Florida.

In addition to these chlorophyll measurements, water samples preserved in formalin were taken at all three stations from August 28, 1953 through January 21, 1954 and at the upper Harbor station during the previous summer and the following spring. These were examined after settling. The observations may be summarized as follows:

In terms of mass, and especially in terms of numbers, most of the pelagic plants are nannoplankters, chiefly small diatoms, commonly of the naviculoid group. Perhaps small flagellates were equally important, though their form and identity were destroyed in preserved samples. Many of these minute plankters are unattached forms associated with the bottom, but they continuously mix into the pelagic area. Such a component of the phytoplankton is not adequately recognized in the literature; however, it seems probable that further studies of estuarine habitats will bring a wider recognition of this plankton component.

Associated with this population that mixes in from the bottom is a large amount of inorganic and organic detritus, including fragments and whole cases of dead diatoms.

Of the larger and better known plankton diatoms (all tentatively named due to lack of taxonomic study in the locality), the more numerous include *Rhizosolenia* spp., *Chaetoceros* spp., *Skeletonema costatum*, *Melosira sulcata*, *Thallassionema nitzchioides*, *Thallasiothrix frauenfeldii*, *Asterionella japonica*, species of *Gyrosigma*

and *Pleurosigma*, and *Nitzchia* spp. Though individual counts have not been made, it is clear that species of *Rhizosolenia*, *Chaetoceros*, *Nitzchia* and others undergo pronounced fluctuations in numbers, but there is little indication that any tend to multiply in such proportions that they dominate in the pattern commonly regarded as a bloom.

Counts of the total number of phytoplankton cells, extremely rough due to the difficulties of distinguishing and enumerating these heterogeneous small forms, show a range that is generally between 1–15 million/l. Of the larger forms named above, the species of *Nitzchia* greatly exceeded others in numbers.

Though there may be qualitative differences between stations in the Harbor, they are not sufficiently obvious to be reported from the present general observations.

A large bottom diatom, *Eupodiscus radiatus*, is often the most abundant form in collections made by net; however, for unstrained collections, a count of 15,000/l (by Herbert Curl, Jr.) is the highest known to the author.

From these comments on the contribution of bottom flora to the phytoplankton, it is apparent that the gradient to higher chlorophyll concentrations toward the upper estuary is due in part to the fact that the up-Harbor waters are shallower and present a larger bottom to volume ratio than that toward the mouth. Thus, in the headwaters the mixing of bottom forms into the plankton is proportionately greater. As a corollary, the Harbor gradient decreases when mixing is decreased. This can be seen in day-to-day changes but it is most readily illustrated by reference to the low gradients of the winter months and to the deeper secchi disc readings of that period (Table I).

The contrasts in circulation from one end of the estuary to the other may also contribute to the phytoplankton gradient. The headwaters of the Harbor are partially cut off by oyster bars and other shoals. This and the lack of tributary flow reduce tidal currents and other major circulation effects. By contrast, circulation is much freer at mid-Harbor and at the mouth. These comparisons stand out quite clearly in a twelve-hour tidal cycle observation conducted on April 11, 1953, a day with a relatively even diurnal tide and with a minimum of complicating wind effects. These observations, taken every 15 minutes, give the following average currents:

Sta. 308 (Head of Harbor) 0.03 knots
Sta. 313 (Mid-Harbor) 0.14 knots
Sta. 318 (Mouth of Harbor) 0.19 knots

Since there are no persistent gradients in salinity and temperature along the length of the estuary (Table I), and since vertical gradients are slight and transitory in these shallow depths, these surface circu-

TABLE I. Surface Salinity (‰), Temperature (°C) and Secchi Disc Depths (Meters at Disappearance) Near the Mouth in Alligator Harbor (St. 318), at mid-Harbor (St. 313), and Near the Head (St. 308). Number of Readings Is Given in ( ) When There Was More Than One.

	Near mouth			*Mid-Harbor*			*Near head*		
Date	*Sal.*	*Temp.*	*S.D.**	*Sal.*	*Temp.*	*S.D.**	*Sal.*	*Temp.*	*S.D.**
2/14/53	31.4(3)	15.4(3)	—	31.1(3)	15.5(3)	—	31.1(3)	15.2(3)	—
2/27/53	28.9(3)	17.4(3)	—	29.7(3)	17.0(3)	—	30.0(3)	17.7(3)	—
3/8/53	30.1(3)	18.9(3)	—	30.5(3)	18.9(3)	—	30.0(3)	19.3(3)	—
3/19/53	30.4	21.7	1.7	29.9	21.9	1.7	29.5	22.3	1.2
3/20/53	30.6(3)	21.3(3)	1.5(3)	30.6(3)	21.0(3)	1.2(3)	29.8(3)	21.5(3)	0.9(3)
4/11/53	30.0(37)	24.1(37)	—	29.1(38)	24.3(38)	—	29.0(38)	24.8(38)	—
5/21/53	24.2	26.9	2.3	26.8	28.4	1.4	29.7	28.1	0.8
5/25/53	26.7	29.4	2.3	27.6	29.9	1.5	27.8	30.4	0.8
5/29/53	30.7	27.9	0.9	31.6	27.7	0.9	29.3	27.9	0.6
6/5/53	31.0	27.1	0.8	31.8	27.1	0.5	32.4	27.1	0.5
6/12/53	30.0	29.7	1.4	28.8	29.9	1.5	28.6	30.2	0.9
7/5/53	30.4	30.8	0.9	30.6	30.5	0.6	30.3	30.7	0.5
7/14/53	32.1	28.7	2.0	31.3	28.1	1.1	30.0	27.9	0.5
7/21/53	29.4	30.9	—	29.7	30.1	—	32.1	30.4	—
7/27/53	31.5	29.9	1.7	31.7	29.9	0.9	31.3	27.9	0.6
8/3/53	32.1	31.1	—	31.8	31.9	—	31.0	31.7	—
8/22/53	29.1	27.5	0.9	27.2	27.2	0.6	27.1	27.2	0.5
8/28/53	26.7	27.2	1.2	25.9	27.2	0.6	25.5	28.2	0.5
9/24/53	29.2	25.2	0.8	27.5	24.7	0.5	29.8	25.2	0.5
10/3/53	27.3	26.2	1.1	27.7	26.2	0.5	27.8	26.2	0.3
10/8/53	29.4	23.0	0.9	28.9	23.0	0.6	29.6	23.0	0.8
10/20/53	30.9	24.0	1.1	30.5	24.0	0.8	30.9	24.5	0.6
10/28/53	31.0	22.5	0.9	30.6	22.0	0.8	29.9	21.5	0.6
11/4/53	31.7	20.0	1.4	31.2	19.6	1.1	31.1	20.0	1.1
11/12/53	30.7	15.5	v.	30.3	14.5	v.	30.0	14.0	v.
11/19/53	32.2	19.5	2.1	32.1	19.5	1.7	31.7	19.7	1.4
11/29/53	31.9	15.7	v.	31.4	14.5	v.	30.6	14.0	v.
12/8/53	29.9	15.8	1.5	29.8	15.7	v.	28.5	15.0	v.
12/17/53	29.9	10.4	v.	30.4	10.2	1.2	29.7	9.0	0.9
12/30/53	26.8	14.2	v.	28.1	14.2	v.	28.1	14.2	v.
1/7/54	29.8	12.5	v.	29.7	12.5	v.	29.4	11.4	v.
1/21/54	30.8	15.5	v.	30.8	15.8	v.	30.7	16.6	v.

* When visible on bottom, the letter "v" is entered in column.

lation figures can be used as an index of comparative dispersal rates. The minimum circulation at the head of this estuary could permit an accumulation of nutrients and a building of phytoplankton populations through recruitment and growth. In comparison, the nutrients and populations would tend to be dispersed more toward the mouth where stronger currents exist.

TAMPA BAY

Fig. 2 presents the chlorophyll *a* measurements for samples from Tampa Bay. Though sampling was not frequent enough to observe seasonal averages or short term fluctuations, the data do show a gradient that ranges from high concentrations in the head waters (near tributary sources) to lower concentrations toward the mouth; the lowest values occur offshore.

Accompanying these measurements are some records of the total phosphorous as determined by Dr. H. T. Odum. The total P, high in all instances, is probably a direct result of the high P found in the tributary rivers by Odum (1953). Toward the mouth the P values decline in the same general pattern as that observed in the chlorophyll determinations. This suggests a correlation between the phytoplankton crop and the general nutrient level.

COASTAL WATERS

Table II presents miscellaneous offshore measurements. Characteristically, these offshore records are appreciably lower than those of the estuaries.

Red tide waters, caused by the intense bloom of *Gymnodinium brevis*, are listed separately in Table II. Though red tide was once regarded as a rare and unique phenomenon, outbreaks of this condition have been observed with sufficient frequency of late to throw some doubt on the validity of dealing with this as an atypical occurrence. Unfortunately the red tide measurements presented here are subject to fading error; however, the data show chlorophyll in quantities of 20–40 mg/m^3, which are characteristic of algal blooms observed by Conover (1955) for spring flowering in Long Island Sound. The red tide measurements also indicate the patchiness of the bloom, some areas having a far greater chlorophyll concentration than others. Such contrasting areas are often separated by sharp lines of demarcation easily seen at the surface.

DISCUSSION OF COMPARATIVE MEASUREMENTS

The chlorophyll gradients in Alligator Harbor and Tampa Bay, sloping as they do to lower values offshore, are in accord with evident

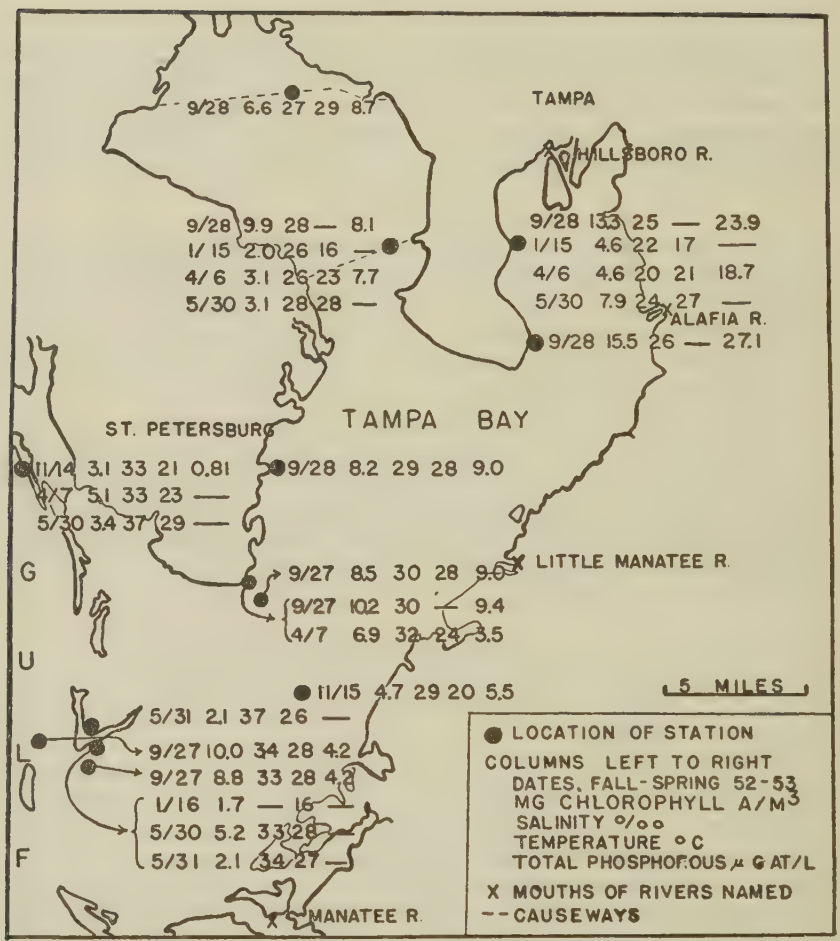

Figure 2. Measurements of chlorophyll *a*, temperature, salinity and total phosphorous in Tampa Bay, Florida. Phosphorous data are from H. T. Odum (1953). (A causeway which now extends across the mouth of the Bay was in the early stages of construction when the above observations were made.)

trends obtained from assorted data in the literature which deal with various indices of basic production (Table III). In general, enclosed freshwater ponds and lakes have a greater phytoplankton biomass than estuaries and embayments, which in turn have a greater biomass than coastal offshore waters, which have a greater biomass than open seas.

These are rough rule-of-thumb relationships, so rough in fact

TABLE II. Miscellaneous Chlorophyll *a* Measurements (mg/m³) on Surface Samples from Coastal Waters of Florida.

Gulf waters; no exceptional conditions		
30 miles west of Panama City, near shore	8/27/53	0.8
3 miles offshore from Panama City	5/1/53	0.4*
3 miles south of Alligator Point	6/12/53	0.4
1 mile south of Alligator Point	8/28/53	3.4
Boca Ciega Key west of St. Petersburg, near shore	11/14/53	3.1
	4/7/53	5.1
	5/30/53	3.4
Naples pier	11/17/52	1.6
Gulf waters off Sanibel Island during red tide†		
4 miles west of Sanibel in red water, Sta. 6a‡	11/16/52	30.7,30.7
4 miles west of Sanibel in clear water, Sta. 7‡	11/16/52	6.5,5.9
9 miles west of Sanibel in clear water, Sta. 9‡	11/16/52	4.4,6.6
12 miles west of Sanibel in red water, Sta. 8‡	11/16/52	5.1,14.3
Florida Keys, Atlantic Ocean side		
Plantation Key, near shore	11/19/52	1.8
Upper Matecumbe Key, near shore	11/19/52	0.7

* Sample taken in estuary, St. Andrews Bay, for comparison = 1.5.

† Intense bloom of *Gymnodinium brevis* making water reddish, viscous and toxic to fishes and other marine life.

‡ Station numbers used by the University of Miami crew which took author to stations for samples.

that, when one attempts to explain them, he may prefer instead to discard the generalizations in favor of more specific comparisons between given environments. However, note that the first group (ponds and lakes) constitutes a type that would tend to have proportionately large shallow areas favorable for the mixing of settled nutrients and benthic flora into the pelagic zone. Also, a small lake or relatively enclosed body of water may provide optimum conditions for accumulating a high concentration of nutrients and for building up a high concentration of plankters through recruitment with little dispersion. At the other extreme the features of the open seas are least likely to provide these conditions.

The retention of phytoplankton populations, permitting recruitment and growth, may be regarded as the more fundamental of these reasons for such contrasts in production. Without this feature, as in a fast flowing river such as the Silver River, phytoplankton production may be negligible. Though moderately supplied with nutrients (correspondence with H. T. Odum), the Silver River supports a low phytoplankton population (Table III) and affords little chance

TABLE III. Some Chlorophyll Values in mg/m³ for Different Regions from Surface Samples Obtained by Centrifuge, Filter Paper or Millipore Filter. *a* Was Determined Specifically as Chlorophyll *a*.

Author	*Region*	*Mean*	*Max.*
Freshwater			
Wolschlag and Hasler (1951)	Lake Mendota	23.8	199.0
Marshall	Lakes of Florida (10 samples from 9 lakes)	19.2*a*	112.0*a*
Riley (1940)	Linsley Pond, Conn.	15.0	38.2
Marshall	Silver River, Fla. (3 samples, 7/3/53)	0.2*a*	0.4*a*
Estuaries			
Riley (1941a)	Long Island Sound	17.4	62.0
Marshall (Fig. 2)	Tampa Bay	6.6*a*	15.5*a*
Chesapeake Bay Institute (unpubl. data)	Tidewaters of Chesapeake Bay tributaries*	5.6*a*	47.4*a*
Marshall (Fig. 1)	Alligator Harbor	4.3*a*	14.0*a*
Chesapeake Bay Institute (unpubl. data)	Chesapeake Bay*	4.1*a*	21.7*a*
Coastal Offshore Waters			
Riley (1941b)	Georges Bank	5.6	27.2
Marshall (Table II)	Florida West Coast†	2.3*a*	30.7*a*
Marshall (Table II)	Florida Keys	1.2*a*	1.8*a*
Riley (1938)	Dry Tortugas, Fla.	0.3	0.5
Western N. Atlantic Slope (Ocean)			
Riley (1939)	Northern waters	2.1	—
Riley (1939)	Southern waters	1.0	—

* Averaged by Marshall from records for surface samples listed in the Chesapeake Bay Institute mimeographed data reports.

† Mean does not include determinations in red tide area; maximum is a red tide determination.

for phytoplankton recruitment over its short course from Silver Springs.

Others have made similar generalizations with differing emphases. Motoda (1940) pointed out the presence of higher plankton populations in a coral atoll as compared with ocean waters outside the reef. Rawson (1953) stated, "the inverse relationship between standing crop of plankton and mean depth suggests that morphometric factors are predominant in determining the trophic type of most lakes under consideration." Riley, et al. (1949), in numerous data and comments on the western North Atlantic, showed quite consistently a relatively low phytoplankton crop in the open ocean, intermediate conditions in coastal waters, and a high standing crop inshore, particularly in Long Island Sound. Ketchum (1954), in an analysis of the relationship of plankton reproduction and the rate of water circulation in estuaries, indicated that plankton populations are likely to be greater where there is less water exchange.

Table III throws some light on conditions in the eastern Gulf waters as compared to other areas similarly measured. The chlorophyll values for Tampa Bay and Alligator Harbor compare favorably with those for Chesapeake Bay, which is usually regarded as a highly productive estuarine system. The data suggest that none of these estuaries compares favorably with Long Island Sound; however, Riley has recently obtained measurements in which he has greater confidence, and he advises that these data would break down this contrast.

EXPERIMENTS ON CHLOROPHYLL *a* RELATIVE TO DEPTH

Concurrent with observations on chlorophyll values in natural waters, observations were made on the chlorophyll *a* histories of bottled water samples from Alligator Harbor. These involved a series of exploratory experiments, with different set-ups being repeated only as they clarified points in question or helped point the way to successive steps. Most of the emphasis here is placed on the last few experiments.

The experimental patterns and the resulting chlorophyll determinations are presented in Appendix I. The samples of natural populations observed in these experiments were held either in open bottles or flasks or in closed bottles with air pockets. This encouraged splashing and mixing in the containers. For Experiments 1 and 2 the containers were filled by dipping them at the surface, thus individual samples probably varied slightly. In the remaining experiments, the initial similarity of all samples was assured by filling the containers from a common supply poured from an ordinary watering can.

Considering the mixed nature of the plankton associations used and the differences in populations and their physiological condition from one experiment to the next, the variations observed for these chlorophyll histories are readily understandable. But in spite of the variations, a relationship to depth and to the amount of light available can be discerned. Light bottles at the surface commonly showed a decline in chlorophyll or, if there was a gain, it tended to be less than that in bottles held one and two meters below the surface (Appendix I; Fig. 3). At depths where conditions reduced the light appreciably, a chlorophyll increase was usual. Actually, the most rapid increases in chlorophyll concentrations were obtained in samples which were subjected to the low radiation that penetrated through brown jugs held one meter below the surface in the turbid waters of Alligator Harbor.

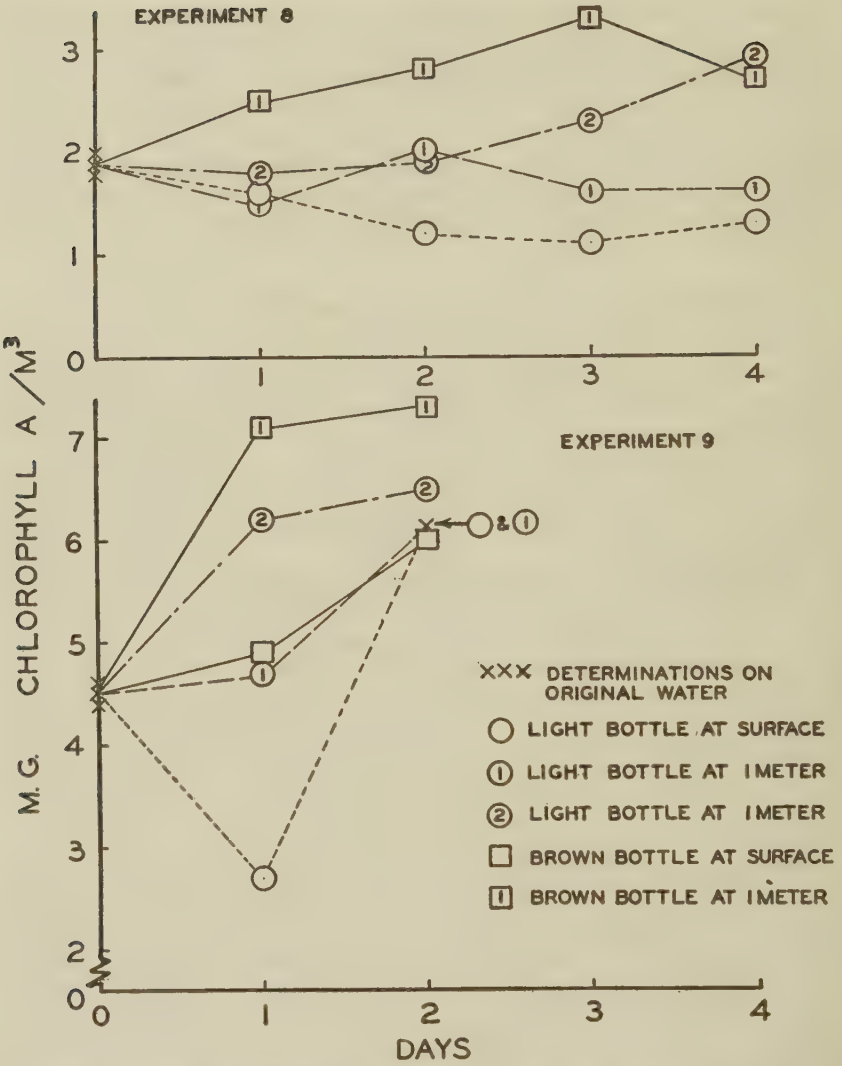

Figure 3. Graphic representation of Experiments 8 and 9 (see description and data in Appendix I).

The early experiments, which were carried out before chlorophyll decline at surface light intensities had been anticipated, involved only surface exposures. Of these early trials, Experiment 2 is especially noteworthy. The clear bottles that floated in the Harbor exhibited decline while those in a laboratory tank illuminated by

two 40W daylight fluorescent bulbs (dim light compared to sunlight) showed a chlorophyll gain.

Several of the experiments included observations on dark bottles (painted black on the outside or covered with opaque oilskin). These showed both increases and decreases, but in general the chlorophyll values held rather steady.

The populations used for these experiments, the same as those described previously for Alligator Harbor, were difficult to identify and enumerate. Nevertheless, counts were attempted on samples from the beginning and end of each experiment. These counts (Table IV) were made with a compound microscope at 430X on aliquots taken after formalin preserved samples had been concentrated by settling.

From the data it appears that the filtration process used in setting up half of the initial samples for Experiment 1 caused a concentration of minute cells that passed through the net. Otherwise the counts, though sketchy, are readily followed. They show clearly that the decline or lack of increase in chlorophyll values in bottles exposed to intense light was not associated with corresponding changes in population size. In fact, there were instances of population growth in the face of chlorophyll decline, as illustrated by the counts for Experiment 8.

It is possible that the chlorophyll histories observed could be due to differential species development under these experimental conditions. However, in spite of the lack of identification, the characteristic types could be followed, and in doing so the writer is of the impression that the same types were generally in abundance at both beginning and end of each experiment.

Considered together, the counts and chlorophyll values indicate that at high light intensities, such as those which occur at and near the surface, there may be at times a rapid decrease in the chlorophyll content of individual plankters. Since these light intensities must exceed the average light to which the plankters are exposed as they mix through the water column, this chlorophyll loss is probably not unlike that which many terrestrial plants undergo when subjected to light in excess of their normal range. Also, it appears that there are wide variations in these chlorophyll-light relationships, some of which are probably associated with the physiological condition of the plankters, some with species differences.

The observations on dark bottles are not readily explained. It is not uncommon to observe short term increases in chlorophyll in the dark, and such might tend to offset losses due to destructive processes. One might expect, however, that grazing, respiration and

TABLE IV. Cells $\times 10^6$/L in the Phytoplankton Populations of the Experiments Reported. Letter and Number in Parenthesis Give Counts on *Nitzchia* spp. (N), *Rhizosolenia* spp. (R), and *Chaetoceros* spp. (C).

		Samples in containers at termination of experiments					
		Light			*Brown*		*Dark*
*Exp. No.**	*Initial water*	*Surface*	*1 meter*	*2 meters*	*Surface*	*1 meter*	
1 sea water	3.4 (N 0.1)	11.6 (N 1.1)	—	—	—	—	—
1 filtered water	6.3 (N 0.4)	6.1 (N 0.3)	—	—	—	—	—
2 in Harbor	7.7 (N 0.3)	6.6 (N 0.4)	—	—	—	—	—
2 in tank	7.7 (N 0.3)	12.8 (N 0.7)	—	—	—	—	†11.4 (N 0.1)
3	6.8 (N 1.8)	6.0 (N 1.9)	—	—	—	—	—
	(R 0.016)	(R .015)	—	—	—	—	—
4	3.0 (R 0.035)	2.3 (R .012)	—	—	—	—	2.8 (R .003)
5	1.4 (N 0.1)	2.8 (N 0.2)	—	—	—	—	1.9 (N 0.2)
6	3.6 (N 0.4)	—	3.0 (N 0.5)	—	—	—	2.0 (N 0.2)
7	0.7	1.6	1.1	0.5	—	—	1.1
8	1.6 (C 0.2)	2.2 (C 0.3)	2.0 (C 0.2)	2.3 (C 0.2)	—	2.1 (C 0.3)	—
9	4.6 (N 1.0)	6.6 (N 2.7)	4.2 (N 0.7)	6.6 (N 0.8)	7.0 (N 0.4)	6.3 (N 0.6)	—

* Experiments numbered as in Appendix I.
† Sample at termination missing. This sample was taken 12 hrs. earlier.

decay would result in noticeable chlorophyll declines in the longer experiments. Possibly the following factors are important in explaining these sustained chlorophyll values: (1) Grazing may be inhibited in bottled samples, particularly when the water is not sufficiently agitated to keep the phytoplankton in suspension. (2) Many of the physiological and dynamic processes of the pelagic association may be slowed down considerably in a dark container. Possibly chlorophyll quantities remained little changed in the dark even though the population was changing due to multiplication, consumption, death, decay, etc. Edmondson and Edmondson (1947) offered such an explanation for what would otherwise appear to be discrepancies in their growth experiments.

Some results of earlier work are more readily understood in terms of the observations reported here. For example, Riley (1941a) compared the oxygen and chlorophyll histories in light and dark bottles suspended one meter below the surface. In some instances, when the oxygen indicated considerable synthesis in light bottles, the chlorophyll values dropped below those of the dark containers. Chlorophyll stability in dark bottles and decline in light ones readily account for this.

Jenkin (1937), Riley, et al. (1949), and Steeman Nielsen (1952), observed that photosynthesis is optimal somewhat below the surface. Kallio (1953) indicated a chloroplast breakdown in desmids under continued high illumination. Such relationships and the chlorophyll decline at high light intensities suggest that surface conditions may be not only suboptimal but even deleterious to some populations.

Though it is obvious that the chlorophyll history of a bottled sample cannot be used to indicate growth and productivity, the observations reported here do not discredit the use of chlorophyll values as an index of phytoplankton abundance. Of the variations that might occur in the relation between chlorophyll values and phytoplankton mass, this depth and light effect should be kept in mind; however, mixing processes in nature tend to minimize variability due to light alone.

REFERENCES

Conover, S. M.
1955. Oceanography of Long Island Sound, 1952–1954. IV. Phytoplankton. Bull. Bingham Ocean. Coll., *15:* 62–112.

Edmondson, W. T. and Yvette H. Edmondson
1947. Measurements of production in fertilized salt-water. J. Mar. Res., *6* (3): 228–246.

Graham, H. W.
1943. Chlorophyll-content of marine plankton. J. Mar. Res., *5*(2): 153–160.

Jenkin, Penelope M.
1937. Oxygen production by the diatom *Coscinosdiscus exentricus* Ehr. in relation to submarine illumination in the English channel. J. Mar. biol. Ass. U. K., *22:* 301–342.
Kallio, Paavo
1953. The effect of continued illumination on the desmids. Arch. Zool. Bot. Fenn. "Vanamo," *8* (1): 58–74.
Ketchum, B. H.
1954. Relation between circulation and planktonic populations in estuaries. Ecology, *35* (1): 191–200.
Motoda, Sigeru
1940. Comparison of the conditions of water in the bay, lagoon, and open sea in Palao. Stud. Palao Trop. biol. Sta., *2* (1): 41–48.
Odum, H. T.
1953. Dissolved phosphorous in Florida waters. Rep. Fla. Geol. Survey, No. 9 (1): 1–40.
Rawson, D. S.
1953. The standing crop of net plankton in lakes. J. Fish. Res. Bd. Canada, *10* (5): 224–237.
Richards, F. A. with T. G. Thompson
1952. The estimation and characterization of plankton populations by pigment analyses. II. A spectrophotometric method for the estimation of plankton pigments. J. Mar. Res., *11* (2): 156–172.
Riley, G. A.
1938. Plankton studies. I. A preliminary investigation of the plankton of the Tortugas region. J. Mar. Res., *1* (4): 335–352.
1939. Plankton studies. II. The western North Atlantic, May–June, 1939. J. Mar. Res., *2* (2): 145–162.
1940. Limnological studies in Connecticut. Part III. The plankton of Linsley Pond. Ecol. Monogr., *10:* 279–306.
1941a. Plankton studies. III. Long Island Sound. Bull. Bingham oceanogr. Coll., *7* (3): 1–93.
1941b. Plankton studies. IV. Georges Bank. Bull. Bingham oceanogr. Coll., *7* (4): 1–73.
Riley, G. A., Henry Stommel and D. F. Bumpus
1949. Quantitative ecology of the plankton of the western North Atlantic. Bull. Bingham oceanog. Coll., *12* (3): 1–169.
Steeman Nielsen, E.
1952. The use of radio-active carbon (C^{14}) for measuring organic production in the sea. J. Cons. int. Explor. Mer, *18* (2): 117–140.
Wohlschlag, D. E. and A. D. Hasler
1951. Some quantitative aspects of algal growth in Lake Mendota. Ecology, *32* (4): 581–593.

APPENDIX I

Procedures and Observed Chlorophyll *a* Changes in Samples of Natural Phytoplankton Populations Held in Jugs or Flasks

Determinations are on 90% acetone extracts of phytoplankton concentrated with a Foerst centrifuge for experiments 1–4 and with AA millipore filters for experiments 5–9. Readings are listed at the nearest 6-hour interval. Each reading represents a determination on a different container. Values are in milligrams of chlorophyll *a* per cubic meter.

Surface water from the upper end of Alligator Harbor was used for all experimental set-ups. Determinations for this water are listed under 0 hours exposure for each experiment. Dark bottle determinations are listed without depth notations; these would be of no consequence since the water was without vertical temperature differences.

The light and dark bottles consisted of either a one gallon jug or a two liter Erlenmeyer flask of clear glass; the dark bottle was rendered opaque with outer coats of paint or cloth wrappings. The brown bottles consisted of one gallon jugs of brown glass.

Experiment 1. VII/16/53 @ 0700 h. to VII/17/53 @ 1900 h.

Light bottles, some with unstrained surface water, others with surface water strained through No. 10 bolting cloth to remove bulk of larger zooplankters (a relatively small proportion of the phytoplankton was also removed from straining).

All bottles were floated in Alligator Harbor.

VII/16 @ 0700: surf. temp. 28.2°C, sal. 30.6‰. Slightly cloudy the first day; clear the second day. No appreciable change in water temperature during experiment.

Exposure in h.	*Unstrained*	*Strained*
0	4.9	4.4
12 (1 day)	7.1	4.4
24 (1 day and 1 night)	6.2	4.9
36 (2 days and 1 night)	6.5	6.8

Experiment 2. VII/30/53 @ 0700 h. to VIII/1/53 @ 0700 h.

Some light bottles were floated in Alligator Harbor and others were held in the lab tank under two new 40-watt daylight fluorescent bulbs mounted about 8 inches above the bottles. Dark bottles were also kept in the same lab tank.

VII/30 @ 0700: surf. temp. 29.5°C (temp. in tank 28.0°C), sal. 31.4 ‰. Sky quite clear for duration. Water temperature showed little change either in tank or in Harbor.

Exposure in h.	*Light bottles in Harbor*	*—Bottles in tank—* *Light*	*Dark*
0	5.4, 5.2, 5.4	5.4, 5.2, 5.4	5.4, 5.2, 5.4
12 (1 day)	5.2, 3.9, 5.0	7.3	5.6
24 (1 day and 1 night)	3.3, 5.5, 4.9	6.8	4.7
36 (2 days and 1 night)	3.5, 3.9, 3.5	5.8	5.4
48 (2 days and 2 nights)	3.5, 3.5, 3.6	6.0	5.2

Experiment 3. X/30/53 @ 1000 h. to XI/1/53 @ 1600 h.

Light and dark bottles floated in an outdoor tank and tied to a rig that provided constant shaking.

X/30/53 @ 1000: surf. temp. 15.7°C (temp. in tank 15.7°C), sal. 30.1‰. Sky remained quite clear for duration. Water temperature in tank tended to rise slightly, the maximum measured being 18.0°C.

Exposure in h.	*Light bottles*	*Dark bottles*
0	12.5, 11.2, 12.1	12.5, 11.2, 12.1
6 (part of 1 day)	11.4, 11.6	11.4, 11.6
30 (2 days and 1 night)	6.9, 7.6, 7.6	No samples
54 (3 days and 2 nights)	4.8, 5.3, 5.6	No samples

Experiment 4. XI/4/53 @ 1130 h. to XI/10/53 @ 1130 h.

Same set-up as in Experiment 3.

XI/4/53 @ 1130: surf. temp. 20.0°C (temp. in tank 21.5°C), sal. 31.1 ‰. Sky tended to be cloudy on four of the six days. Water temperature in tank dropped, the lowest reading being 15.7°C.

Exposure in h.	*Light bottles*	*Dark bottles*
0	4.5, 4.5, 4.5	4.5, 4.5, 4.5
48 (2 days and 2 nights)	3.0, 4.1, 3.6	4.7, 4.5, 4.7
144 (6 days and 6 nights)	1.5, 1.3, 1.8	4.3, 4.3, 3.9

Experiment 5. XI/12/53 @ 1200 h. to XI/20/53 @ 1000 h.

Light and dark bottles were placed in outdoor tank, one of each being floated at the surface and one of each being held one meter below surface.

XI/12/53 @1200: surf. temp. 14.0°C (temp. in tank at 1600, 15.8°C), sal. 30.0 ‰. Water in tank was so turbid that bottles could not be seen at one meter. Sky was quite clear for duration. Temperature in tank rose as high as 20.0°C.

	Light bottles		*Dark bottles*
Exposure in h.	*Surface*	*One meter*	
0	1.5, 1.9	1.5, 1.9	1.5, 1.9
192 (8 days and 8 nights)	3.8	4.4	1.6, 2.1

Experiment 6. XI/24/53 @ 0800 h. to XI/29/53 @ 1100 h.

Light and dark bottles floated at surface and at one meter below; of the clear bottles only those at one meter survived.

XI/24/53 @ 0800: surf. temp. 18.5°C, sal. 30.6 ‰, secchi disc barely visible on bottom, which was just over one meter. Sky generally clear for duration. Water temp. dropped as low as 13.7°C. Water remained turbid till the last day or so.

Exposure in h.	*Light bottles, one meter*	*Dark bottles*
0	4.4, 4.8	4.4, 4.8
48 (2 days and 2 nights)	5.1	3.6, 3.5
120 (5 days and 5 nights)	4.4	3.6

Experiment 7. XII/28/53 @ 1200 h. to I/1/54 @ 1300 h.

Light bottles held in Harbor at surface and at one and two meters, with dark bottles held at depths in between.

XII/28/53 @ 1200: surf. temp. 10.6°C, sal. 28.6 ‰, secchi disc visible on bottom at 4 meters. Sky was hazy till third day, then remained clear. Water remained relatively clear and increased in temperature to 14.0°C.

	Light bottles			*Dark bottles*
Exposure in h.	*Surface*	*1m*	*2m*	
0	0.7	0.7	0.7	0.7
	0.7	0.7	0.7	0.7
	0.7	0.7	0.7	0.7
24 (1 day and 1 night)	0.7	0.7	0.9	0.7, 0.7
48 (2 days and 2 nights)	1.1	1.1	1.1	0.9, 0.7
72 (3 days and 3 nights)	1.2	1.1	1.2	0.7, 0.8
96 (4 days and 4 nights)	1.1	1.1	1.0	0.8, 0.7

Experiment 8. II/13/54 @ 1130 h. to II/17/54 @ 1000 h.

Light bottles held at surface and at one and two meters below. Brown bottles held one meter below surface.

II/13/54 @ 1130: surf. temp. 13.4°C, sal. 30.9 ‰, secchi disc disappeared at 2.25 m. Sky generally clear for duration. Water temp. rose to 18.0°C; transparency did not change greatly.

	Light bottles			*Brown bottles*
Exposure in h.	*Surface*	*1m*	*2m*	*1m*
0	1.8	1.8	1.8	1.8
	1.9	1.9	1.9	1.9
	2.0	2.0	2.0	2.0
24 (1 day and 1 night)	1.6	1.5	1.8	2.5
48 (2 days and 2 nights)	1.2	2.0	1.9	2.8
72 (3 days and 3 nights)	1.1	1.6	2.3	3.1
96 (4 days and 4 nights)	1.3	1.6	2.9	2.7

A bottle with formalin added and held at the surface showed no chlorophyll when tested after 24 hours exposure.

Experiment 9. IV/14/54 @ 1200 h. to IV/16/54 @ 1200 h.

Same set-up as Experiment 8, but with brown bottles at surface as well as at one meter.

IV/14/54 @ 1200: surf. temp. 26.3°C, sal. 33.0 ‰, secchi disc disappeared at one meter. Sky clear for duration. Water temperature changed little and the transparency changed but little till the end, when it decreased.

	Light bottles			*Brown bottles*	
Exposure in h.	*Surface*	*1m*	*2m*	*Surface*	*1m*
0	4.5	4.5	4.5	4.5	4.5
	4.4	4.4	4.4	4.4	4.4
	4.6	4.6	4.6	4.6	4.6
24 (1 day and 1 night)	2.7	4.7	6.2	4.9	7.1
48 (2 days and 2 nights)	6.1	6.1	6.5	6.0	7.3

THE DYNAMIC STRUCTURE OF A COASTAL PLAIN ESTUARY[1]

By

D. W. PRITCHARD

Chesapeake Bay Institute, The Johns Hopkins University

ABSTRACT

The time mean equations of motion applicable to a coastal plain estuary are developed and discussed. Time series observations of temperature, salinity, and current velocity from two sections in the James River are utilized to obtain the mean lateral and longitudinal components of the relative pressure field, the Coriolis force, and the field accelerations. Using appropriate boundary conditions, the equations of motion are then solved for the nonadvective or eddy flux of momentum. As a consequence of this solution, the depths of the pressure surfaces which are level relative to the longitudinal and lateral coordinates are found. The variations with depth of the longitudinal and lateral components of the pressure force are discussed, and the relative importance of the various terms in the equations of motion are evaluated.

INTRODUCTION

Notable advances in our understanding of the dynamics of estuarine circulation have been made by Stommel (1951) and Cameron (1951). It has not been possible thus far to solve the general hydrodynamic equations completely, hence it was necessary that these investigators make certain assumptions as to the relative importance of the various processes governing the dynamic structure of the estuary being investigated. Both Stommel and Cameron treated the relatively deep fiord estuary. Analysis of chemical and physical observations in Chesapeake Bay and its tributary estuaries shows that the existing treatments of the dynamics and mixing do not adequately describe conditions in this particular type of estuary.

In order to evaluate the relative importance of the various processes involved in controlling the dynamic structure in an estuary, extensive field observations have been combined with certain basic hydrodynamic equations. The procedure employed involves the treatment of the hydrodynamic equations in such a manner that unknown terms can be determined from observations of the mean distribution of tem-

[1] Contribution No. 24 from the Chesapeake Bay Institute. This work was supported by the Office of Naval Research, the State of Maryland (Department of Research and Education), and the Commonwealth of Virginia (Virginia Fisheries Laboratory).

perature, salinity, and current velocity. The purpose of such an investigation is to lay a firm foundation for a more complete attack on the dynamics of estuarine circulation.

Extensive field studies of the distribution of chemical and physical properties have been under way in Chesapeake Bay and its tributary estuaries for the last several years. These investigations reveal that the general features of the salinity distribution and of the circulation pattern are similar among the several major estuaries which comprise the Chesapeake Bay system. During the summer of 1950 an intensive investigation was undertaken in the James River estuary; a summary discussion of the general features of salinity and current observations in the Chesapeake Bay system, with particular emphasis on the detailed study of the James River, has been reported (Pritchard, 1952).

Data collected from the James River estuary were employed in a detailed analysis of the salt balance in a coastal plain estuary. This study (Pritchard, 1954) showed that when time mean values of the various parameters over several tidal cycles are considered, the two most important terms involved in maintaining the salinity distribution are the mean horizontal advection and the nonadvective vertical flux of salt; the nonadvective horizontal flux of salt was found to be small. Use will be made of this latter fact in the present analysis.

We will consider a left-handed coordinate system with its origin in fresh water at the head of the estuary. The coordinate axes will be designated as x_i, the x_1-axis being directed longitudinally along the central axis of the estuary toward the ocean. The x_2-axis is directed vertically downward, the x_3-axis laterally toward the right-hand shore of the estuary.

THE LONGITUDINAL COMPONENT OF THE EQUATION OF MOTION

The purpose of this study is to investigate the relative magnitudes of the various terms which comprise the equation of motion as applied to a coastal plain estuary. We will first consider the x_1-component, which, for instantaneous values of the various parameters, may be written as

$$(1)\quad \frac{\partial v_1}{\partial t} + v_1\frac{\partial v_1}{\partial x_1} + v_2\frac{\partial v_1}{\partial x_2} + v_3\frac{\partial v_1}{\partial x_3} = -\alpha\,\partial p/\partial x_1 - f v_3 + \alpha\left(\frac{\partial P_{11}'}{\partial x_1} + \frac{\partial P_{12}'}{\partial x_2} + \frac{\partial P_{13}'}{\partial x_3}\right).$$

Here f designates the Coriolis parameter, p the hydrostatic pressure, and P_{ij}' the appropriate components of the molecular stress related

to the motion. It is assumed here that the Coriolis term related to the vertical motion is sufficiently small to be neglected.

THE MEAN LONGITUDINAL COMPONENT OF THE EQUATION OF MOTION

The instantaneous velocity v_i may be considered to be composed of three terms:

(a) A time mean velocity $\bar{v}_i$, obtained by averaging over one or more tidal cycles. This mean velocity has components along the longitudinal (x_1) and vertical (x_2) axis, but the lateral component is assumed to be negligible.

(b) An oscillatory tidal velocity U_1 which is directed up and down the longitudinal axis of the estuary. This term is assumed to be a function of x_1 only and to vary according to the simple harmonic function $U_1 = U_0 \cos \varphi$, where U_0 is the amplitude of the tidal current and φ represents the sum of an angular time argument of tidal period plus a phase angle. Both the phase angle φ and the amplitude U_0 may be functions of the longitudinal coordinate.

(c) A velocity deviation v_i', which results from those turbulent fluctuations which have a time scale smaller than the period employed in the averaging process. The period of averaging used here is one tidal cycle.

The three components of the instantaneous velocity are thus given by

$$(2) \qquad v_1 = \bar{v}_1 + U_1 + v_1' ; \qquad v_2 = \bar{v}_2 + v_2' ; \qquad v_3 = v_3' .$$

Our next step is to introduce the velocity terms from eq. (2) into eq. (1) and to take the time mean over one or more tidal cycles of this latter equation. Before doing this, however, we note that:

(a) Since $U_1 = U_0 \cos \varphi$, a time mean over one or more tidal cycles results in $\overline{U_1} = 0$. Hence any of the cross products involving $\overline{U_1}$ will not appear in the resulting mean equation of motion.

(b) A field acceleration term will result from $\overline{U_1^2}$, since the mean value of $U_0^2 \cos^2 \varphi$ over a tidal cycle is $\frac{1}{2} U_0^2$.

(c) There is no reason to expect a correlation between the velocity deviations v_1', v_2', or v_3' on the one hand and the tidal component U_1 on the other, hence terms of the type $U_1 v_i'$ will not appear in the mean equation of motion. (There may be a correlation between the root mean square velocity deviations and U_1, since the magnitude of the turbulent velocities may be directly affected by the magnitude of the tidal velocities.)

(d) The mean value of the x_1-component of the pressure force $-<\alpha\frac{\partial p}{\partial x_1}>$ may be determined from the distribution of temperature and salinity, providing the depth of a level pressure surface is known. If we designate $-<\alpha\frac{\partial p}{\partial x_1}>_0$ as the x_1-component of the pressure force at any depth x_2 relative to the x_1-component of the pressure force at the surface, and if the actual longitudinal component of the pressure force at the surface is designated as b_0, then $-<\alpha\frac{\partial p}{\partial x_1}>$ $= -<\alpha\frac{\partial p}{\partial x_1}>_0 + b_0$. Note that $-<\alpha\,\partial p/\partial x_1>_0$ can be determined from the distribution of temperature and salinity, while b_0 remains as yet an undetermined constant with respect to the vertical.

(e) Because the vertical gradient of the horizontal mean velocity is much larger than other components of the velocity gradient, the only molecular stress term which will be of any importance in the mean equation is $<P_{12}'>$. This term can be expressed by $\mu\frac{\partial \bar{v}_1}{\partial x_2}$, where μ is the molecular viscosity; hence it is seen that $<P_{12}'>$ is of significant size only near surface and near bottom, where the mean velocity gradient may approach significant magnitudes. Both $<P_{12}'>$ and $<v_2'v_1'>$ represent momentum transports due to velocity deviations, one on a molecular scale, the other on a macro-scale. In what follows, $<P_{12}'>$ will be included with $<v_2'v_1'>$, and at the boundaries (surface and bottom) $<v_2'v_1'>$ will take on the appropriate value representing the total flux of momentum across the boundaries. Within the interior of the fluid, only the so-called eddy processes need be considered.

Under these conditions, the time mean of eq. (1) over one or more tidal cycles is given for mean steady state by

$$(3)\quad \bar{v}_1\frac{\partial \bar{v}_1}{\partial x_1} + \bar{v}_2\frac{\partial \bar{v}_1}{\partial x_2} + U_0\frac{\partial U_0}{\partial x_1} = -<\alpha\frac{\partial p}{\partial x_1}>_0 + b_0 - \frac{\partial}{\partial x_1}<v_1'v_1'> - \frac{\partial}{\partial x_2}<v_2'v_1'> - \frac{\partial}{\partial x_3}<v_3'v_1'>.$$

THE LATERAL COMPONENTS OF THE EQUATION OF MOTION

The x_3 component of the equation of motion, for instantaneous values of the various parameters, may be expressed as

$$(4)\quad \frac{\partial v_3}{\partial t} + v_1\frac{\partial v_3}{\partial x_1} + v_2\frac{\partial v_3}{\partial x_2} + v_3\frac{\partial v_3}{\partial x_3} = -\alpha\frac{\partial p}{\partial x_3} + f v_1 + \alpha\left(\frac{\partial P_{31}'}{\partial x_1} + \frac{\partial P_{32}'}{\partial x_2} + \frac{\partial P_{33}'}{\partial x_3}\right).$$

Before taking the time mean of this equation we note that

(a) The mean values of the molecular stress terms at the longitudinal axis of the estuary are zero, since the assumption is made that, along the longitudinal axis, $\bar{v}_3 = \dfrac{\partial \bar{v}_2}{\partial x_3} = \dfrac{\partial \bar{v}_1}{\partial x_3} = 0$.

(b) Since $\bar{v}_3 = 0$, all the mean field acceleration terms vanish.

(c) As in the longitudinal component, the mean value of the x_3-component of the pressure force may be expressed as the x_3-component of the pressure force relative to that at the surface, which can be computed from the distribution of temperature and salinity, plus a constant with respect to the vertical, representing the actual x_3-component of the pressure force at the surface.

Under mean steady state conditions, the time mean of eq. (4) over one or more tidal cycles then becomes

$$(5)\quad 0 = -\langle\alpha\frac{\partial p}{\partial x_3}\rangle_0 + b_0' + f\bar{v}_1 - \frac{\partial}{\partial x_1}\langle v_1'v_3'\rangle - \frac{\partial}{\partial x_2}\langle v_2'v_3'\rangle - \frac{\partial}{\partial x_3}\langle v_3'v_3'\rangle.$$

THE MEAN EQUATIONS OF MOTION AS APPLIED TO THE JAMES RIVER ESTUARY

In a study of the salt balance in the James River estuary (Pritchard 1954), the horizontal component of the turbulent flux of salt was shown to be negligible compared to the horizontal advection and the vertical component of the turbulent flux of salt. If we assume by analogy that the horizontal component of the turbulent flux of momentum is also negligible compared to the other terms in the equation of motion, then the terms $\dfrac{\partial}{\partial x_1}\langle v_1'v_1'\rangle$, $\dfrac{\partial}{\partial x_1}\langle v_1'v_3'\rangle$, $\dfrac{\partial}{\partial x_3}\langle v_3'v_3'\rangle$,

and $\frac{\partial}{\partial x_3} <v_3'v_1'>$ will drop from eqs. (3) and (5). Under these conditions we have

$$(6) \quad \bar{v}_1 \frac{\partial \bar{v}_1}{\partial x_1} + \bar{v}_2 \frac{\partial \bar{v}_1}{\partial x_2} + U_0 \frac{\partial U_0}{\partial x_1} = - <\alpha \frac{\partial p}{\partial x_1}>_0 + b_0 - \frac{\partial}{\partial x_2} <v_2'v_1'>,$$

and

$$(7) \quad 0 = - <\alpha \frac{\partial p}{\partial x_3}>_0 + b_0' + f \bar{v}_1 - \frac{\partial}{\partial x_2} <v_2'v_3'>.$$

Solving (6) for $< v_2'v_1'>$ and (7) for $<v_2'v_3'>$, we have

$$(8) \quad <v_2'v_1'> = - \left[\int \left(\bar{v}_1 \frac{\partial \bar{v}_1}{\partial x_1} + \bar{v}_2 \frac{\partial \bar{v}_1}{\partial x_2} + U_0 \frac{\partial U_0}{\partial x_1} + <\alpha \frac{\partial p}{\partial x_1}>_0 - b_0 \right) dx_2 + C_1 \right],$$

and

$$(9) \quad <v_2'v_3'> = \left[\int \left(f \bar{v}_1 - <\alpha \frac{\partial p}{\partial x_3}>_0 + b_0' \right) dx_2 + C_2 \right].$$

Assume for the moment that velocity data are available in sufficient detail to evaluate both the mean acceleration terms and the term involving the amplitude of the tidal velocity, $U_0 \frac{\partial U_0}{\partial x_1}$. From temperature and salinity data the relative pressure field could also be determined, leaving an unknown constant representing the absolute mean pressure force at the surface as an unknown quantity in each equation. There is also a second unknown constant, the constant of integration, in each equation. These constants can be evaluated providing the two boundary values for $< v_2'v_1'>$ and $<v_2'v_3'>$ are known.

At the surface and at the bottom, $\rho <v_2'v_1'>$ and $\rho <v_2'v_3'>$ will be equal to the net flux of momentum across these boundaries. During the period of study, the vector mean of the wind was close to zero, hence there was no appreciable momentum flux across the surface. The net longitudinal velocity at the bottom would lead to a net momentum flux across this interface directed along the x_1-axis. Hence $\rho <v_2'v_1'>$ would be equal to this momentum flux, or stress, at the bottom. Our best estimate of the boundary values of $<v_2'v_3'>$ is that it equals zero at the bottom as well as at the surface.

In a recent paper Lesser (1951) has shown that velocity measurements near the bottom in the open ocean satisfy the Prandtl-von

Karman boundary layer theory for a "rough" boundary. If z represents the vertical distance up from the bottom and v the magnitude of the mean horizontal velocity at the point z in the boundary layer, then the stress at the boundary is given by

$$\tau_h = \rho K_0^2 V_*^2 \Big/ \left[\ln \frac{z + z_0}{z_0}\right]^2, \tag{10}$$

where k_0 is von Karman's constant and z_0 is the roughness parameter.

According to Lesser's analysis, the boundary layer within which the logarithmic velocity distribution characteristic of the Prandtl-von Karman boundary layer theory occurs is approximately one meter thick. Lesser has determined values of z_0 for three different types of bottom sediment. For a mud bottom the value of z_0, based on Lesser's measurements, was 0.02 cm, for a sand-gravel bottom 0.13 cm, and for a sand-mud bottom 0.16 cm. Lesser attributes the high value for the sand-mud bottom to the possible presence of ripples.

Taking $z_0 = 0.02$ cm as representative of the character of the mud bottom found in the central channel of the James River, it is possible to evaluate the boundary value of $< v_2' v_1' >$ from a single mean velocity measurement within the boundary layer, using eq. (10), since at the bottom $< v_2' v_1' > = \alpha \tau_h$.

Data from two sections in the James River have been employed in the evaluation of eqs. (8) and (9). Typical plots of $< v_2' v_1' >$ and of $< v_2' v_3' >$ vs. depth are given in Fig. 1. The determination of the constant b_0 in each equation also provides for evaluation of the depth of the level pressure surface, and, in fact, of the actual distribution of the pressure field.

These determinations reveal that a pressure surface which is level in regard to the longitudinal coordinate exists at near mid-depth. Above this depth, at which $\partial \bar{p}/\partial x_1 = 0$, the pressure surfaces slope downward from the river toward the sea. Below this reference depth the pressure surfaces slope in the opposite direction.

Based on an evaluation of eq. (9) for the James River estuary, there is also some mid-depth where $\partial \bar{p}/\partial x_3 = 0$, but it is not necessarily the same reference depth as that found from the longitudinal equation. Above this reference depth the pressure surfaces slope downward from the right side of the estuary (facing the mouth) to the left side. Below this reference depth the lateral slope is in the opposite direction.

In the James River estuary there is a net horizontal velocity directed down-estuary in an upper layer and up-estuary in a lower

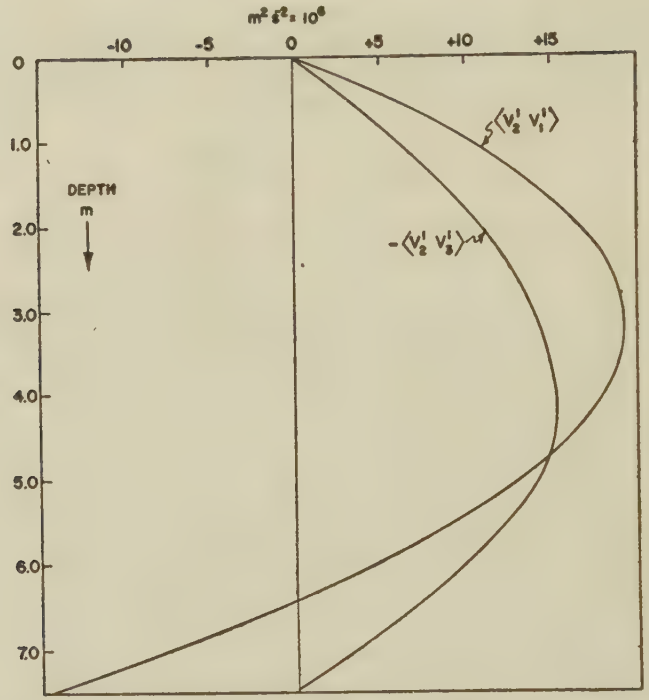

Figure 1. A typical variation of $\langle v_3' v_1' \rangle$ and of $-\langle v_2' v_3' \rangle$ vs. depth for the James River estuary.

layer. At some mid-depth there is a surface of no net motion. The pressure surface which is level in the lateral direction occurs at a depth close to but slightly below the depth of no net motion. The depth of the pressure surface which is level with respect to the longitudinal coordinate may be above or below the depth of no net motion, the departure depending primarily on the sign and magnitude of the term $U_0 \dfrac{\partial U_0}{\partial x_1}$. Table I gives the observed depths of no net motion, as well as computed depths at which $\partial \bar{p}/\partial x_1 = 0$ and $\partial \bar{p}/\partial x_3 = 0$.

These computations also allow a determination of the relative importance of the various terms which comprise the equation of motion. In the case of the longitudinal component, the pressure force is primarily balanced by the eddy frictional term $\dfrac{\partial}{\partial x_2} \langle v_2' v_1' \rangle$. However, a significant portion of the pressure force may be balanced by the

TABLE I.

Station	Period	Bottom Depth	$\bar{v}_1$	Depth (m) of Zero value for: $<\alpha \frac{\partial p}{\partial x_1}>$	$<\alpha \frac{\partial p}{\partial x_2}>$	$\left(<\alpha \frac{\partial p}{\partial x_1}> + U_0 \frac{\partial U_0}{\partial x_1}\right)$
J-11	I	7.0	2.5	4.6	—	3.0
	II	7.0	2.5	5.4	—	2.7
	III	7.0	2.6	5.1	—	3.1
J-17	I	7.5	2.9	4.1	3.6	3.2
	II	7.5	2.9	3.9	3.3	3.0
	III	7.5	3.0	3.9	—	3.1
	IV	7.5	3.0	—	3.0	—

field change in the amplitude of the tidal velocity, $U_0 \frac{\partial U_0}{\partial x_1}$. When this latter term is small, the depth at which $\frac{\partial \bar{p}}{\partial x_1} = 0$ is nearly the same as the depth of no net motion. When the tidal velocity amplitude increases downstream, then the depth at which $\frac{\partial \bar{p}}{\partial x_1} = 0$ is greater than the depth of no net motion. If the tidal velocity amplitude decreases downstream, then the depth at which $\frac{\partial \bar{p}}{\partial x_1} = 0$ is less than the depth of no net motion. The field acceleration terms related to the mean motion are relatively small.

In the lateral component of the equation of motion, the Coriolis force resulting from the net horizontal motion is balanced primarily by the lateral pressure force. Of secondary importance is the eddy

TABLE II. Variation with Depth of the Terms in the Longitudinal Component of the Mean Equation of Motion—For a Typical Section in the James River Expressed in $ms^{-2} \times 10^6$

Depth (meters)	$\bar{v}_1 \frac{\partial \bar{v}_1}{\partial x_1}$	$\bar{v}_2 \frac{\partial \bar{v}_1}{\partial x_2}$	$U_0 \frac{\partial U_0}{\partial x_1}$	$-<\alpha \frac{\partial p}{\partial x_1}>$	$\frac{\partial}{\partial x_2}<v_2' v_1'>$
0	0.03	0.01	2.97	14.30	11.29
1	0.12	0.09	2.97	10.56	7.38
2	0.08	0.28	2.97	6.83	3.50
3	0.01	0.42	2.97	3.10	−0.30
4	0.09	0.20	2.97	−0.64	−3.90
5	0.11	0.04	2.97	−4.38	−7.50
6	−0.04	0.01	2.97	−8.09	−11.03
7	−0.04	0.02	2.97	−11.77	−14.72

frictional term, $\frac{\partial}{\partial x_2} <v_2'v_3'>$. The depth at which $\partial\bar{p}/\partial x_3 = 0$ is nearly the same as the depth of no net motion.

Tables II and III give the variation with depth of the various terms in the longitudinal and lateral components of the equation of motion for a typical section in the James River.

TABLE III. Variation with Depth of the Terms in the Lateral Component of the Mean Equation of Motion—For a Typical Section in the James River Expressed in $ms^{-2} \times 10^6$

Depth (meters)	$-<\alpha\frac{\partial p}{\partial x_3}>$	$f\bar{v}_1$	$\frac{\partial}{\partial x_2}<v_2'v_3'>$
0	−16.49	10.18	−6.31
1	−11.64	6.23	−5.41
2	−6.26	3.07	−3.19
3	−0.53	−1.23	−1.76
4	+5.08	−4.92	+0.16
5	+9.73	−6.15	+3.58
6	+12.63	−6.67	+5.96
7	+13.29	−5.97	+7.32

REFERENCES

Cameron, W. M.

1951. On the dynamics of inlet circulations. Doctoral Dissertation, Scripps Institution of Oceanography, University of California.

Lesser, R. M.

1951. Some observations of the velocity profile near the sea floor. Trans. Amer. geophys. Un., *32* (2): 207–211.

Pritchard, D. W.

1952. Salinity distribution and circulation in The Chesapeake Bay Estuarine system. J. Mar. Res., *11* (2): 106–123.

1954. A study of the salt balance in a coastal plain estuary. J. Mar. Res., *13* (1): 133–144.

Stommel, Henry

1951. Recent developments in the study of tidal estuaries. Technical Report, Woods Hole Oceanographic Institution, Ref. No. 51–33.

THE ACTION OF VARIABLE WIND STRESSES ON A STRATIFIED OCEAN[1, 2]

By

G. VERONIS and HENRY STOMMEL

Institute for Advanced Study, Princeton, N. J.

ABSTRACT

The forced response of a horizontally infinite ocean on a rotating earth to a transient wind system is investigated. In an equilibrium state, the ocean consists of two homogeneous layers of fluid of finite depth, the fluid in the lower layer being slightly denser than that in the upper. The wind system is periodic in space, and its time-dependence is periodic or is given by a step function.

Little energy goes into the inertio-gravity waves for winds that blow longer than a half pendulum day; most of the energy appears as geostrophically balanced Rossby (planetary) waves. Wind systems with periods from a day to a year excite motions which are in part barotropic and in part baroclinic. Winds of long period (100 years or more) excite the (internal) baroclinic Rossby mode, in which the currents are confined to the upper layer. The applicability and oceanographic implications of the model are discussed quantitatively.

1. INTRODUCTION

This paper treats the response of a stratified ocean to time-dependent wind stress systems of various dimensions. The model of the ocean is infinite horizontally, but the wind systems are of finite dimensions.

We anticipate that the density stratification of the ocean will play an important role in the response of ocean to wind. To account for the effect of density variation, a highly idealized structure is introduced, viz., a two-layer ocean with each layer homogeneous in density. This structure is supposed to correspond roughly to the two masses of water above and below the main thermocline in the real ocean.

In accordance with the theoretical framework for the dynamics of

[1] Work was sponsored by the Office of Naval Research under Contract No. N-6-ORI-139, Task Order I. Reproduction in whole or in part is permitted for any purpose of the U. S. government.

[2] Contribution No. 859 of the Woods Hole Oceanographic Institution.

Note added in proof. In a recent publication (Veronis, 1956) it was pointed out that this article in the *Journal of Marine Research* contained a wrong conclusion. The mistake referred to has been corrected in this article subsequent to publication of the Veronis (1956) article in *Deep Sea Research.*

currents in central oceanic areas as given by Sverdrup (1947) and Reid (1948), we will neglect horizontal friction due to large scale lateral turbulent processes.

Cases where the effects of coastal boundaries are involved are not considered because of the complexity of the general problem. It is not generally possible therefore to apply the results of this paper to the real ocean in an enclosed basin in the same satisfactory way that theories of the mean steady-state circulation (e. g. Munk, 1950) have been applied. Application of theoretical results must be limited to types of motion (or initial stages of certain types) in which boundaries or coasts do not exert an immediate influence.

Essentially, what we have sought is an understanding of how the two-layer ocean responds to changes in the applied wind. Is the wind-induced velocity (a) confined to the upper layer, (b) nearly the same throughout the depth of the ocean, or (c) a combination of a and b? Correspondingly, how does the interface between the two layers respond in relation to the free surface? (a) Does it respond in such fashion as to keep the horizontal pressure gradients (and hence velocities) negligible in the deep layer? (b) Does it remain essentially unaffected, hence permitting the horizontal pressure gradients to be nearly equal in both layers? (c) Or does it respond as a combination of a and b?[3] From a practical oceanographic point of view, a clear picture as to which of these alternative modes of motion is probable is of great importance in any attempt to relate changes of oceanic circulations to changes in the applied wind stress.

The surface wind-drift currents within the top 100 m are almost always in equilibrium with the wind stress and are measured directly by discrepancies in navigation of ships, while currents in deeper portions of the ocean are inferred from dynamic computations only. It is well known that the latter method fails to detect the barotropic component of velocity.

Despite the fact that there are no satisfactory *direct* measurements of velocity distribution in deep waters beneath the main thermocline, it is quite obvious from a study of the distribution of certain properties such as salinity and dissolved oxygen that these deep waters do not move with the same high mean velocity of the water masses above the main thermocline. Therefore, so far as the mean circulation is concerned, it is certain that the time-mean velocity is essentially baroclinic, and one may be sure that any theory which results in a barotropic mean circulation has some essential physical feature lacking. Barotropic mean currents are excluded by observation; but

[3] Motion of the type (a) will be called baroclinic or internal; motion of the type (b) will be referred to as barotropic or external.

time-periodic barotropic currents are permissible provided they do not involve horizontal displacements large enough to confuse the picture of the mean distribution of deep ocean properties. For example, ordinary tidal currents are barotropic, but, since the amplitude of the periodic horizontal displacement associated with them is of the order of one kilometer, they produce unobservably small periodic variations in the mean distribution of deep water properties at any fixed point. It is necessary to examine the theoretical implications of any time-variable barotropic flow which might result from the passage of storms, from prolonged disturbances to the circulation, or even from seasonal variations in wind. If the theoretical result requires barotropic modes with periodic horizontal displacements of the deep water of more than, say, 300 km, then it seems safe to say that such a result is in conflict with observation.

Finally, one further test by observation should be mentioned. Barotropic currents set up by a storm might involve a permanent displacement of the deep water in addition to the periodic displacements. The passage of a number of storms, more or less at random, would then result in deep water particles executing horizontal "random walks." This type of mixing process can then be expressed in terms of a coefficient of eddy diffusivity. If theoretically predicted motions of the deep water layers imply an eddy coefficient of much more than 10^8 cm^2 sec^{-1} (Sverdrup, 1939), they are in conflict with observational material.

The history of previous theoretical work on this subject goes back to Rossby (1938) who, in a pioneer theoretical investigation, came to the conclusion that the ocean responds barotropically to variable applied wind stress. Because this result was so surprising and since it might lead to contradictions with observation in some one of the ways mentioned above, Rossby re-examined his results by means of several different models. In addition to the simple case of two homogeneous layers with an abrupt density discontinuity, he studied a case where the density stratification was continuous in the lower layer; and he even considered the effect of placing another thick homogeneous layer beneath the layer of constant stability. Despite these elaborations he was unable to escape the disconcerting conclusion that currents produced by changes in wind stress are almost independent of depth and are not affected significantly by density stratification.

Since Rossby's conclusion is independent of frequency of applied stress (except that it must be less than the inertial frequency), it seems that one must infer that even seasonal fluctuations of winds produce barotropic changes in the circulation, although in this case the boundaries must certainly have some influence on the circulation.

However, if the boundary conditions are *linear*, then they would change only the horizontal distribution of the velocity field, not the fact that velocity is independent of depth. Finally, it is impossible, on the basis of Rossby's model, to account for the fact that the observed mean wind-induced circulation is confined to the upper layer of the ocean. In the latter case, one can point out that bottom friction, which is not included in Rossby's model, might well be important in preventing the mean wind-induced circulation from extending to the bottom, but it could hardly be effective on a time scale such as that of a storm. Despite difficulties in interpreting Rossby's model for long-period wind variations, in which a completely naïve application of the model leads to results that contradict observation, the theoretical conclusions regarding short-period wind variations seemed quite inescapable.

Rossby's model involves a uniform Coriolis parameter. It is important to see what effect the introduction of a *variable* Coriolis parameter would have on Rossby's conclusions, on the grounds that the variable Coriolis parameter is a vital feature of the steady-state wind-driven circulation theories (Sverdrup, Reid, Stommel, Munk, et al.). Its presence in the vorticity equation might modify the response of the ocean to a variable wind system.

A number of other theoretical studies on the time-response of the ocean have been published in the intervening time, and it may be helpful to the reader to see explicitly the relation of the present study to some of the previous ones. A brief summary of the essential characters of these studies is given in Table I.

The theories of Sverdrup (1947), Reid (1948), Stommel (1948), and Munk (1950) are steady-state theories of the circulation set up by a steady wind system. They provide the justification for neglecting horizontal frictional forces in the interior of the ocean.

The theories of Ichiye (1951) and of Veronis and Morgan (1955) are concerned with changes in the total circulation in an enclosed basin due to variations in wind. The papers deal with a homogeneous ocean.

A recent study by Groves (1954) shows some of the features produced in the Rossby (1938) type of model in the presence of a coast, but since the influence of boundaries is not included in the present study, there will be no further occasion to refer to the Groves paper.

An equation for predicting the change in depth of the seasonal thermocline, in terms of the applied wind-stress field alone, has recently been published (Freeman, 1954); this is based on the assumption that the induced velocity field is baroclinic. In view of the fact that no reason has been formed to dismiss Rossby's 1939 demonstration that

TABLE I.

	Boundaries	*Variation of Coriolis parameter*	*Time variability of wind*	*Stratification*
Sverdrup, 1947	+(one)	+	−	−
Stommel, 1948	+	+	−	−
Reid, 1948	+(one)	+	−	+
Stockmann, 1946	+	+	−	+
Munk, 1950; and other similar theories	+	+	−	−
Ichiye, T., 1951	+	+	+	−
Veronis & Morgan, 1955	+	+	+	−
Rossby, 1938	−‡	−	+	+
Cahn, 1945	−‡	−	+	−
Bolin, 1953	−‡	−	+	+
Groves, 1954	+(one)	−	+	+
Charney, 1955	+(two)†	+†	+	+
Freeman, 1954	−	−	+	−*
Present study	−	+	+	+

‡ No fixed boundaries, but initial stream restricted in extent.

† Charney does consider variation of Coriolis parameter with latitude in one portion of his study, but not in the model with boundaries.

* In this case the response of the interface is specified, not determined.

short-period response must be barotropic, such an assumption seems unsubstantiable.

During the latter half of 1954, when J. G. Charney (1955) was preparing a contribution for The Convocation held at Woods Hole in connection with the dedication of the new U. S. Navy Laboratory of Oceanography at Woods Hole, we had an opportunity to read his manuscript and to discuss it at length with him; we are indebted to Dr. Charney for many valuable suggestions. His paper uses the quasigeostrophic approximation throughout. Starting with Rossby's two-layer model, he studies the effects of coastal boundaries and of the variation of Coriolis parameter with latitude. The presence of a coastal boundary tends to favor the baroclinic mode (even in the absence of the variation of Coriolis parameter with latitude), a result which may be of fundamental importance in future theoretical studies of such coastal currents or of the Gulf Stream.

Finally, mention should be made of two papers, by Cahn (1945) and Bolin (1953), in which particular attention is paid to the dispersal of energy from an initially concentrated current system by means of inertio-gravitational waves. Whereas the present study does include gravitational and inertial waves, it cannot produce many of the

interesting features of the Cahn and Bolin models. This shortcoming arises from the periodic spatial distribution of applied wind stress in the present study.

2. THE VORTICITY EQUATIONS IN NORMAL MODES

The model which will be considered in the subsequent analysis consists of a horizontally infinite rotating ocean which is of constant depth in the equilibrium state. The density stratification, an idealization of the observed (continuous) density distribution of the ocean, consists of two layers of homogeneous water separated by a surface of discontinuity which corresponds to the mean thermocline. It is assumed that the motions are quasihydrostatic and that no momentum is transmitted across the interface by friction. If the motions are small, the equations may be linearized. Thus

$$\frac{\partial u_1}{\partial t} - fv_1 = -g\frac{\partial \eta_1}{\partial x} + \frac{\tau'}{D_1}, \tag{2.1}$$

$$\frac{\partial v_1}{\partial t} + fu_1 = -g\frac{\partial \eta_1}{\partial y} + \frac{\tau}{D_1}, \tag{2.2}$$

$$\frac{\partial}{\partial t}(\eta_1 - \eta_2) + D_1\left(\frac{\partial u_1}{\partial x} + \frac{\partial v_1}{\partial y}\right) = 0 \quad , \tag{2.3}$$

$$\frac{\partial u_2}{\partial t} - fv_2 = -g\left[a\frac{\partial \eta_1}{\partial x} + b\frac{\partial \eta_2}{\partial x}\right], \tag{2.4}$$

$$\frac{\partial v_2}{\partial t} + fu_2 = -g\left[a\frac{\partial \eta_1}{\partial y} + b\frac{\partial \eta_2}{\partial y}\right], \tag{2.5}$$

$$\frac{\partial \eta_2}{\partial t} + D_2\left(\frac{\partial u_2}{\partial x} + \frac{\partial v_2}{\partial y}\right) = 0 \quad , \tag{2.6}$$

where x (directed eastward) and y (directed northward) are the horizontal co-ordinates; t is time; u_i and v_i ($i = 1, 2$) are the velocities in the x and y directions respectively; D_1 is the equilibrium thickness of the upper layer;[4] η_1 is the deviation of the free surface from its equilibrium position; g is gravity; $f = 2\,\Omega$ sin (latitude) is the Coriolis parameter; Ω is the angular speed of the earth's rotation; $a = \rho_1/\rho_2$, $b = (\rho_2 - \rho_1)/\rho_2$; ρ_1 is the density of the upper layer; and τ' and τ are stresses in the x and y directions, respectively, exerted on the ocean surface by a wind. Charney (1955) has shown in some detail that it is justifiable to treat the wind stress, which is, of course, actually applied

[4] The terms with subscript 2 define similar quantities in the lower layer.

at top surface, as a body force distributed evenly with depth over the entire top layer.

If

$$\eta = \eta_1, \phi = \eta_1 - \eta_2 \tag{2.7}$$

are substituted above, one finds

$$\frac{\partial u_1}{\partial t} - fv_1 = -g\frac{\partial \eta}{\partial x} + \frac{\tau'}{D_1}, \tag{2.8}$$

$$\frac{\partial v_1}{\partial t} + fu_1 = -g\frac{\partial \eta}{\partial y} + \frac{\tau}{D_1}, \tag{2.9}$$

$$\frac{\partial \phi}{\partial t} + D_1\left(\frac{\partial u_1}{\partial x} + \frac{\partial v_1}{\partial y}\right) = 0 \quad , \tag{2.10}$$

$$\frac{\partial u_2}{\partial t} - fv_2 = -g\left[\frac{\partial \eta}{\partial x} - b\frac{\partial \phi}{\partial x}\right], \tag{2.11}$$

$$\frac{\partial v_2}{\partial t} + fu_2 = -g\left[\frac{\partial \eta}{\partial y} - b\frac{\partial \phi}{\partial y}\right], \tag{2.12}$$

$$\frac{\partial}{\partial t}(\eta - \phi) + D_2\left(\frac{\partial u_2}{\partial x} + \frac{\partial v_2}{\partial y}\right) = 0 \quad . \tag{2.13}$$

In the subsequent analysis we propose to take account of the variability of the Coriolis parameter by writing $df/dy = \beta =$ constant whenever f appears in differentiated form. Otherwise f will be assumed constant. Cross differentiating (2.8) and (2.9) and (2.11) and (2.12), we obtain the vorticity equations

$$\frac{\partial \zeta_1}{\partial t} - \frac{f}{D_1}\frac{\partial \phi}{\partial t} + \beta v_1 = \frac{1}{D_1}\left(\frac{\partial \tau}{\partial x} - \frac{\partial \tau'}{\partial y}\right), \tag{2.14}$$

$$\frac{\partial \zeta_2}{\partial t} - \frac{f}{D_2}\frac{\partial}{\partial t}(\eta - \phi) + \beta v_2 = 0\,, \tag{2.15}$$

where $\zeta_1 = \partial v_1/\partial x - \partial u_1/\partial y$ and $\zeta_2 = \partial v_2/\partial x - \partial u_2/\partial y$ are the relative vorticities of the upper and lower layers respectively.

At this point it is assumed that the motions are independent of the y co-ordinate. The effect of β is thereby incorporated into the equations of the simple one-dimensional model. Care must be exercised, however, in the choice of equations which describe the system; otherwise the trivial and uninteresting condition $\beta \equiv 0$ results. Thus, in eliminating all but a single dependent variable, one must not include the curl operation, since now $\partial/\partial y \equiv 0$, and the only possible consequence is $\beta \equiv 0$.

The only set of equations which is consistent with the above remarks is:

$$\frac{\partial^2 v_1}{\partial x \partial t} - \frac{f}{D_1}\frac{\partial \phi}{\partial t} + \beta v_1 = \frac{1}{D_1}\frac{\partial \tau}{\partial x}, \tag{2.16}$$

$$\frac{\partial u_1}{\partial t} - f v_1 = -g\frac{\partial \eta}{\partial x}, \tag{2.17}$$

$$\frac{\partial \phi}{\partial t} + D_1\frac{\partial u_1}{\partial x} = 0, \tag{2.18}$$

$$\frac{\partial^2 v_2}{\partial x \partial t} - \frac{f}{D_2}\frac{\partial}{\partial t}(\eta - \phi) + \beta v_2 = 0, \tag{2.19}$$

$$\frac{\partial u_2}{\partial t} - f v_2 = -g\left[\frac{\partial \eta}{\partial x} - b\frac{\partial \phi}{\partial x}\right], \tag{2.20}$$

$$\frac{\partial}{\partial t}(\eta - \phi) + D_2\frac{\partial u_2}{\partial x} = 0 \quad . \tag{2.21}$$

Eliminating u_1 from (2.17) and (2.18) and substituting the value of v_1 in (2.16) we find for the upper layer

$$r\lambda^2\eta_{xxxt} - \frac{\phi_{xttt}}{f^2} - \phi_{xt} + r\beta\lambda^2\eta_{xx} - \frac{\beta}{f^2}\phi_{tt} = \frac{\tau_{xx}}{f}, \tag{2.22}$$

where $r = D_1/D_2$ and $\lambda^2 = gD_2/f^2$; λ is the quantity Rossby called the radius of deformation.

A similar procedure in the last three equations results in the following equation for the lower layer

$$\lambda^2(\eta - b\,\phi)_{xxxt} - \frac{(\eta - \phi)_{xttt}}{f^2} - (\eta - \phi)_{xt} + \beta\lambda^2(\eta - b\,\phi)_{xx} - \frac{\beta}{f^2}(\eta - \phi)_{tt} = 0 \quad . \tag{2.23}$$

The two equations (2.22) and (2.23) may be used for a detailed study of the response of η and ϕ to the variable wind stress τ, but from an analytical point of view it is much simpler to introduce normal modes, which enable one to separate the two dependent variables in the two vorticity equations without increasing the order of the differential form. Equation (2.23), multiplied by the arbitrary constant α, is added to (2.22) to obtain

$$\lambda^2\left[(r+\alpha)\,\eta-\alpha b\phi\right]_{xxxt}-\frac{1}{f^2}\left[(1-\alpha)\,\phi+\alpha\eta\right]_{xttt}$$
$$-\left[(1-\alpha)\,\phi+\alpha\eta\right]_{xt}+\beta\lambda^2\left[(r+\alpha)\,\eta-\alpha b\phi\right]_{xx}$$
$$-\frac{\beta}{f^2}\left[(1-\alpha)\,\phi+\alpha\eta\right]_{tt}=\frac{\tau_{xx}}{f}\quad.\qquad(2.24)$$

The conditions

$$(1+\alpha)\,\phi+\alpha\eta=R\quad\text{and}\quad(r+\alpha)\,\eta-\alpha b\phi=kR\,,\qquad(2.25)$$

where k is a constant of proportionality, are sufficient to reduce the equations to a single variable. The above conditions determine α and k by the necessity that

$$k=-\frac{\alpha b}{1-\alpha}=\frac{r+\alpha}{\alpha}\quad.\qquad(2.26)$$

Therefore

$$\alpha=\frac{1-r\pm\sqrt{(1+r)^2-4rb}}{2(1-b)}\,,$$

and

$$\alpha_1\approx\frac{1+r-rb}{(1+r)\,(1-b)}\,,\qquad\alpha_2\approx\frac{-r\,(1+r-b)}{(1+r)\,(1-b)}\,,$$
$$k_1\approx 1+r\,,\qquad k_2\approx\frac{rb}{1+r}\,.\qquad(2.27)$$

The two values of R (two normal modes corresponding to the two values of α) are

$$R_i=(1-\alpha_i)\,\phi_i+\alpha_i\eta\qquad(i=1,2)\,.\qquad(2.28)$$

Thus (2.24) may be written

$$\lambda^2k_i\,R_{ixxxt}-\frac{1}{f^2}\,R_{ixttt}-R_{ixt}+\beta\lambda^2k_i\,R_{ixx}-\frac{\beta}{f^2}\,R_{itt}=\frac{\tau_{xx}}{f}\quad.\qquad(2.29)$$

These will be referred to as the equations of normal modes. Once the normal modes have been determined, it is possible to obtain other more primitive quantities, such as elevation of the free surface and interface, as well as the velocities in each layer from definitions (2.27), (2.28) and equations (2.17), (2.18), (2.20), (2.21); e.g.,

$$\phi=\frac{\alpha_2\,R_1-\alpha_1\,R_2}{\alpha_2-\alpha_1}\,,\qquad(2.30)$$

$$\eta = \frac{(\alpha_2 - 1) R_1 - (\alpha_1 - 1) R_2}{\alpha_2 - \alpha_1} \quad . \tag{2.31}$$

3. FREE WAVES

In subsequent sections we shall have occasion to refer to various wave motions which are induced by the action of a transient wind stress on the sea surface. It is appropriate therefore to consider the free waves which are inherent in the normal mode equations and to study thereby the behavior of the solutions. A clear picture of the free wave motions is also desirable because it helps in visualizing certain resonance phenomena which occur in cases where the wind stress is periodic in time.

Consider a normal mode of the form

$$R_i = S_i \sin (lx + \omega_i t) \quad , \tag{3.1}$$

where S_i = const. and where l is the wave number associated with the wave length L, i.e. $l = 2\pi/L$. The assumed form of the normal mode is therefore a wave progressing in the negative x direction when the frequency ω_i is positive. Substituting R_i into (2.29), we find that the equations reduce to a pair of frequency equations of the form

$$\left(\frac{\omega_i}{f}\right)^3 - \frac{\beta}{fl}\left(\frac{\omega_i}{f}\right)^2 + (1 + \mu_i^2)\frac{\omega_i}{f} + \frac{\beta\mu_i^2}{lf} = 0 \quad (i = 1, 2) \, , \tag{3.2}$$

where $\mu_i^2 = k_i l^2 \lambda^2$. The solutions of the algebraic equations (3.2) give the frequency ω_i in terms of the wave number l.

From an oceanographic point of view, only a limited range of values of l is of interest, and it will be demonstrated that the approximate roots of the cubic equation within this range of values of l are:

$$\omega_{i1} = \frac{\beta}{l}\frac{\mu_i^2}{\gamma_i} \, , \tag{3.3}$$

$$\omega_{i2} = \frac{\beta}{2l\gamma_i} + \sqrt{\left(\frac{\beta}{2\gamma_i l}\right)^2 + \frac{4\beta^2\mu_i^2}{l^2\gamma_i^2} + 4f^2\gamma_i} \, , \tag{3.4}$$

$$\omega_{i3} = \frac{\beta}{2l\gamma_i} - \sqrt{\left(\frac{\beta}{2\gamma_i l}\right)^2 + \frac{4\beta^2\mu_i^2}{l^2\gamma_i^2} + 4f^2\gamma_i} \, , \tag{3.5}$$

where $\gamma_i = 1 + \mu_i^2$. In order to indicate the degree of approximation involved in these expressions for the roots, the original cubic equation may be compared with the expression

$$\frac{1}{f^3}(\omega_i - \omega_{i1})(\omega_i - \omega_{i2})(\omega_i - \omega_{i3}) = 0$$

or

$$\left(\frac{\omega_i}{f}\right)^3 - \frac{\beta}{fl}\left(\frac{\omega_i}{f}\right)^2 - (1+\mu_i^2)\left(\frac{\omega_i}{f}\right) + \frac{\beta\mu_i^2}{fl}(1+\varepsilon_i) = 0\,,$$

where $\varepsilon_i = \dfrac{\beta^2\mu_i^2}{l^2f^2\gamma_i^3}$. The original cubic frequency equation is distinguished from the approximate equation only by the absence of the term ε_i. In order to ascertain the limitations of the approximations, we consider an ocean model with the following properties

$D_1 = 500$ m $\qquad \beta = 2 \times 10^{-11}\text{m}^{-1}\text{sec}^{-1}$
$D_2 = 3500$ m $\qquad f = 10^{-4}\text{sec}^{-1}$
$r = 1/7 \qquad b = 2 \times 10^{-3}$.

Then

$\lambda^2 = 3.5 \times 10^{12}\text{m}^2 \qquad \varepsilon_1 \leq .16$ for all l
$k_1 \approx 8/7 \qquad \varepsilon_2 \leq 4 \times 10^{-6}$ for all l.
$k_2 \approx 2.5 \times 10^{-4}$

The largest values of ε_i occur for $l = 0$, i.e., for an infinite wave length L. Since L will be restricted by $L \leq 12{,}000$ km, the practical upper limit of ε_1 is .02. Therefore the approximate roots are actually close to the real ones.

The phase velocity and frequency of these various waves are shown in Fig. 1 for the range of wave lengths 10 km $\leq L \leq$ 12,000 km.

The six wave motions may be separated into two categories. The waves with frequency ω_{11} and ω_{21} represent the geostrophically balanced current motions; ordinarily they contain the measurable flow in the ocean. The remaining four waves arise from a completely different source, viz., the unbalance between Coriolis and pressure forces. These inertio-gravitational motions will often be referred to as "transient" motions, since in a nonperiodic model their energy would be rapidly dispersed into the outlying regions (see Cahn, 1945).

Specifically, the waves with frequency ω_{11} and ω_{21} are barotropic and baroclinic Rossby waves, respectively, moving toward the west. They determine the external and internal geostrophic response of the ocean to an applied wind stress. For scales of motion most often encountered in the ocean, i.e. $L \geq 1{,}000$ km, the isostatic Rossby wave merges into a nondispersive type of wave.

For the smaller wave lengths ($L \leq 2{,}000$ km), the ω_{12} and ω_{13} waves are barotropic gravity waves of the familiar nondispersive type moving to the west and east respectively. For larger wave lengths, the waves become dispersive waves of the Sverdrup type (Sverdrup, 1926), although this characteristic of their behavior is practically unnoticeable except for long waves, $L \geq 6{,}000$ km. In

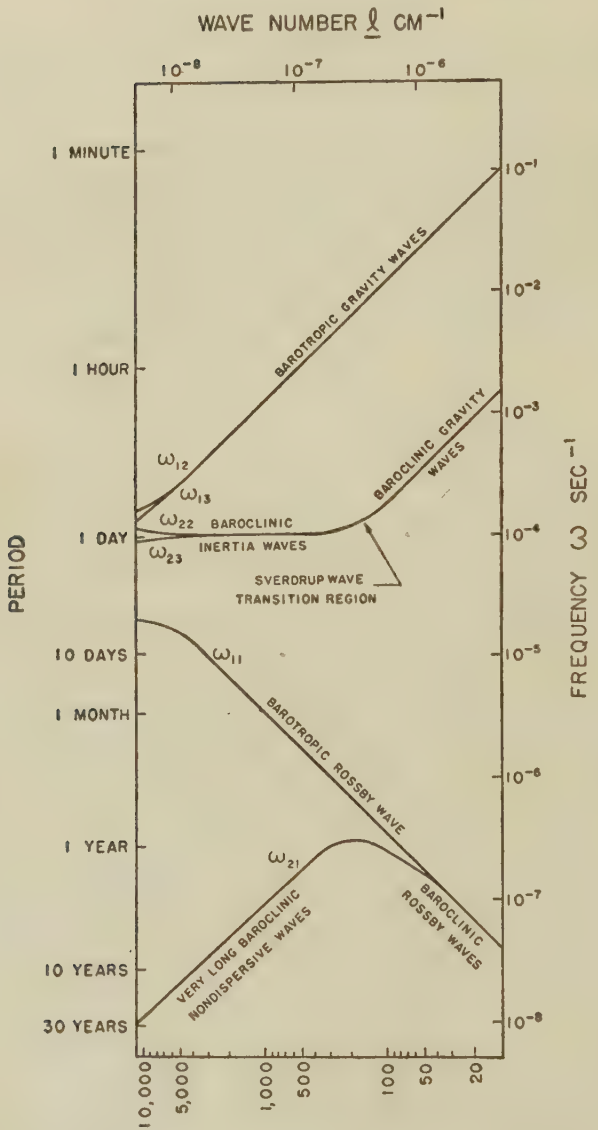
WAVE NUMBER l CM⁻¹
10⁻⁸
10⁻⁷
10⁻⁶
1 MINUTE
1 HOUR
1 DAY
10 DAYS
1 MONTH
1 YEAR
10 YEARS
30 YEARS
PERIOD
BAROTROPIC GRAVITY WAVES
BAROCLINIC GRAVITY WAVES
ω12
ω13
ω22 BAROCLINIC
INERTIA WAVES
ω23
SVERDRUP WAVE
TRANSITION REGION
ω11
BAROTROPIC ROSSBY WAVE
ω21
VERY LONG BAROCLINIC
NONDISPERSIVE WAVES
BAROCLINIC
ROSSBY WAVES
10⁻¹
10⁻²
10⁻³
10⁻⁴
10⁻⁵
10⁻⁶
10⁻⁷
10⁻⁸
FREQUENCY ω SEC⁻¹
10,000
5,000
1,000
500
100
50
20
WAVE LENGTH, KM

Figure 1

the latter range, both the earth's rotation and the variation of the Coriolis parameter affect the velocities of propagation; thus the westward moving waves ω_{12} move faster than long gravity waves and the eastward moving waves ω_{13} move more slowly.

The waves ω_{22} and ω_{23} are baroclinic waves moving to the west and east respectively. For extremely small scale motions ($L \leq 100$ km), they take the form of internal long gravity waves (speed $\sqrt{bgD_1}$). For somewhat larger wave lengths (100 km $\leq L \leq$ 400 km) they are of the Sverdrup type. For the more realistic values $L > 400$ km they are essentially inertial waves with a period of a half pendulum day.

Since the properties of the various types of waves have been discussed in the literature they will not be considered here in any more detail. Baroclinic and barotropic long gravity, Sverdrup, and inertial waves are discussed in Proudman (1953). Barotropic Rossby waves are discussed by Rossby (1949) and Yeh (1949).

4. MOTIONS CAUSED BY MOVING WIND SYSTEM

As the simplest case of a time-dependent wind stress, consider the y component of wind stress to be of the form

$$\tau = W \sin (lx + \nu t).^5 \tag{4.1}$$

The modes excited by the present form of τ are

$$R_i = S_i \sin (lx + \nu t) \quad , \tag{4.2}$$

where frequency and wave number of the forced motion are the same as those of the stress field. The amplitudes S_i of the normal modes are determined from the vorticity equations (2.29) and are

$$S_i = \frac{Wl}{f^2 \mathfrak{D}_i(\nu, l)} , \tag{4.3}$$

where

$$\mathfrak{D}_i(\nu, l) = \left(\frac{\nu}{f}\right)^3 - \frac{\beta}{lf}\left(\frac{\nu}{f}\right)^2 - (1 + \mu_i^2)\frac{\nu}{f} + \frac{\beta}{lf}\mu_i^2 . \tag{4.4}$$

From S_i, the physical quantities may be determined immediately by means of relations

[5] In this case, τ could be interpreted as wind stress caused by (slowly) moving large-scale wind systems such as those obtained from five-day-mean weather charts. Reasonable values for the frequency ν and for the wave-number l are $\nu = -5 \times 10^{-6}$ sec^{-1} and $l = 10^{-6}$ m^{-1}. These correspond to a period of about two weeks and to a wave-length of 6,000 km. The system moves toward the east and ν is therefore negative. W, the amplitude of stress, is constant.

$$\phi' = \frac{rS_1 + S_2}{1 + r} \qquad u_1' = -\frac{\nu}{D_1 l}\phi'$$

$$\eta_1' = S_1 + \frac{b}{(1 + r)^2} S_2 \qquad u_2' = -\frac{\nu}{D_2 l}\eta_2' \tag{4.5}$$

$$\eta_2' = \frac{S_1 - S_2}{1 + r} \qquad v_1' = \frac{\nu}{f} u_1 + \frac{gl}{f}\eta_1'$$

$$v_2' = \frac{\nu}{f} u_2' + \frac{gl}{f}(\eta_1' - b\phi') ,$$

where

$$(\phi, \eta_1, \eta_2, u_1, u_2) = (\phi', \eta_1', \eta_2', u_1', u_2') \sin(lx + \nu t)$$
$$(v_1, v_2) = (v_1', v_2') \cos(lx + \nu t) . \tag{4.6}$$

The exact forms for the solutions will not be written here since they will not be used.

It is apparent that resonance will occur in the present system where the denominator $\mathfrak{D}_i(\nu, l)$ vanishes. Specifically, the resonant frequencies correspond to those of the various free waves (Section 3). An eastward moving wind system can excite resonance only for the internal and barotropic inertio-gravity waves since there are no eastward moving Rossby waves. Since natural wind systems rarely move to the west, there is no point in considering the cases $\nu > 0$.

In footnote 4 we noted that the present form of the wind stress could correspond to slowly moving patterns of ridges and troughs in the atmosphere. The frequencies of these atmospheric motions correspond to periods of the order of several weeks. If such low frequencies are assumed, the quantities $\mathfrak{D}_i(\nu, l)$ are given approximately by

$$\mathfrak{D}_1(\nu, l) = -(1 + \mu_1^2)\frac{\nu}{f} + \frac{\beta}{lf}\mu_1^2$$

$$\mathfrak{D}_2(\nu, l) = -(1 + \mu_2^2)\frac{\nu}{f} + \frac{\beta}{lf}\mu_2^2 , \tag{4.7}$$

where ν/f is negative.

Consider the case where $l = 10^{-6}\text{m}^{-1}$ (corresponding to a wave length of approximately 6,000 km). If we use here the values of the physical quantities D_1, D_2, etc. which were perscribed in Section 3, then $\mu_1^2 = 4$ and $\mu_2^2 = .88 \times 10^{-3}$. It is apparent, therefore, that the $\mathfrak{D}_i(\nu, l)$ given by (4.7) can be further simplified for certain ranges of ν/f. Thus

$$\left.\begin{array}{l}\text{Range 1: } 10^{-2} \leq -\dfrac{\nu}{f} \leq 10^{-1} \\ \text{or } 70 \text{ days} \geq T \geq 7 \text{ days}\end{array}\right\} \text{yields} \begin{cases}\mathfrak{D}_1(\nu, l) = -(1+\mu_1^2)\dfrac{\nu}{f} + \dfrac{\beta}{lf}\mu_1^2 \\ \mathfrak{D}_2(\nu, l) \approx -\dfrac{\nu}{f}\end{cases},$$

$$\left.\begin{array}{l}\text{Range 2: } 2 \times 10^{-3} \leq -\dfrac{\nu}{f} < 10^{-2} \\ \text{or 1 year} \geq T > 70 \text{ days}\end{array}\right\} \text{yields} \begin{cases}\mathfrak{D}_1(\nu, l) \approx \dfrac{\beta}{lf}\mu_1^2 \\ \mathfrak{D}_2(\nu, l) \approx -\dfrac{\nu}{f}\end{cases}, \tag{4.8}$$

$$\left.\begin{array}{l}\text{Range 3: } 0 \leq -\dfrac{\nu}{f} \leq 2 \times 10^{-5} \\ \text{or } T \geq 100 \text{ years}\end{array}\right\} \text{yields} \begin{cases}\mathfrak{D}_1(\nu, l) \approx \dfrac{\beta}{lf}\mu_1^2 \\ \mathfrak{D}_2(\nu, l) \approx \dfrac{\beta}{lf}\mu_2^2\end{cases},$$

where $T = -2\pi/\nu$ is the period.

The first range, corresponding to periods which are considerably longer than those of the inertio-gravitational motions, is still comparable to the period of the barotropic Rossby wave; this initial range contains magnitudes that are comparable to observed phenomena in the atmosphere (see footnote 4). Range 2 represents periods which are much longer than the barotropic but shorter than the baroclinic Rossby wave period. The final range exceeds the internal Rossby wave period by at least a factor of 10.

In Range 1, the crosswind velocity component in the upper layer u_1 is simply the Ekman frictional wind-drift velocity directed to the right of the applied wind stress. It is independent of period. This is depicted in Fig. 2, which contains the amplitudes of the four velocities as well as the two surface heights for Range 1, with the magnitude of the wind-stress $W = 1$ cm^2/sec^2. Since the crosswind velocity in the upper layer is independent of period, its total effect on the mass distribution is increased with increasing period. Thus the divergences are larger and the thermocline is displaced further. Fig. 2 shows that the thermocline response is linearly proportional to the period. The free surface deviation is small in this range (less than 2 cm), and for larger periods in the range it is also proportional to the period. The crosswind velocity in the lower layer u_2 tends to compensate for the divergence caused by u_1 in the upper layer. Since it is a function of the free surface deviation as well as of the thermocline response, it is not exactly constant in this range.

The downwind velocities, mainly geostrophic in the large period end of this range, are proportional to period there. It is interesting to note that, for the small periods, the accelerative (nongeostrophic)

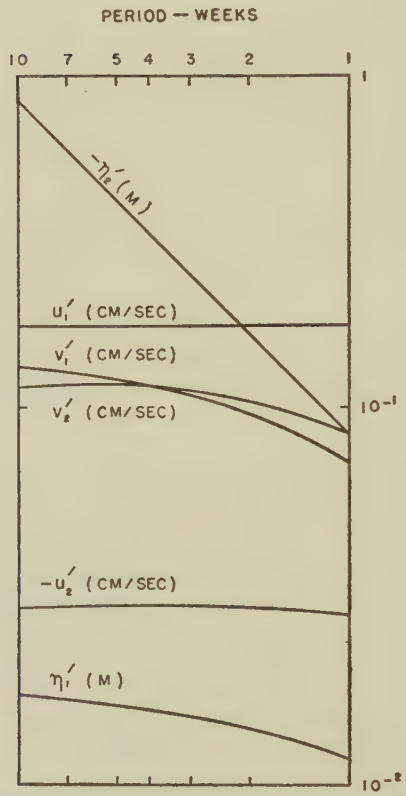

Figure 2

effects which tend to retard the motion are quite prominent, representing roughly 20% of the contribution to the downstream velocity. Since these effects are considerably stronger in the upper layer (where wind stress is a direct cause of the unbalanced state), the downwind velocity of the upper layer is actually smaller than that of the lower layer. The accelerative effects become negligible for a period longer than four weeks. It is evident also that the principal response of the system throughout Range 1 is barotropic. Near the large period end of the range, internal effects become important.

The periods contained in Range 2 represent the seasonal to yearly variations in the wind stress systems. Although boundary effects must certainly become important for such long periods, the results of the present investigation yield some features which are of interest and which will therefore be given here.

The solutions of the two modes are

$$S_1 = \frac{Wf}{\beta g(D_1 + D_2)}, \qquad S_2 = -\frac{Wl}{f^2(\nu/f)}, \tag{4.9}$$

and the physical variables become (approximately)

$$\eta_1' = \frac{Wf}{\beta g(1+r)D_2} - \frac{Wlb}{(1+r)^2 f^2(\nu/f)}, \tag{4.10}$$

$$\eta_2' = \frac{Wl}{(1+r) f^2(\nu/f)}, \tag{4.11}$$

$$u_1' = \frac{W}{(1+r) D_1 f}, \tag{4.12}$$

$$u_2' = -\frac{W}{(1+r) D_2 f}, \tag{4.13}$$

$$v_1' = \frac{Wgl}{(1+r)f}\left[\frac{f}{\beta g D_2} - \frac{bl}{(1+r) f^2(\nu/f)}\right], \tag{4.14}$$

$$v_2' = \frac{Wl}{(1+r)\beta D_2}. \tag{4.15}$$

When interpreting results for the present range, one must keep in mind the fact that Range 2 corresponds to periods which are considerably longer than the barotropic Rossby wave period but shorter than the baroclinic Rossby wave period. However, in η_1' and v_1' the effect of the internal Rossby wave period appears. The longer the period, the larger the effect of this internal wave.

The following facts are evident from an inspection of (4.10) to (4.15):

(a) The crosswind velocity component in the upper layer is simply the Ekman frictional wind-drift current and is independent of the period. In the lower layer there is a compensating (baroclinic) counterflow.

(b) The thermocline response is directly proportional to the period.

(c) The downwind lower layer velocity, essentially constant, is unaffected by variations in the period.

The free surface deviation η_1' and the downwind upper layer velocity v_1' are dependent on the period. In each case the variable has a constant value upon which is superposed the baroclinic Rossby wave effect (proportional to period). The velocity v_1' exceeds the lower layer velocity v_2' by the amount $-\dfrac{bgl^2W}{(1+r)f^3(\nu/f)} = 1.53 \times 10^{-4}$

(f/ν) cm sec^{-1}. For the longest period in this range, i.e., $T \approx$ one year, this excess value is approximately half of the constant value $\frac{Wl}{(1+r)D_2\beta}$. The baroclinic effect has therefore become quite important for this extreme value.

For Range 3, the periods are much longer than the internal Rossby wave period. Both D_1 and D_2 and consequently all of the coefficients of the physical quantities are independent of frequency. The flow in this range is now a quasisteady flow. Thus

$$\begin{aligned} n_1' &= \frac{1}{r}\frac{Wl^2}{\beta f \mu_1^2}, \\ \eta_2' &= \frac{1}{rb(1+r)}\frac{Wl^2}{\beta f \mu_1^2}, \\ v_2' &= u_1' = u_2' = 0, \\ v_1' &= \frac{Wl}{\beta D_1} . \end{aligned}$$

The velocities are all contained in the upper layer. The total transport Wl/β is equal to that given by Munk (1950) for the steady-state model $\nu/f \to 0$. In this range of long period variations the flow is geostrophic.

5. MOTIONS CAUSED BY STORMS

We shall consider next a simple transient model, i.e., one in which all of the wave motions discussed in Section 3 are present. It is assumed that the ocean is initially at rest and that a wind stress begins to act on the ocean surface at time $t = 0$. The y-component of the stress is

$$\begin{aligned} \tau &= 0, & t &< 0, \\ \tau &= W \cos lx, & t &> 0. \end{aligned} \tag{5.1}$$

The effect of a storm on oceanic motions can be investigated with the present model by the simple expedient of adding the new condition $\tau = 0$ for $t > t_0$, where t_0 is, say, four or five days. A more realistic wind stress resulting from the passage of a storm is a moving wave which starts at $t = 0$, i.e.

$$\begin{aligned} \tau &= 0, & t &< 0, \\ \tau &= W \cos(lx + \nu t), & t &> 0. \end{aligned} \tag{5.2}$$

Except for possible resonance effects, the progressive storm, as opposed to a fixed storm, reduces the importance of the inertio-gravitational motions. However, since we are primarily interested in the qualitative effect of the initial unbalance and since the moving storm adds nothing new to the qualitative behavior, we shall confine our attention to the wind stress defined by (5.1).

The solution of the normal mode equations (2.29), with the wind stress τ given by (5.1), is[6]

$$R_1 = Wlf\left\{\frac{\cos lx - \cos(lx + \omega_{11}t)}{\frac{\beta}{l}f^2\mu_1^2} + \frac{\cos(lx + \omega_{12}t)}{2f^3[1 + \mu_1^2]^{3/2}} - \frac{\cos(lx + \omega_{13}t)}{2f^3[1 + \mu_1^2]^{3/2}}\right\}, \quad (5.3)$$

$$R_2 = Wlf\left\{\frac{\cos lx - \cos(lx + \omega_{21}t)}{\frac{\beta}{l}f^2\mu_2^2} + \frac{\cos(lx + \omega_{22}t)}{2f^3(1 + \mu_2^2)^{3/2}} - \frac{\cos(lx + \omega_{23}t)}{2f^3(1 + \mu_2^2)^{3/2}}\right\}, \quad (5.4)$$

where

$$\omega_{11} = \frac{\beta\mu_1^2}{l(1 + \mu_1^2)}, \quad \omega_{12} = \frac{\beta\mu_2^2}{l(1 + \mu_2^2)},$$

$$\omega_{12} = f\sqrt{1 + \mu_1^2} + \frac{\beta}{2l(1 + \mu_1^2)}, \quad \omega_{22} = f\sqrt{1 + \mu_2^2} + \frac{\beta}{2l(1 + \mu_2^2)}, \quad (5.5)$$

$$\omega_{13} = -f\sqrt{1 + \mu_1^2} + \frac{\beta}{2l(1 + \mu_1^2)}, \quad \omega_{23} = -f\sqrt{1 + \mu_2^2} + \frac{\beta}{2l(1 + \mu_2^2)}.$$

The velocities and surface heights can now be determined from (2.30), (2.31), (2.8), (2.10), (2.11), (2.13)

[6] The solution is approximate, terms of order $\beta^2 k_i^2 \lambda^2 / f^2 \gamma_i^3$ having been considered small when compared to unity. This restriction is the same as the one used in Section 3 for the approximate roots of the frequency equation. The simpler forms for the frequencies, as given below, are also subject to the same approximation within the range of wave lengths of interest.

$$\phi = \frac{Wlf}{r+1}\left\{\frac{l}{\beta f^2}\left[\frac{r}{\mu_1^2}+\frac{1}{\mu_2^2}\right]\cos lx - \frac{lr\cos(lx+\omega_{11}t)}{\beta f^2\mu_1^2} - \frac{l\cos(lx+\omega_{21}t)}{\beta f^2\mu_2^2} + \frac{r}{2f^3(1+\mu_1^2)^{3/2}}\left[\cos(lx+\omega_{12}t) - \cos(lx+\omega_{13}t)\right] + \frac{1}{2f^3(1+\mu_2^2)^{3/2}}\left[\cos(lx+\omega_{22}t) - \cos(lx+\omega_{23}t)\right]\right\}, \quad (5.6)$$

$$\eta = \eta_1 = Wl\left\{\frac{l\cos lx}{\beta fr(r+1)\mu_1^2} - \frac{l\cos(lx+\omega_{11}t)}{\beta f\mu_1^2} - \frac{l\cos(lx+\omega_{21}t)}{\beta rf\mu_1^2} + \frac{1}{2f^2(1+\mu_1^2)^{3/2}}\left[\cos(lx+\omega_{12}t) - \cos(lx+\omega_{13}t)\right] + \frac{b}{2f^2(1+r)^2(1+\mu_2^2)^{3/2}}\left[\cos(lx+\omega_{22}t) - \cos(lx+\omega_{23}t)\right]\right\}, \quad (5.7)$$

$$\eta_2 = \frac{Wla}{1+r}\left\{\frac{l}{\beta f}\left(\frac{1}{\mu_1^2}-\frac{1}{\mu_2^2}\right)\cos lx - \frac{l\cos(lx+\omega_{11}t)}{\beta f\mu_1^2} + \frac{l\cos(lx+\omega_{21}t)}{\beta f\mu_2^2} + \frac{\cos(lx+\omega_{12}t) - \cos(lx+\omega_{13}t)}{2f^2(1+\mu_1^2)^{3/2}} - \frac{\cos(lx+\omega_{22}t) - \cos(lx+\omega_{23}t)}{2f^2(1+\mu_2^2)^{3/2}}\right\}, \quad (5.8)$$

$$u_1 = -\frac{W}{D_1(1+r)}\left\{-\frac{l\omega_{11}r\cos(lx+\omega_{11}t)}{\beta f\mu_1^2} - \frac{l\omega_{21}\cos(lx+\omega_{21}t)}{\beta f\mu_2^2} + \frac{r}{2f^2(1+\mu_1^2)^{3/2}}\left[\omega_{12}\cos(lx+\omega_{12}t) - \omega_{13}\cos(lx+\omega_{13}t)\right] + \frac{1}{2f^2(1+\mu_2^2)^{3/2}}\left[\omega_{22}\cos(lx+\omega_{22}t) - \omega_{23}\cos(lx+\omega_{23}t)\right]\right., \quad (5.9)$$

$$u_2 = -\frac{Wa}{D_2(1+r)}\left\{-\frac{l\omega_{11}\cos(lx+\omega_{11}t)}{\beta f\mu_1^2} + \frac{l\omega_{21}\cos(lx+\omega_{21}t)}{\beta f\mu_2^2} + \frac{\omega_{12}\cos(lx+\omega_{12}t) - \omega_{13}\cos(lx+\omega_{13}t)}{2f^2(1+\mu_1^2)} - \frac{\omega_{22}\cos(lx+\omega_{22}t) - \omega_{23}\cos(lx+\omega_{23}t)}{2f^2(1+\mu_z^2)^{3/2}}\right\}, \quad (5.10)$$

$$v_1 = -\frac{W}{(1+r)D_1}\left\{\frac{\omega_{11}^2 rl\sin(lx+\omega_{11}t)}{\beta f^2\mu_1^2} + \frac{l\omega_{21}^2\sin(lx+\omega_{21}t)}{\beta f^2\mu_2^2}\right.$$
$$+\frac{r}{2f^3(1+\mu_1^2)^{3/2}}\left[-\omega_{12}^2\sin(lx+\omega_{12}t)+\omega_{13}^2\sin(lx+\omega_{13}t)\right]$$
$$\left.+\frac{1}{2f^3(1+\mu_2^2)^{3/2}}\left[-\omega_{22}^2\sin(lx+\omega_{22}t)+\omega_{23}^2\sin(lx+\omega_{23}t)\right]\right\}$$
$$+Wl^2g\left\{\frac{-l(1+r)\sin lx}{\beta f^2 r\mu_1^2}+\frac{l\sin(lx+\omega_{11}t)}{\beta f^2\mu_1^2}+\frac{l\sin(lx+\omega_{21}t)}{\beta f^2 r\mu_1^2}\right.$$
$$-\frac{1}{2f^3(1+\mu_1^2)^{3/2}}\left[\sin(lx+\omega_{12}t)-\sin(lx+\omega_{13}t)\right]$$
$$\left.-\frac{b}{2f^3(1+r)^2(1+\mu_2^2)^{3/2}}\left[\sin(lx+\omega_{22}t)-\sin(lx+\omega_{23}t)\right]\right\}, \tag{5.11}$$

$$v_2 = -\frac{Wa}{(1+r)D_2}\left\{\frac{l\omega_{11}^2\sin(lx+\omega_{11}t)}{\beta f^2\mu_1^2}-\frac{l\omega_{21}^2\sin(lx+\omega_{21}t)}{\beta f^2\mu_2^2}\right.$$
$$-\frac{\omega_{12}^2\sin(lx+\omega_{12}t)-\omega_{13}^2\sin(lx+\omega_{13}t)}{2f^3(1+\mu_1^2)^{3/2}}$$
$$\left.+\frac{\omega_{22}^2\sin(lx+\omega_{22}t)-\omega_{23}^2\sin(lx+\omega_{23}t)}{2f^3(1+\mu_2^2)^{3/2}}\right\}$$
$$+Wl^2g\left\{\frac{-l\sin(lx+\omega_{21}t)+l\sin(lx+\omega_{11}t)}{\beta f^2\mu_1^2}\right.$$
$$-\frac{\sin(lx+\omega_{12}t)-\sin(lx+\omega_{13}t)}{2f^3(1+\mu_1^2)^{3/2}}$$
$$\left.+\frac{br\left[\sin(lx+\omega_{22}t)-\sin(lx+\omega_{23}t)\right]}{2f^3(1+r)^2(1+\mu_2^2)^{3/2}}\right\}. \tag{5.12}$$

From the above form of the solutions it can be seen that the various contributions consist of a stationary meridional flow and/or the six progressive waves discussed in Section 3. Comparison of the upper and lower layer velocities shows that amplitudes of the barotropic waves in the lower layer are essentially equal to those of the upper layer. The amplitude of the internal wave contributions of the lower layer differ by the factor $-r$. The stationary wave is not present in the lower layer since it is a direct consequence of wind action. With these facts in mind, only upper layer velocities and

surface heights will be discussed in the remaining portion of this section.

As stated earlier, the waves with second subscript equal to unity are the geostrophically balanced Rossby waves (see also Charney, 1955). Representing the geostrophic current motions, they are the features of flow which are ordinarily measurable. The remaining four terms are accelerative effects and have periods of less than a half pendulum day. Thus, for studies of motions with a sufficiently large time scale (say, two weeks or longer), the Rossby waves represent the essential form of the solution.

TABLE II.

Values of ω_i for three values of L.

	L = 200 km	L = 2000 km	L = 8000 km
ω_{11}	6.32×10^{-7} sec^{-1}	6.17×10^{-6} sec^{-1}	1.81×10^{-5} sec^{-1}
ω_{12}	6.22×10^{-3} sec^{-1}	6.3×10^{-4} sec^{-1}	1.91×10^{-4} sec^{-1}
ω_{13}	-6.22×10^{-3} sec^{-1}	-6.3×10^{-4} sec^{-1}	-1.83×10^{-4} sec^{-1}
ω_{21}	2.95×10^{-7} sec^{-1}	5.53×10^{-3} sec^{-1}	1.38×10^{-3} sec^{-1}
ω_{22}	1.37×10^{-4} sec^{-1}	1.03×10^{-4} sec^{-1}	1.13×10^{-4} sec^{-1}
ω_{23}	-1.37×10^{-4} sec^{-1}	$-.97 \times 10^{-4}$ sec^{-1}	$-.87 \times 10^{-4}$ sec^{-1}

The coefficients of the various wave contributions of η_1, η_2 and u_1. The three (vertical) values given for each coefficient are for L = 200, 2000, and 8000 km.

Coefficient of	η_1 (in m)	η_2 (in m)	u_1 (in cm/sec)
	.3	−150	—
cos lx	.3	−150	—
	.3	−150	—
	.0375	3.3×10^{-2}	1.9×10^{-5}
cos($\omega_{11}t+lx$)	.0375	3.3×10^{-2}	1.8×10^{-3}
	.0375	3.3×10^{-2}	2.1×10^{-3}
	.2625	150	.276
cos($\omega_{21}t+lx$)	.2625	150	.54
	.2625	150	.153
	1.8×10^{-6}	1.65×10^{-6}	-9.2×10^{-6}
cos($\omega_{12}t+lx$)	1.8×10^{-6}	1.6×10^{-4}	-9×10^{-4}
	1.8×10^{-6}	-1.6×10^{-4}	-1.1×10^{-2}
	-1.8×10^{-6}	-1.65×10^{-6}	-9.2×10^{-6}
cos($\omega_{13}t+lx$)	-1.8×10^{-6}	-1.6×10^{-4}	-9×10^{-4}
	-1.8×10^{-6}	-1.6×10^{-4}	-1.1×10^{-2}
	2.8×10^{-4}	1.6×10^{-1}	− .11
cos($\omega_{22}t+lx$)	7.3×10^{-5}	4.1×10^{-2}	− .27
	1.8×10^{-5}	1.0×10^{-2}	− .30
	-2.8×10^{-4}	-1.6×10^{-1}	− .11
cos($\omega_{23}t+lx$)	-7.3×10^{-5}	-4.1×10^{-2}	− .27
	-1.8×10^{-5}	-1.0×10^{-2}	− .23

TABLE II. (*Continued*)

The coefficients of the various wave contributions of v_1. The first column represents the $\partial u_1/\partial t$ (or acceleration) contribution to the v_1 term, the second column gives the geostrophic or $g\ \partial\eta/\partial x$ contribution to v_1.

Coefficient of:	v_1 (in cm/sec) ($\partial u_1/\partial t$ contribution)	v_1 (in cm/sec) ($g\ \partial\eta/\partial x$ contribution)
	—	-96
$\sin lx$	—	$-\ 9.6$
	—	$-\ 2.4$
	-1.2×10^{-7}	12
$\sin(\omega_{11}t+lx)$	-1.1×10^{-4}	1.2
	$-\ 4 \times 10^{-3}$	.3
	-8.4×10^{-4}	84
$\sin(\omega_{21}t+lx)$	$-\ 3 \times 10^{-4}$	8.4
	-7.2×10^{-5}	2.1
	5.7×10^{-4}	$-\ .6 \times 10^{-4}$
$\sin(\omega_{12}t+lx)$	5.7×10^{-3}	$-\ 5.7 \times 10^{-3}$
	2.1×10^{-2}	$-\ 1.4 \times 10^{-2}$
	-5.7×10^{-4}	6×10^{-4}
$\sin(\omega_{13}t+lx)$	-5.7×10^{-3}	5.7×10^{-3}
	-1.9×10^{-2}	1.4×10^{-2}
	.19	$-\ 9 \times 10^{-3}$
$\sin(\omega_{23}t+lx)$	.28	$-\ 2.1 \times 10^{-3}$
	.34	$-\ 1.4 \times 10^{-4}$
	$-$ .19	9×10^{-3}
$\sin(\omega_{23}t+lx)$	$-$ .25	2.1×10^{-3}
	$-$ .20	1.4×10^{-4}

Table II gives compilations of the amplitudes of the various wave motions for three separate values of l corresponding to wave lengths of 200, 2000 and 8000 km. The 200 km wave length does not represent any actual wind-driven motions, but it does give a picture of the type of motion which can be expected for such a scale length. The other two cases, i.e., wave lengths of 2,000 and 8,000 km, represent the practical scale limits of wind-driven oceanic motions. The numerical values shown in Table II are based on the physical properties of the ocean (D_1, D_2, b, etc.) prescribed in Section 3. The wind-stress amplitude, taken as 3 dynes/cm^2, corresponds to wind velocities commonly found in storms.

In interpreting the results of Table II, it is necessary to consider the frequencies of the various waves. For example, in the values for surface heights η_1, η_2 and downstream velocity v_1, the amplitudes of the internal Rossby wave and of the standing wave are much larger than any of the other individual amplitudes. However, these two amplitudes differ in sign and, because of the low frequency of the baroclinic

Rossby wave, their net effect is small (comparable in magnitude to the external Rossby wave amplitude) for quite a long period of time. On the other hand, the barotropic Rossby wave, which has a considerably smaller amplitude, actually attains its maximum value after just a few days. For practical purposes, therefore, the geostrophic response of the ocean is a combination of the barotropic and baroclinic modes.

In order to extend the results to storms of finite duration, it is necessary to subtract from the above form of the solution a similar contribution with t replaced by $t - t_0$, where t_0 is the length of time during which the wind acts. From the values of the frequencies it is then clear that the internal Rossby wave does not attain its maximum amplitude for storms of, say, five days duration. The remaining terms execute at least a fourth of one oscillation in that time—that is, their maximum values are attained.

Note that the barotropic long gravity wave amplitude in the velocity terms is always at least an order of magnitude smaller than that of the baroclinic inertial wave. In the lower layer the internal amplitudes are reduced by a factor of $-r = -1/7$ and the two terms may become comparable.

We have separated the magnitudes of the various waves of the downstream velocity v_1 into two sections that correspond to the contributions from the acceleration term $\partial u_1/\partial t$ and the pressure term $g\,\partial\eta/\partial x$ in the first equation of motion:

$$v_1 = \frac{1}{f}\left(\frac{\partial u_1}{\partial t} + g\,\frac{\partial \eta}{\partial x}\right).$$

The purpose of this separation is to compare the relative effects of acceleration and pressure in building up the downwind velocity. As one would expect, the pressure terms are the dominant forces in producing the barotropic and internal Rossby waves, since these motions are essentially geostrophically balanced. However, the high frequency inertio-gravitational motions present an entirely different picture. These motions result primarily from acceleration effects.

Separation of acceleration and pressure terms has resulted in a rather surprising characteristic of the baroclinic inertio-gravitational motions. Rossby (1938) presented an intuitive picture of inertial motions in a homogeneous ocean. He suggested that an unbalanced stream is shifted to the right (in the northern hemisphere) of its downstream direction and that its inertia carries it beyond the equilibrium position to a point where the pressure gradients caused by the resultan

piling up of mass force it back again. The stream thus oscillates about its equilibrium position with a period of a half pendulum day. This intuitive picture was confirmed by the quantitative results of Cahn (1945). In a note following Cahn's paper, Starr (1945) suggested that the extension to a stratified system was relatively simple—that one can extend the results to a baroclinic ocean with relatively minor changes. Inspection of the internal inertial wave amplitudes for v_1 in Table I shows that such an extension is unjustified. It is seen that the Coriolis force is almost completely balanced by the acceleration terms and that neither the free surface nor the interface changes much in this contribution to the flow. *Thus the transient internal motion is purely an inertial motion* of the type such as a bead may execute when constrained to move on a rotating frictionless sphere.

At the outset of the investigation we had the impression that a possible indication of distant storms would be a measure of the change of the interface and that the period of oscillation would be roughly a half pendulum day. However, unless other effects, such as sloping bottom or resonance, contribute to amplification of the interface changes, this quantity would be quite unmeasurable. The velocities[7] resulting from such storms at distant regions are also quite small. Possibly the only noticeable effect would be the amplitude of the barotropic Rossby wave contribution to the free surface height. Perhaps such measurements could be made with tide gauges on isolated oceanic islands.

As stated earlier, the "permanent" current velocity is a combination of the barotropic and internal Rossby wave contributions to the downwind velocity. Rossby's conclusion, viz., that changes in the winds must produce motions which extend to the ocean bottom, is verified here. These velocities are so small, however, that they are comparable only to the slow deep-water drift which results from large sources of heating and cooling. For example, a storm with a scale of 2,000 km, applying a wind stress of 3 dynes/cm^2 to the sea surface, gives rise to a maximum velocity of approximately 1 cm/sec in the deep layers of the ocean (result of barotropic Rossby wave contribution). The maximum value is attained in a period of three days. Thus the maximum possible mixing length attributable to such a storm is approximately 3×10^5 cm. This leads to a coefficient of lateral eddy diffusivity considerably smaller ($3 \times 10^5 \text{cm}^2\text{sec}^{-1}$) than the one assumed by Sverdrup (1939), viz. $10^8 \text{cm}^2\text{sec}^{-1}$. His justification for using such a value is found in the following quotation from his paper (Sverdrup,

[7] Frictionally wind-driven surface velocities would be measurable. However, these are in the direct vicinity of the storm area.

1939: 196): "Rossby (1938) has, however, shown that changes in the winds over the ocean may produce currents reaching from the surface to the greatest depths. All such motions will be directed at random and Rossby's conclusions, therefore, can be interpreted as showing that changing wind conditions may produce variable currents in the deep water, but no flow in a definite direction. If this is the case, a large scale lateral mixing may take place." His reasoning is probably based on the following excerpt from Rossby (1938: 262): "However, since the large scale atmospheric wind systems which drive the ocean circulation change from day to day and from season to season, it is permissible to state with a reasonable degree of assurance, that it is entirely inappropriate to consider the homogeneous bottom water as inert beyond the slow thermal circulation maintained by antarctic cooling."

Both of these statements are qualitatively correct. However, from quantitative considerations these statements appear to be misleading. The deep lateral mixing due to storms is probably negligible on the basis of the present investigation.

A few remarks should probably be made concerning the effect of the change of the Coriolis parameter with latitude. An investigation of a model with constant Coriolis parameter reveals that the geostrophically balanced downwind velocities must increase linearly with time. The essential effect of β is to keep the velocities finite (in the form of moving waves). The two solutions become comparable for sufficiently small values of t (less than a day) where the sinusoidal time-dependent Rossby wave terms can be linearized. In none of the inertio-gravitational wave frequencies does the β term contribute an effect of more than two percent. Therefore the effect of β on inertial oscillations is essentially negligible, whereas its effect on the geostrophically balanced motions is such as to alter the solution completely (from a linear function of time to a moving wave form) for time scales larger than the inertial period.

An important question which has been raised by various authors in the past concerns the amount of energy absorbed by the inertial oscillations when a transient wind blows over the ocean. This question may be partially answered by the present model, although a complete investigation would necessarily embrace many more features than those included here. By restricting our attention to the initial stages of the motion, say, to the first day or so, we may investigate the case of $\beta = 0$ as a good approximation to the present model. The total energy E of the flow between the limits $-L \leq \times \leq L$ and per unit thickness in the y direction may be derived from a combination of equations (2.1) to (2.6) (with $\beta = 0$)

$$D_1 \frac{\rho_1}{2} \int_0^t \int_{-L}^{L} \frac{\partial}{\partial t}\left(u_1^2 + v_1^2 + \frac{g\eta_1^2}{D_1}\right) dydt + \frac{D_2\rho_2}{2} \int_0^t \int_{-L}^{L} \frac{\partial}{\partial t}\left(u_2^2 + v_2^2 + \frac{\Delta\rho g}{D_2}\eta_2^2\right) dydt = \rho_1 \int_0^t \int_{-L}^{L} \tau v_1 dydt .$$

The term on the left represents the total (kinetic and potential) energy of the flow. The right-hand term, the energy input, can be evaluated directly

$$\rho_1 \int_{-L}^{L} \int_0^t \tau v_1 dtdy = \frac{W^2\rho_1 L}{D_1}\left\{\frac{f^2 D_2}{Dp_1^4}(1 - \cos p_1 t) + \frac{f^2 D_1}{Dp^4}(1 - \cos pt) + \frac{1}{2}\left[1 - \frac{f^2 p_2^2}{p^2 p_1^2}\right] t^2\right\} ,$$

where $p^2 = f^2 + gDl^2$, $p_1^2 = f^2 + \dfrac{bgD_1D_2l^2}{D}$, $p_2^2 = f^2 + gD_2l^2$, and $D = D_1 + D_2$. The two sinusoidal terms represent the input energy which is absorbed by the inertio-gravitational motions; the remaining term (t^2) is the geostrophic current energy. For a wave length of 2,000 km, the term $\dfrac{f^2 D_1}{Dp^4}(1 - \cos pt)$ (corresponding to the barotropic inertio-gravitational motions) is negligible as compared to either of the other terms. Hence a comparison of inertio-gravitational energy with geostrophic current energy is afforded by the ratio

$$\frac{E_i}{E_g} = \frac{\dfrac{f^2 D_2}{Dp_1^4}(1 - \cos p_1 t)}{\dfrac{1}{2}[1 - f^2 p_2^2/p^2 p_1^2]t^2} .$$

Time t in this expression is to be interpreted as the time during which energy is added to the system by a wind stress. If the length of time is considerably shorter than a half pendulum day, most of the energy is absorbed by transient oscillatory motions. For times longer than a half pendulum day, the maximum amount of energy is contained in the geostrophic current field. These facts are shown in Fig. 3, which gives the ratio E_i/E_g as a function of time of wind duration for $t < 1$ pendulum day. The graph cannot be carried any

further as a function of time because linearization of the Rossby waves is no longer valid. The tendency, however, is clearly indicated even for the short period shown in Fig. 3.

The case which we have chosen is conducive to strong inertial oscillations. If the wind system were moving with a speed of 10 m/sec, the reverse action of the wind after a day or so would have a destruc-

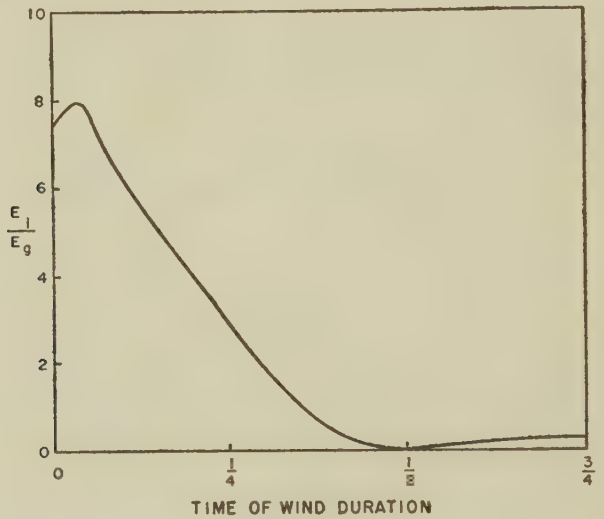

Figure 3

tive influence on the inertio-gravitational motions. However, the transient motions will dominate in the initial period ($< 1/2$ pendulum day) regardless of whether the wind system is moving, unless the frequency of the moving system is unrealistically large. Therefore, for motions with a sufficiently large time scale (> 1 pendulum day), the flow may be considered as essentially quasigeostrophic (Charney, 1955).

6. APPLICABILITY OF THE MODEL TO THE OCEAN

There are several questions concerning the applicability of the present model to the ocean which merit particular consideration: (1) To what extent are variable motions in the ocean independent of the presence of boundaries? (2) How justifiable is the neglect of friction? (3) Are other forces such as atmospheric pressure important in setting up oceanic currents? and (4) What are the effects of bottom topography on the induced motions?

(1) The disturbance set up by an instantaneous change in wind is propagated toward the boundaries in the form of waves. The length of time required for the influence of the boundaries to become evident at an interior point of the ocean therefore depends upon the time required for a wave to move from that point to the boundary. Since the wave velocities differ for each mode of motion, strict application of the model is limited by the time it takes the fastest wave (barotropic gravity wave) to reach the coast (a matter of a few hours). However, there are two reasons for assuming that the essential results of this model would not be affected by coastal influences for a considerably longer period. First, there is no interaction between the various modes in the interior of the ocean and there is no reason to suppose that there is any interaction between the transient and Rossby modes at the coast. Therefore, so far as the balanced motion is concerned, the model may be used in the interior of the oceans for the time it takes a barotropic Rossby wave to reach the coast (a matter of a few days). Second, the amount of energy contained in the transient motions is considerably smaller than that in the balanced motions. The reflection of this energy from the coasts would exert a relatively negligible influence on any observable motions. It seems likely, therefore, that the geostrophically balanced motion of the real ocean should respond to a three or five day storm much like the theoretical model—that is, during the "active phase" or life time of a central oceanic storm, the effect of coastal boundaries should be negligible.

It is clear that, for periods longer than a week, the barotropic Rossby mode of motion may be strongly influenced by the coasts. The length of time over which the internal Rossby mode is unaffected by the coasts could be as much as several years were it not for the uncertainty as to whether the two Rossby modes can interact at the coasts. There is a possibility that the proper boundary conditions are nonlinear in a coastal current such as the Gulf Stream, in which case there might be an interaction between the barotropic and baroclinic Rossby modes. This is the reason why we hesitate to extend the discussion of the internal Rossby mode to wind fluctuations of a seasonal time scale.

If there is, in fact, no interaction between Rossby modes at the coasts, this model leads us to the conclusion that equilibrium adjustment of the main thermocline in the central ocean does not occur even in response to wind variations with periods as long as a year.

(2) The effect of friction is neglected in the model under discussion, and it is important to form some estimate of the frictional force. For bottom friction, Proudman (1953) gives the frictional force on the ocean

bottom as $F = -k\,\rho u^2$, where $k = 2 \times 10^{-3}$. The bottom velocities involved in the models under discussion are less than those due to deep sea tides. The amplitude of the tidal velocity U may be regarded as purely periodic, in which case the resultant frictional force due to a long period deep sea velocity component u is simply $F = -2k\,U\,u$. If the bottom layer is of depth D, then the time constant K of the frictional damping of the lower layer velocity is $K = kU/D$. Taking representative values $k = 2 \times 10^{-3}$, $U = 2$ cm sec^{-1}, $D = 4 \times 10^5$ cm, one calculates $K = 10^{-8}$sec^{-2}. Thus the length of time necessary for destruction of the velocity of the bottom layer by bottom friction is approximately three years.

The time constant involved in lateral friction is $K' = Al^2$, where l is the wave number and A the coefficient of lateral eddy viscosity. For the largest scale phenomena in the deep sea (Sverdrup, 1939), it appears that a largest possible limit of A is 10^8cm^{2}sec^{-1}. Taking $l = 1/2 \times 10^{-8}$cm^{-1}, the time constant becomes $K' = 0.25 \times 10^{-8}$. Thus lateral friction of the most intense sort can destroy motion in these models in the bottom layer only after 12 years. The conclusion is that the frictionless models are justified only for periods up to about one year, and that physically they should include friction explicitly for longer periods.

(3) There are other surface stresses which may affect the response of the ocean also. These are the variations of atmospheric pressure and the divergence of the wind stress. (The latter term is approximately an order of magnitude smaller than the curl of the wind stress.) Neither of these driving terms contributes to the current motions, but they tend only to increase the transient motions in the ocean. For this reason they have not been considered, although any thorough study of inertial oscillations would necessarily entail a detailed study of these effects.

(4) The effect of bottom topography has been neglected altogether. Perhaps there is no other justification for excluding this feature than the fact that the analysis is quite complex when it is included. It is conceivable that its effect may be important, particularly for the stratified ocean.

7. SUMMARY AND CONCLUSIONS

We have investigated the response of an infinite rotating ocean of finite depth to a transient wind stress applied at the sea surface. The density structure, an idealization of the observed stratification, consists of two layers of homogeneous water. The variation β of the Coriolis parameter f with latitude is included in the equations by taking $\beta = df/dy$ = constant; elsewhere, f is assumed to be constant.

By using normal modes, the equations of motion of a two layer system can be reduced to a vorticity equation in a single variable whose highest order derivative is of the same order as that in the homogeneous system. The vorticity equation contains two separate types of motion corresponding to the two modes of oscillation in the system. In the barotropic case the motion is uniform vertically. The second type, baroclinic motion, occurs when the lower layer responds in such a manner as to offset the pressure gradient caused by deviations of the free surface from its equilibrium position.

Substitution of a moving wave solution in the homogeneous vorticity equation yields a frequency equation which shows that six different types of waves may be excited in the system. Two of the waves, the barotropic and baroclinic Rossby waves, represent the motions which are in geostrophic balance. The remaining four waves (two barotropic and two baroclinic) represent inertio-gravitational motions which result from incomplete balance between pressure and Coriolis forces. Behavior of the latter waves is dependent on both the Coriolis parameter and the static parameters (depth, density, gravity) of the system. Generally, however, the barotropic waves are pure gravity waves travelling with speed $\sqrt{gD}$, and the internal waves are pure inertial waves with a period of a half pendulum day, $2\pi/f$.

Two types of wind-driven motions are treated. The forced motions caused by a moving wave system with a scale comparable to atmospheric patterns as given by five-day mean charts are investigated by assuming a driving force of the type $W \sin(lx + \nu t)$, with $W = 1$ cm^2 sec^{-1}. The resultant motions may be studied by considering three separate ranges of period of the driving wind.

For periods of one to seven weeks (comparable to the barotropic Rossby wave period), the ocean responds principally as a homogeneous body of water. The baroclinic effects increase in importance with longer period.

For longer periods (up to a year, thus lying between the barotropic and baroclinic Rossby wave period) the motion is partly barotropic although the effects of baroclinity are more prominent. The upper layer downwind velocity is approximately half barotropic-half baroclinic when the wind period is a year for the scale chosen. The other variables are effected less by the baroclinity.

When the wind period is long (at least 100 years) the motion is purely baroclinic. The flow is geostrophic and the total transport is equal to that given by Munk for the steady-state model.

The second type of wind-driven motions treated here is that caused by a nonmoving wind which varies sinusoidally in space and which

begins impulsively at some time. In this case all of the possible free wave motions of the system occur, and one can study the relative importance of the inertio-gravitational and geostrophically balanced motions.

When the wind acts for a period of time comparable to the life of a storm, the geostrophically balanced motion is partially external and partially internal. The precise partition of the energy between the two modes depends on the scale of the motion. The thermocline therefore responds to the action of the wind stress and may be measurable (of the order of 10 to 20 m) when the wind blows for three days or more. The currents set up in the deep layers are small and are probably no stronger than the slow thermal currents resulting form antarctic cooling. Consequently, as a result of storms there is probably no mechanism for the formation of large-scale lateral mixing in the oceanic stratosphere.

The isostatic inertio-gravitational motions are much larger than the barotropic inertio-gravitational motions. However, they are not accompanied by any measurable movement of the thermocline; instead, they are purely horizontal inertial motions. In a stratified ocean, therefore, the observed inertial oscillation is not accompanied by pressure gradients resulting from excess piling up of water. Instead, it is mainly a lateral movement with an oscillation caused by the earth's rotation only.

From the present simple analysis, the essential effect of β in a transient problem is to amplify the baroclinic mode for large periods.

A simple investigation of the relative amounts of energy contained in the inertio-gravitational and geostrophically balanced flow indicates that, so long as the wind blows for more than a half pendulum day, most of the energy is contained in the geostrophically balanced flow. For winds of shorter duration the energy is expended in inertio-gravitational motions.

BIBLIOGRAPHY

Bolin, B.

1953. The adjustment of a non-balanced velocity field towards geostrophic equilibrium in a stratified fluid. Tellus, *5* (3): 373–385.

Cahn, A.

1945. An investigation of the free oscillations of a simple current system. J. Meteor., *2* (2): 113–119.

Charney, J. G.

1955. The generation of ocean currents by wind. J. Mar. Res., *14* (4): 477–498.

Freeman, J. C.

1954. Note on a prediction equation for the surface layer of a two-layer ocean. Trans. Amer. geophys. Un., *35* (4): 585–587.

Groves, G. W.
1954. Dynamic model of a two-layer ocean under influence of atmosphere and coastal boundary. Tech. Rept. No. 54–22, Scripps Institution of Oceanography, 27 pp.
Ichiye, T.
1951. On the variation of oceanic circulation. Oceanogr. Mag., *3* (2): 79–82.
Munk, W. H.
1950. On the wind-driven ocean circulation. J. Meteorol., *7* (2): 79–93.
Proudman, J.
1953. Dynamical Oceanography. London Methuen, London. 409 pp.
Reid, R. O.
1948. The equatorial currents of the eastern Pacific as maintained by the stress of the wind. J. Mar. Res., *7* (2): 74–99.
Rossby, C. G.
1938. On the matual adjustment of pressure and velocity distribution in certain simple current systems, II. J. Mar. Res., *1:* 239–263.
1949. On the dispersion of planetary waves in a barotropic atmosphere. Tellus, *1:* 54–58.
Starr, J.
1945. Note on inertial oscillations. J. Meteorol., *2* (2): 120–122.
Stockmann, W. B.
1946. Equations of the field of integrated currents caused by the wind in a non-homogeneous ocean. Doklady Akad. Nauk. SSSR, *54* (5): 403–406.
Stommel, Henry
1948. The westward intensification of wind-driven ocean currents. Trans. Amer. geophys. Un., *29* (2): 202–206.
Sverdrup, H. U.
1926. Dynamic of tides on the North Siberian shelf. Geofys. Publ., *4* (5): 75 pp.
1939. Lateral mixing in the deep water of the South Atlantic Ocean. J. Mar. Res., *2* (3): 195–207.
1947. Wind-driven currents in a baroclinic ocean; with application to the equatorial currents of the eastern Pacific. Proc. Nat. Acad. Sci., *33* (11): 318–326.
Veronis, G.
1956. Partition of energy between geostrophic and non-geostrophic oceanic motions. Deep-Sea Res., *3* (3): 157–177.
Veronis, G. and G. W. Morgan
1955. A study of the time-dependent wind-driven ocean circulation. Tellus, *7* (2): 232–242.
Yeh, T.
1949. On energy dispersion in the atmosphere. J. Meteor., *6* (1): 1–16.

A LIGHT-SCATTERING DIAGRAM[1]

By

WAYNE V. BURT

Department of General Science, Oregon State College
Corvallis, Oregon

ABSTRACT

A diagram is presented which shows the light scattering effectiveness of small particles when they are suspended in water. The effective scattering is plotted as a function of the radius of the particles (0.005 to 5 μ), of the wave length of the energy being scattered (0.35 to 0.8 μ), and of the relative refractive index of the material in the particle when compared to water (1.02 to 1.40). The diagram covers the range of variables for most fine materials which are found suspended in natural waters.

INTRODUCTION

It is of interest to oceanographers and limnologists to be able to estimate the effectiveness of various types and sizes of naturally suspended materials in the scattering of solar energy in water. Such estimates may be used in the study of the light budget for photosynthesis, in underwater visibility studies, and when working with actions of phototropic organisms. Furthermore, relative scattering and related extinction have been used to characterize and trace water masses (Jerlov, 1953; Joseph, 1953) and to determine something about the size range and concentration of suspended materials (Burt, 1954, 1955a, 1955b).

The literature on theoretical results and practical applications of light scattering is found in publications in many fields. Often information is presented in a form which is applicable to a single problem and which may cover such a narrow range of variables that it is of use to that problem alone. In other cases, information is presented in forms which are difficult or impossible to assimilate without extensive training in mathematics and physics.

This note has been written in order to make available to aquatic researchers a reference diagram which will show at a glance some of the effects of the various independent variables on light scattering. More detailed and exact information, if desired, can be obtained for certain conditions from the references (Gumprecht and Sliepcevich, 1951: 3–8; Van de Hulst, 1946; Sinclair and LaMer, 1949).

[1] This work has been supported by Office of Naval Research, Contract Nonr 1286(02) Project NR 083–102, and Oregon State College.

SCATTERING DIAGRAM

The relative ability of particles to scatter light is usually given in terms of their effective area scattering coefficient, K_s, or their efficiency factor. It is defined as the dimensionless number by which the geometric cross-sectional area of a particle (in the plane perpendicular to the direction in which the original direct light beam, or pencil, is traveling) must be multiplied in order to determine its effectiveness in deflecting light from a direct beam by processes of scattering. Thus, K_s is a nondimensional number equal to the energy scattered from the incident beam divided by the energy of the pencil that is geometrically obstructed by the particle. Lines of constant K_s, plotted in the upper part of Fig. 1, range in numerical value from 10^{-7} to 3.75.

The ordinate in the upper part of Fig. 1 is the relative refractive index of the material in the particles. It is found by dividing the refractive index of the material in air (as published in reference tables) by 1.33, the average refractive index of water. The range of the relative refractive indices of some of the particulate matter found in natural waters is shown on the right ordinate (Clay minerals from Grim, 1939; Bacteria and the range of other inorganic materials from Bennett, *et al.*, 1951: 320, table V. 1).

The abscissa in the lower part of Fig. 1 is the radius of the particles in microns. The numerical value of the radius for any position on the abscissa is a function of the wave length of the energy being scattered. Thus, monocromatic light is scattered at different rates depending upon what part of the spectrum it comes from. For example, the position on the abscissa corresponding to particles with radii of 1μ for energy in the infra-red at a wave length of 0.8μ is the same as the position for particles with radii of only 0.45μ for energy in the ultra-violet at a wave length of 0.35μ. Each part of the solar spectrum must be considered separately due to the wave length effect.

The effective area coefficient is obtained from the diagram by entering with the wave length in the left-hand side of the lower diagram or with the color of light in the right-hand side, crossing horizontally to the proper radius and then moving vertically to the relative refractive index of the material in the upper diagram. The effective area coefficient is then read or interpolated for this position on the graph. For example, bacteria with a relative refractive index of 1.10 and a radius of 1μ would have an effective area coefficient ranging from 3.4 for blue light down to 2.4 for red light. The range in effective area coefficient values for fine clay with a radius of 0.1μ would

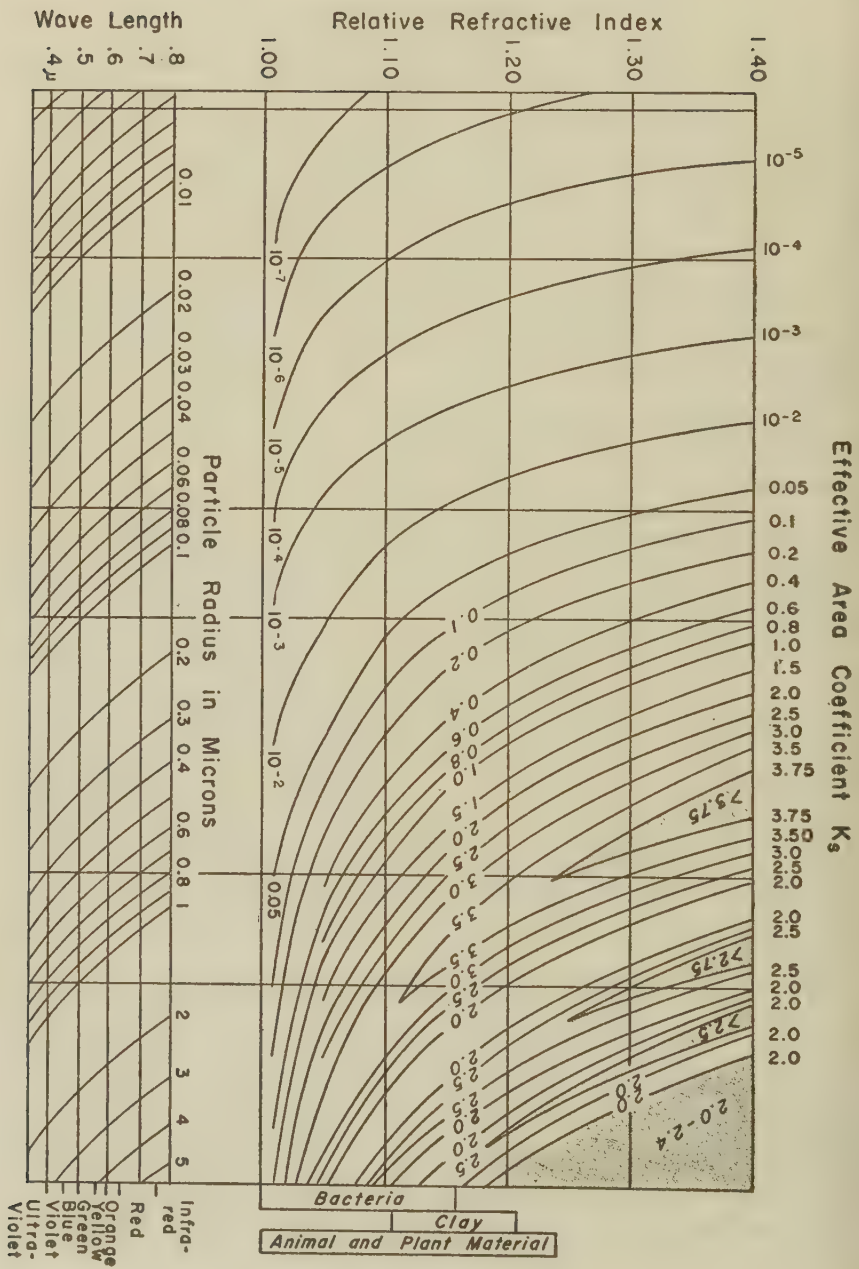
Wave Length
.4μ .5 .6 .7 .8
Relative Refractive Index
1.00 1.10 1.20 1.30 1.40
Particle Radius in Microns
0.01 0.02 0.03 0.04 0.06 0.08 0.1 0.2 0.3 0.4 0.6 0.8 1 2 3 4 5
Effective Area Coefficient Ks
Ultra-Violet
Violet
Blue
Green
Yellow
Orange
Red
Infra-red
Bacteria
Clay
Animal and Plant Material

Figure 1

be 10^{-2} to 0.4 depending on the relative refractive index of the clay and the wave length of the light being scattered.

Note that the effectiveness of particles as scatterers for radii up to about 0.5μ increases directly with the size of the particle and the relative refractive index of the material and inversely as the wave length of the light being scattered. For particles above approximately 0.5μ, the scattering may vary directly or inversely with size, wave length, or relative refractive index, depending upon the position on the diagram. For particles with radii above 5μ, variations in numerical value of the effective area coefficient become less and less with a tendency toward a constant value of 2.0.

The direction of scattering is isotropic for very small particles (left-hand side of diagram). As the particle increases in size, scattering becomes directional. One pronounced effect of the directionality is that a sizable proportion of scattered energy tends to travel in a nearly forward direction.[2] For the larger particles (right-hand side of the diagram), as much as 40% of the scattered energy is concentrated within a cone of only 7° in half angle centered about the direction in which the original light beam was traveling (Gumprecht and Sliepcevich, 1952: table 1).

SOURCES

Scattering by particles much smaller than the wave length of light was computed from Rayleigh's Law (Van de Hulst, 1946: 17). Scattering in the size range of light waves for material with relative refractive indices of 1.20 and greater was interpolated from plots in the tables of Gumprecht and Sliepcevich (1951: 3–6). Van de Hulst's equation (1946: 58) was used to compute scattering for particles with relative refractive indices near unity. Intermediate values were interpolated.

REFERENCES

Bennett, A. H., H. Osterberg, H. Jupnik and O. W. Richards
1951. Phase microscopy. John Wiley and Sons, Inc., New York. 320 pp.

Burt, W. V.
1954. Specific scattering by uniform minerogenic suspensions. Tellus, *6:* 229–231.

[2] To obtain a maximum amount of use from the Mie theory it would be highly desirable to have information on that portion of the light which is scattered in a backward direction only. However, the preparation and presentation in graphical form of such information is not possible without considerable additional study for the range of variables shown in the diagram herewith. An effort to prepare such a diagram or set of diagrams is planned for the future.

1955a. Interpretation of spectrophotometer readings on Chesapeake Bay waters. J. Mar. Res., *14* (1): 33–46.

1955b. Distribution of suspended materials in Chesapeake Bay. J. Mar. Res., *14* (1): 47–62.

GRIM, R. E.

1939. Properties of clay (pp. 466–495) in Recent marine sediments, edited by Parker Trask. 736 pp.

GUMPRECHT, R. O. and C. M. SLIEPCEVICH

1951. Tables of light scattering functions for spherical particles. Engng. Res. Inst., Univ. Mich., Ann Arbor. 574 pp.

1952. Scattering of light by large spherical particles. J. phys. Chem., *57* (1): 90–95.

JERLOV, N. G.

1953. Particle distribution in the ocean. Rep. Swedish deep-sea expedition, 1947–1948, *3* (3): 73–97.

JOSEPH, JOACHIM

1953. Die trubungsverhaltnisse in der sudwestlichen Nordsee. Wahrend der "GAUSS" Fahrt in Februar/Marz 1952. Ber. dtsch. Komm. Meeresforsch., *13* (2): 93–102.

SINCLAIR, DAVID and V. K. LAMER

1949. Light scattering as a measure of particle size in aerosols. Chem. Rev., *44* (2): 245–267.

VAN DE HULST, H. C.

1946. Optics of spherical particles. Rech. astr. Obs. Utrecht, *11* (1): 87 pp.

A METHOD FOR DETERMINING MEAN LONGITUDINAL VELOCITIES IN A COASTAL PLAIN ESTUARY[1]

By

D. W. PRITCHARD and RICHARD E. KENT

Chesapeake Bay Institute, The Johns Hopkins University

ABSTRACT

It is shown that the longitudinal component of the mean velocity in a coastal plain estuary may be computed by indirect methods. To do this, use is made of the lateral and longitudinal components of the equation of motion, the tidal velocity amplitudes, and a deduced relationship between the vertical and lateral eddy stresses. The method is evaluated for a station in the James River estuary. The resultant computed velocities agree quantitatively with the corresponding observed velocities.

Consider a coastal plain estuary in which there exists a mean circulation pattern similar to that shown schematically in Fig. 1. Here the two-dimensional flow pattern consists of a seaward directed flow in the upper portion of the water column and a landward directed flow in the lower portion. This estuarine system has been studied in detail by Pritchard (1952, 1954, 1956), who showed that:

a) the salt balance is maintained primarily by a longitudinal advective salt flux and a vertical nonadvective salt flux,
b) the mean field acceleration terms are small compared with other terms in the equation of motion, and
c) the horizontal and lateral components of the mean equation of motion are given essentially by balances between the forces of pressure, eddy friction, and tidal acceleration; and pressure, eddy friction, and Coriolis, respectively. Thus,

$$U_0 \frac{\partial U_0}{\partial x_1} = - <\alpha \frac{\partial p}{\partial x_1}>_0 + b_0 - \frac{\partial}{\partial x_2} <v_2' v_1'>, \tag{1}$$

and

$$0 = - <\alpha \frac{\partial p}{\partial x_3}>_0 + b_0' + f\bar{v}_1 - \frac{\partial}{\partial x_2} <v_2' v_3'>. \tag{2}$$

A left-handed co-ordinate system is used in which the x_1, x_2, and x_3-axes are directed horizontally seaward, vertically downward, and

[1] Contribution No. 26 from the Chesapeake Bay Institute. This work was supported by the Office of Naval Research, the State of Maryland (Department of Research and Education), and the Commonwealth of Virginia (Virginia Fisheries Laboratory).

laterally across the estuary, respectively. The symbols used in (1) and (2) have the following meanings:

$< \quad >$	designates a time mean taken over one or more tidal cycles. (A superscript bar has the same meaning.)
$-<\alpha \frac{\partial p}{\partial x_1}>_0, \quad -<\alpha \frac{\partial p}{\partial x_3}>_0$	denote the longitudinal and lateral components, respectively, of the mean pressure force at any depth x_2 relative to the pressure force at the surface.
b_0, b_0'	are the longitudinal and lateral components, respectively, of the mean pressure force at the surface.

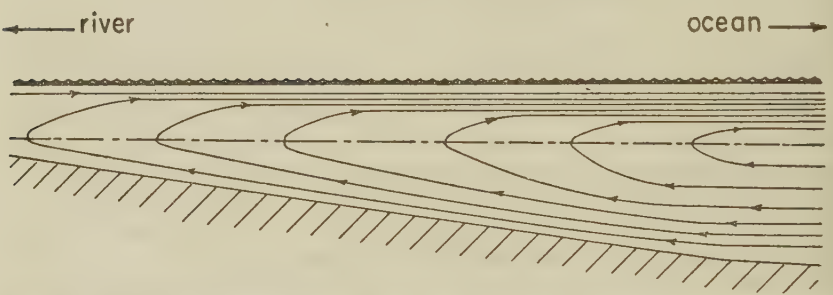

Figure 1. Schematic presentation of the mean circulation pattern in the axial section of the estuary.

U_0	is the tidal velocity amplitude.
$\bar{v}_1$	is the longitudinal component of the mean velocity.
$\bar{s}$	is the mean salt content.
$<v_2'v_1'>, \quad <v_2'v_3'>$	denote the eddy stresses in which v_1', v_2', and v_3' are random deviations from the mean velocities $\bar{v}_1$, $\bar{v}_2$, and $\bar{v}_3$.
R	is the volume rate of freshwater inflow from the river.
w, h	are the width and depth, respectively, of the estuary.

It will be demonstrated through momentum equations (1) and (2) that the mean longitudinal velocity $\bar{v}_1$ as a function of depth can be determined if we know the mean distributions of temperature and salinity, the variation of the tidal velocity amplitude along the estuary, the relationship between the eddy stresses $<v_2'v_1'>$ and $<v_2'v_3'>$, and the magnitudes of these stresses near the bottom of the estuary.

Before proceeding with the formal determination of $\bar{v}_1$ let us consider the evaluation of (1) and (2) for the eddy stresses $<v_2'v_1'>$ and $<v_2'v_3'>$ as well as the evidence that suggests a relationship between these terms.

Since the pressure force components $-<\alpha\frac{\partial p}{\partial x_1}>_0$ and $-<\alpha\frac{\partial p}{\partial x_3}>_0$ can be determined as functions of depth from the distributions of temperature and salinity, it is possible to solve (1) and (2) for $<v_2'v_1'>$ and $<v_2'v_3'>$ providing two boundary values of the stress terms are known. It is assumed here that the wind stress on the surface will give one boundary value of the stress terms. The boundary condition employed for evaluation of the bottom stress stems from two sources: (1) from velocity measurements made by Lesser (1951) near the bottom at several open ocean locations which showed that in the lowest meter of water the velocity-depth variation was logarithmic and that the Prandtl-von Karman boundary layer theory was applicable; and (2) from our measurements in the James River estuary which showed that the region of rapid velocity decrease begins about one meter from the bottom, with the vertical gradient of the mean velocity going to zero at this depth. Pritchard (1955) evaluated eq. (1) for the stress term $<v_2'v_1'>$ and found it equal to zero at one meter from the bottom. In view of Lesser's and Pritchard's results we make the assumptions that the surface values of $<v_2'v_1'>$ and $<v_2'v_3'>$ are given by the appropriate component of the surface wind stress and that these terms pass through the value zero at a distance of one meter from the bottom.

Using these two boundary conditions, the eddy stresses $<v_2'v_1'>$ and $<v_2'v_3'>$ were obtained from (1) and (2) for a station located in the James River estuary. Mean values of temperature, salinity, and velocity observations taken during the period 18–23 June 1950 were employed in the evaluation. The computed values of $<v_2'v_1'>$ and $-<v_2'v_3'>$ are shown as functions of depth in Fig. 2. Also shown is $<v_2'v_1'>$ multiplied by a constant (0.56). The similarity between the latter curve and that for $-<v_2'v_3'>$ suggests the relationship

$$<v_2'v_3'> = \eta<v_2'v_1'>, \tag{3}$$

where η is a constant.

For natural turbulent systems there exists little independent observational support of the hypothesis expressed by eq. (3). However, Fleagle and Badgley (1952) have measured the stress terms $<v_2'v_1'>$ and $<v_2'v_3'>$ in the atmosphere at an elevation of two meters. Their results yield a value of η equal to -0.45. As will be shown subse-

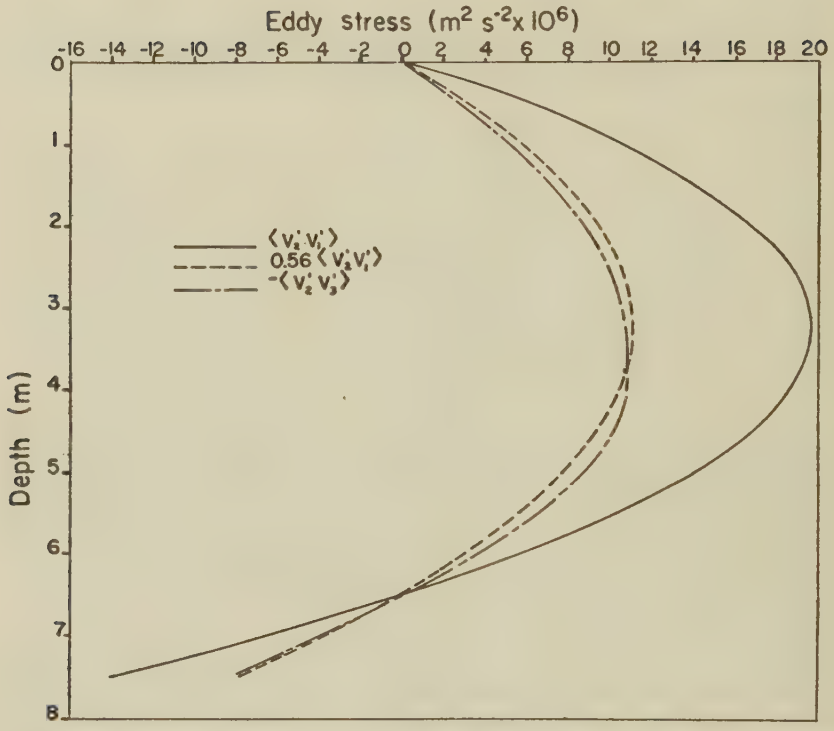

Figure 2. Computed values of $<v_2'v_1'>$, $0.56<v_2'v_1'>$ and $-<v_3'v_2'>$ as functions of depth.

quently, this value of η compares favorably with that calculated from the James River data.

Determination of $\bar{v}_1$ as a Function of Depth. A step-wise procedure by means of which the mean longitudinal velocity $\bar{v}_1$ can be determined will now be presented.

Substitution of eq. (3) into eq. (2) gives

$$0 = -<\alpha \frac{\partial p}{\partial x_3}>_0 + b_0' + f\bar{v}_1 - \eta \frac{\partial}{\partial x_2} <v_2'v_1'>. \tag{4}$$

Applying the equation of continuity in the form

$$\int_0^h w\bar{v}_1 dx_2 = R \tag{5}$$

to eq. (4) yields

$$(6)\quad 0 = -\int_0^h w<\alpha\frac{\partial p}{\partial x_3}>_0 dx_2 + b_0'\int_0^h w dx_2 + f\cdot R - \eta\int_0^h w\frac{\partial}{\partial x_2}<v_2'v_1'>dx_2 .$$

Similarly, applying the concept of salt conservation in the form

$$(7)\qquad \int_0^h w\bar{v}_1\bar{s}dx_2 = 0$$

to eq. (4) yields

$$(8)\quad 0 = -\int_0^h w\bar{s}<\alpha\frac{\partial p}{\partial x_3}>_0 dx_2 + b_0'\int_0^h w\bar{s}dx_2 - \eta\int_0^h w\bar{s}\frac{\partial}{\partial x_2}<v_2'v_1'>dx_2 .$$

Equations (1), (4), (6), and (8) are utilized as follows:

a) $<\alpha\frac{\partial p}{\partial x_1}>_0$ and $<\alpha\frac{\partial p}{\partial x_3}>_0$ are evaluated from the observed temperature and salinity fields.

b) $U_0\frac{\partial U_0}{\partial x_1}$ can be evaluated from the Coast and Geodetic Survey tidal current tables.

c) Using the given boundary values of $<v_2'v_1'>$, eq. (1) can be expressed as

$$(9)\qquad b_0 = \frac{\int_0^{h-1}\left\{U_0\frac{\partial U_0}{\partial x_1} + <\alpha\frac{\partial p}{\partial x_1}>_0\right\}dx_2}{\int_0^{h-1} w dx_2},$$

hence b_0 is determinable.

d) Knowing $U_0\frac{\partial U_0}{\partial x_1}$, $<\alpha\frac{\partial p}{\partial x_1}>_0$, and b_0, the term $<v_2'v_1'>$ can be obtained from eq. (1).

e) All of the integral terms in (6) and (8) now can be evaluated and hence both equations can be solved simultaneously for the constants b_0' and η.

f) As an additional check on the last calculation we note that, since $<v_2'v_1'> = \frac{\partial\bar{v}_1}{\partial x_2} = 0$ one meter from the bottom, eq. (4) yields

Figure 3a (left). Theoretical and observed values of the mean longitudinal velocity as a function of depth for the period 18–23 June 1950 at Station J-17.

Figure 3b (right). Theoretical and observed values of the mean longitudinal velocity as a function of depth for the period 26 June–7 July 1950 at Station J-17.

$$\eta = \frac{\left[\frac{\partial}{\partial x_2} < \alpha \frac{\partial p}{\partial x_3} >_0\right]_{h-1}}{\left[\frac{\partial^2}{\partial x_2^2} < v_2' v_1' >\right]_{h-1}}. \tag{10}$$

g) Eq. (4) now can be solved for $\bar{v}_1$, the required quantity.

Serial observations of temperature and salinity obtained in the James River estuary for periods 18–23 June 1950 and 26 June–7 July 1950 were used in solving for $\bar{v}_1$ in the described manner. Figs. 3a and 3b show the calculated velocities as a function of depth for both periods. Also shown are the corresponding velocities observed at six depths. It is seen that agreement between the theoretical and observed velocities is quite good. Computed values of η and b_0' for two periods at Station J-17 in the James River estuary are as follows:

Period	η (*eqs. 6, 8*)	η (*eq. 10*)	b_0' $m \cdot s^{-2} \times 10^6$
18–23 June 1950	−0.43	−0.32	−16.54
26 June–7 July 1950	−0.38	−0.33	−17.32

The values of η were obtained from the simultaneous solutions of (6) and (8) and were determined also by (10). It is interesting to note that the average value of η obtained from the simultaneous solution of (6) and (8) compares favorably with the value −0.45 obtained from the data of Fleagle and Badgley.

An example of the procedure followed in computing $\bar{v}_1$ from eq. (4), along with the pertinent data, is given in Tables I–IV. Thus: Table I evolves the lateral component of the mean pressure force, $< \alpha \frac{\partial p}{\partial x_3} >_0$;

Table II the gradient of the vertical eddy stress, $\frac{\partial}{\partial x_2} < v_2' v_1' >$;

Table III the parameters η and b_0'; and

Table IV shows finally the evaluation of eq. (4) for the mean longitudinal velocity $\bar{v}_1$ (Fig. 3a).

TABLE I. EVALUATION OF $-<\alpha \frac{\partial p}{\partial x_3}>_0$ FROM THE MASS FIELD FOR THE PERIOD 18–23 JUNE 1950 AT STATION J–17 IN THE JAMES RIVER ESTUARY.

	Station J–17 A			*Station J–17 B*			*Station J–17*	
Depth m	$\bar{S}$ $gm^{-3} \times 10^3$	T °C	$(\Delta D)_0$ m^2s^{-2}	$\bar{S}$ $gm^{-3} \times 10^3$	T °C	$(\Delta D)_0$ m^2s^{-2}	$\frac{\partial}{\partial x_3}(\Delta D)_0$ $ms^{-2} \times 10^6$	$-<\alpha \frac{\partial p}{\partial x_3}>^0$ $ms^{-2} \times 10^6$
0.0			0.00000			0.00000	0.00	
	10.58	24.7		11.41	24.7			1.14
0.5			0.01112			0.01082	2.29	
	10.66	24.6		11.53	24.6			3.47
1.0			0.02220			0.02159	4.66	
	10.68	24.5		11.60	24.5			5.99
1.5			0.03326			0.03230	7.33	
	10.68	24.4		11.64	24.4			8.66
2.0			0.04431			0.04300	10.00	
	10.70	24.3		11.69	24.3			11.37
2.5			0.05534			0.05367	12.75	
	10.83	24.2		11.85	24.2			14.20
3.0			0.06631			0.06426	15.65	
	11.52	24.1		12.54	24.1			17.10
3.5			0.07701			0.07458	18.55	
	11.86	24.0		12.85	24.0			19.96
4.0			0.08757			0.08477	21.37	
	12.98	23.9		13.92	23.9			22.71
4.5			0.09770			0.09455	24.05	
	13.26	23.8		14.10	23.8			25.22
5.0			0.10771			0.10425	26.41	
	13.45	23.8		14.15	23.8			27.36
5.5			0.11765			0.11394	28.32	
	13.63	23.7		14.16	23.7			29.04
6.0			0.12751			0.12361	29.77	
	13.84	23.7		14.24	23.7			30.26
6.5			0.13728			0.13325	30.76	
	14.23	23.6		14.30	23.6			30.84
7.0			0.14691			0.14286	30.92	
	14.57	23.6		14.57	23.6			30.92
7.5			0.15641			0.15236	30.92	

1. When looking seaward, Stations J–17A and J–17B are laterally to the right and left, respectively, of Station J–17. The distance separating J–17A and J–17B is 1.31×10^3 m.

2. $[(\Delta D)_0]_{x_2} = \int_0^{x_2} \delta dp$, where $\delta = f(s_{17}, x_3)$.

3. $\left(\frac{\alpha}{10} \frac{\partial p}{\partial x_3}\right) = \frac{\partial}{\partial x_3}(\Delta D)$.

TABLE II. Evaluation of $\frac{\partial}{\partial x_2}\langle v_2'v_1'\rangle$ as a Function of Depth for the Period 18–23 June 1950 at Station J–17 in the James River Estuary

Depth m	$\langle \alpha \frac{\partial p}{\partial x_1} \rangle$ $ms^{-2} \times 10^6$	$\langle \alpha \frac{\partial p}{\partial x_1} \rangle_0 + U_0 \frac{\partial U_0}{\partial x_1}$ $ms^{-2} \times 10^6$	$\langle -\alpha \frac{\partial p}{\partial x_2} \rangle$ $ms^2 \times 10^6$	$\frac{\partial}{\partial x_2}\langle v_2'v_1' \rangle$ $ms^{-2} \times 10^6$	$\langle v_2'v_1' \rangle$ $ms^{-2} \times 10^6$
0					0.00
	0.89	3.86	14.17	11.20	
.5					5.60
	2.75	5.72	12.31	9.34	
1.0					10.27
	4.63	7.60	10.43	7.46	
1.5					14.00
	6.50	9.47	8.56	5.59	
2.0					16.80
	8.36	11.33	6.70	3.73	
2.5					18.66
	10.22	13.19	4.84	1.87	
3.0					19.60
	12.09	15.06	2.97	0.00	
3.5					19.60
	13.96	16.93	1.10	−1.87	
4.0					18.66
	15.83	18.80	−0.77	−3.74	
4.5					16.79
	17.68	20.65	−2.62	−5.59	
5.0					14.00
	19.57	22.54	−4.51	−7.48	
5.5					10.26
	21.41	24.38	−6.36	−9.32	
6.0					5.60
	23.28	26.25	−8.22	−11.19	
6.5					0.00
	25.11	28.08	−10.05	−13.02	
7.0					−6.51
	26.96	29.93	−11.90	−14.87	
7.5					−13.95

1. $U_0 \frac{\partial U_0}{\partial x_1} = 2.97 \times 10^{-6}\ ms^{-2}$.

2. $b_0 = \frac{\sum_0^{h=1} \left[\langle \alpha \frac{\partial p}{\partial x_1} \rangle_0 + U_0 \frac{\partial U_0}{\partial x_1} \right] a x_2}{(h-1)} = \frac{195.78 \times 10^{-6}}{13} = 15.06 \times 10^{-6}\ ms^{-2}$.

3. Assume $\langle v_2'v_1' \rangle_0 = \langle v_2'v_1' \rangle_{h-1} = 0$.

TABLE III. Evaluation of Equations (6) and (8) for b' and η for the Period 18–23 June 1950 at Station J–17 in the James River Estuary

Depth m	$\bar{S}$ $gm^{-3} \times 10^3$	w $m^2 \times 10^3$	$w\bar{s}$ $gm^{-2} \times 10^6$	$\frac{\partial}{\partial x_2}\langle v_2'v_1'\rangle$ $ms^{-2} \times 10^6$	$-\langle a\frac{\partial p}{\partial x_2}\rangle$ $ms^{-2} \times 10^6$	$-w\langle a\frac{\partial p}{\partial x_2}\rangle$ $m^2s^{-2} \times 10^3$	$\bar{w}\langle a\frac{\partial p}{\partial x_2}\rangle$ $gm^{-1}s^{-2} \times 10^{-1}$	$-w\frac{\partial}{\partial x_2}\langle v_2'v_1'\rangle$ $m^2s^{-2} \times 10^3$	$-\bar{w}\bar{s}\frac{\partial}{\partial x_2}\langle v_2'v_1'\rangle$ $gm^{-1}s^{-2} \times 10^{-1}$
0	10.93	3.03	33.12	11.20	1.14	3.45	0.38	−33.94	−3.71
.5	11.03	3.03	33.42	9.34	3.47	10.51	1.16	−28.30	−3.12
1.0	11.07	3.03	33.54	7.46	5.99	18.15	2.01	−22.60	−2.50
1.5	11.10	3.03	33.63	5.59	8.66	26.24	2.91	−16.94	−1.88
2.0	11.13	3.01	33.50	3.73	11.37	34.22	3.81	−11.23	−1.25
2.5	11.27	2.48	27.95	1.87	14.20	35.22	3.97	−4.64	−0.52
3.0	11.96	2.24	26.79	0.00	17.10	38.30	4.58	0.00	0.00
3.5	12.28	2.10	25.79	−1.87	19.96	41.92	5.15	3.93	0.48
4.0	13.36	1.91	25.92	−3.74	22.71	43.38	5.80	7.14	0.95
4.5	13.60	1.71	23.26	−5.59	25.22	43.13	5.87	9.56	1.30
5.0	13.72	1.59	21.81	−7.48	27.36	43.50	5.97	11.89	1.63
5.5	13.83	1.56	21.57	−9.32	29.04	45.30	6.26	14.54	2.01
6.0	14.02	1.49	20.98	−11.19	30.26	45.09	6.32	16.67	2.34
6.5	14.28	1.39	19.85	−13.02	30.84	42.87	6.12	18.10	2.58
7.0	14.57	1.28	17.92	−14.87	30.92	38.03	5.54	18.29	2.66
7.5									

Calculations for b_0' and η:

From Equations (6) and (8):

$$0 = 254.65 \times 10^{-3} + 16.42 \times 10^3\, b_0' + 10.98 \times 10^{-3} + 8.77 \times 10^{-3},$$

$$0 = 32.93 \times 10^2 + 199.28 \times 10^5\, b_0' - 0.49 \times 10^2,$$

$$\therefore b_0' = -16.54 \times 10^{-6}\ ms^{-2};\ \eta = -0.43.$$

TABLE IV. Evaluation of Eq. (4) for the Mean Longitudinal Velocity $\bar{v}_1$ for the Period 18–23 June 1950 at Station J–17 in the James River Estuary.

Depth	$< a \frac{\partial p}{\partial x_1} >$	$\eta \frac{\partial}{\partial x_2} < v_2' v_1' >$	$f_1 \bar{v}_1$	$\bar{v}_1$	$\bar{v}_1$ *observed*
m	$ms^{-2} \times 10^6$	$ms^{-2} \times 10^6$	$ms^{-2} \times 10^6$	ms^{-1}	ms^{-1}
0.0					
	15.40	−4.82	10.58	0.121	0.116
0.5					
	13.07	>4.02	9.05	0.103	0.092
1.0					
	10.55	−3.21	7.34	0.084	0.071
1.5					
	7.88	−2.40	5.48	0.062	0.054
2.0					
	5.17	−1.60	3.57	0.041	0.035
2.5					
	2.34	−0.80	1.54	0.018	0.012
3.0					
	−0.56	0.00	−0.56	−0.006	−0.014
3.5					
	−3.42	0.82	−2.62	−0.030	−0.038
4.0					
	−6.17	1.60	−4.57	−0.052	−0.056
4.5					
	−8.68	2.41	−6.27	−0.071	−0.065
5.0					
	−10.82	3.22	−7.60	−0.087	−0.070
5.5					
	−12.50	4.02	−8.48	−0.097	−0.074
6.0					
	−13.72	4.82	−8.90	−0.101	−0.076
6.5					
	−14.30	5.60	−8.70	−0.099	−0.076
7.0					
	−14.38	6.39	−7.99	−0.091	−0.068
7.5					

1. $b_0' = -16.54 \times 10^{-6}\ ms^{-1}$.
2. $\eta = -0.43$.

REFERENCES

Fleagle, R. G. and F. I. Badgley
1952. Atmospheric turbulence study. Occ. Rep. Dept. Meteorology and Climatology, Univ. of Washington, No. 2: 47 pp.

Lesser, R. M.
1951. Some observations of the velocity profile near the sea floor. Trans. Amer. geophys. Un., *32*(2): 207–211.

Pritchard, D. W.
1952. Salinity distribution and circulation in the Chesapeake Bay estuarine system. J. Mar. Res., *11*(2): 106–123.
1954. A study of the salt balance in a coastal plain estuary. J. Mar. Res., *13*(1): 133–144.
1956. The dynamic structure of a coastal plain estuary. J. Mar. Res., *15*(1): 33–42.

PLANKTON PIGMENT NOMOGRAPHS[1]

By

A. C. DUXBURY and CHARLES S. YENTSCH[2]

Department of Oceanography
University of Washington
Seattle 5, Washington

ABSTRACT

Nomographs for computing the amounts of plankton pigments as determined by the spectrophotometric method have been constructed. The methods used for alignment and scaling are discussed. The use of the nomographs shortens computation time considerably.

Introduction. The semi-micro method described by Richards with Thompson (1952) for analysis of plankton samples may be used to determine pigment types in plankton populations. In this method the total absorbencies of plankton extracts are measured at specified wave lengths. In brief, the plankton samples are concentrated, the pigments are extracted in 90% acetone, and the optical density of the extract is measured at wave lengths 665, 645 and 630 mμ for chlorophylls *a*, *b*, and *c* and at 480 and 510 mμ for animal and plant carotenoids. Where large numbers of samples are involved, considerable time is spent in computing the pigment types because of the numerous steps involved in solving the simultaneous equations of three or four variables. This time may be shortened considerably by converting the Richards with Thompson equations into nomographic form.

Development of the Nomographs. The nomographs designed for solving these equations comprise a series of alignment diagrams which are readily constructed and which can be used rapidly for determining the amounts of pigment types. The nomographs consist of a series of parallel lines which are spaced and scaled by means of ratios between scale moduli. The scale modulus is a factor which will reduce the coefficient of a component of an equation, such as that of Richards with Thompson, to a unit value. The use of scale moduli allows the different components to be treated with equal scale spacing and

[1] This work was supported in part by the Office of Naval Research under Contract No. N8onr/III with the University of Washington.

[2] Present address: Woods Hole Oceanographic Institution, Woods Hole, Mass.

facilitates the construction of uniform scales for these components. The method used in preparing these nomographs is taken, in part, from Levens (1948) and Kulmann (1954).

The Richards with Thompson equations for determining chlorophyll are:

$$C_a \text{ (mg/L)} = 15.6\ D_{665} - 2.0D_{645} - 0.8D_{630}$$
$$C_b \text{ (mg/L)} = 25.4\ D_{645} - 4.4D_{665} - 10.3D_{630}$$
$$C_c \text{ (MSPU/L)} = 109\ D_{630} - 12.5D_{665} - 28.7D_{645},$$

where the D terms to the right are optical densities. The equations for determining animal and plant carotenoids, knowing the optical densities and chlorophyll values, are:

$$D_{res510} = D_{510} - 0.0026C_a - 0.0035C_b - 0.0021C_c$$
$$D_{res480} = D_{480} - 0.0019C_a - 0.0136C_b - 0.0054C_c$$

or

$$\text{Nonastacian (MSPU/L)} = 7.6\ (D_{res480} - 1.49\ D_{res510})$$
$$\text{Astacian (MSPU/L)} = 2(4.45\ D_{res510} - D_{res480}) \quad .$$

The nomograph of the equation for determining chlorophyll *a* is set up in the following manner. Since the equation has three components or variables that are multiplied by constant coefficients, scale moduli that reduce or change these coefficients to equal values must be determined. This can be done by multiplying each coefficient by its reciprocal, which reduces all coefficients in the equations to unity. These reciprocals are the scale moduli. The equation now has all components weighted equally.

A vertical line is drawn for D_{645} near the left side of the paper, and then another line at some distance is drawn parallel to it for D_{630}. The distance between these lines is quite arbitrary. The D_{665} line is then drawn parallel and at an arbitrary distance to the right of the first two lines. On an 8 × 10 piece of paper the distance between D_{645} and D_{630} can conveniently be about three inches, the distance between D_{630} and D_{665} about four inches. The D_{645} line should be subdivided from zero to about 0.7 unit in optical density, zero being placed at the top. The spacing of the subdivisions should be great enough to assure reading accurately to about .002 unit. The D_{630} line is now graduated similarly with corresponding divisions located on a line perpendicular to the divisions on D_{645}. To allow for both positive and negative signs that occur in the equation, the direction from bottom to top of the page is considered positive. The D_{665} line is now scaled with zero at the bottom on a common perpendicular with the 0.7 mark of the D_{645} and D_{630} lines, the 0.7 at the top in line with the zero mark of the latter lines.

The equation C_a (mg/L) $= 15.6D_{665} - 2.0D_{645} - 0.8D_{630}$ is now divided into two parts. The last two components are set equal to a factor called Q. Thus, $-1.0D_{645} - 0.8D_{630} = Q$ and $15.6D_{665} + Q = C_a$ (mg/L)

The scale moduli for D_{645} and D_{630} are 1/2.0 and 1/0.8 respectively. The Q line is placed between D_{645} and D_{630} at a location determined by the ratio of these scale moduli. In this case the ratio is 1/2.0 divided by 1/0.8 or 0.8/2.0. The position of Q is conveniently determined by assuming that the number of units of distance between D_{645} and D_{630} is 2.8 units and by locating Q 0.8 units from D_{645} and 2.0 units from D_{630}. To simplify further calculations, a substitution is made by referring to the scale moduli with letters and subscripts as follows:

$$M_{645} = 1/2.0;\ M_{630} = 1/.08;\ \text{and}\ M_{665} = 1/15.6 \quad .$$

Q is now located on the nomogram, but a scale modulus for it, Mq, must now be determined. Mq gives the ratio between the size of the divisions of Q and those of D_{665}, D_{645} and D_{630}. However, Q need not be graduated, and Mq is merely used later for determining the placement of the chlorophyll a line. Mq is found in the following manner:

$$\frac{M_{645} \times M_{630}}{M_{645} + M_{630}} = Mq = \frac{1/2.0 \times 1/0.8}{1/2.0 + 1/0.8} = \frac{1}{2.8} \quad .$$

The chlorophyll a line is now positioned. The ratio of Mq/M_{665} or 1/2.8/1/15.6 places the C_a line 15.6 units from Q and 2.8 units from D_{665}, if the distance between Q and D_{665} is assumed to be 18.4 units. The final calculation is the scale modulus for chlorophyll a. It is determined in much the same manner as for Mq. Thus,

$$M_{Ca} = \frac{Mq \times M_{665}}{Mq + M_{665}} = \frac{1/2.8 \times 1/15.6}{1/2.8 + 1/15.6} = \frac{1}{18.4} \quad .$$

This means that each unit on the C_a scale is 1/18.4 times as large as the units on the optical density scales. Since the optical density scales are in tenths, the scale modulus, M_{Ca}, may be multiplied by ten to convert the chlorophyll units from tenths to units. Thus, 1(mg/L) is equal in length to 1/1.84 times the length devoted to 0.1 optical density. Graduation of the chlorophyll a line is accomplished by solving the nomogram to determine the zero point on the chlorophyll a line and then marking off the successive units along the scale.

The nomogram is used in the following manner. A straight edge is employed to line up the values of D_{645} and D_{630} as determined by the analysis; the intersection of this edge with Q is then noted. The

straight edge is then moved to join the intersection on Q with the value obtained for D_{665}. This line now crosses the chlorophyll *a* line, and the value of chlorophyll *a* (in mg/L) is read directly.

All other nomograms in this series are constructed in the same manner, using appropriate scale moduli. It should be noted that the equations for the carotenoids necessitate solving first for the D_{res480} and D_{res510}. These equations involve four variables instead of the three as in the case of chlorophyll; otherwise, the same procedure is followed. Chlorophyll *a* and chlorophyll *b* combine to designate an intersection on the Q line; Q and chlorophyll *c* combine to designate a W line intersection and W and D_{480} or D_{610} combine to designate the intersecting D_{res} lines. The solving of these diagrams consists of the same stepwise procedure described for chlorophyll *a*.

Errors and Range of Values. The amount of error introduced by using the nomographs depends largely upon the accuracies to which

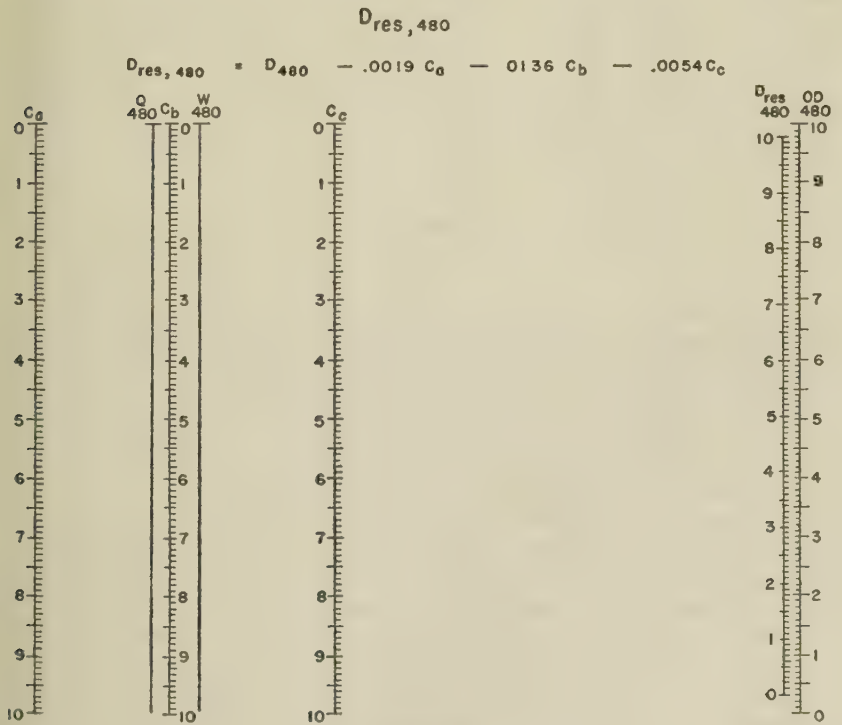

Figure 1

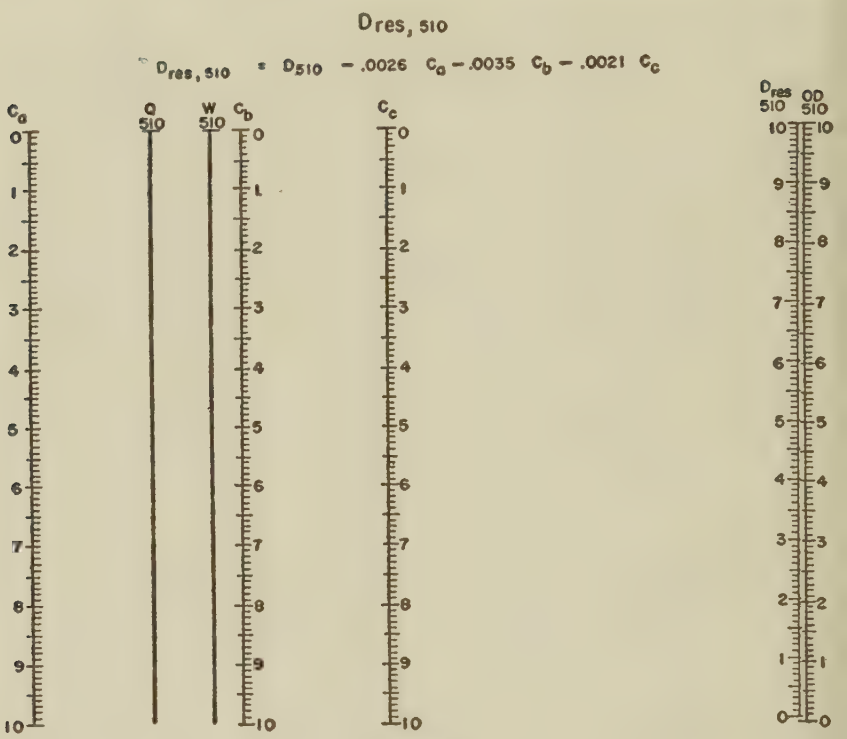

Figure 2

the nomographic scales may be read. In all instances the reading obtained from the nomographs are indicative of the number of significant decimal places to which the pigment values should be calculated. In some instances the equations have constants that approximate the errors in the optical density readings. This reduction in accuracy will show quite distinctly on the nomographs. However, the significant accuracy and relative accuracy is still maintained.

The range of values shown on the nomographs (Figs. 1–6) have been based largely on pigment values commonly found in the waters of Puget Sound and adjacent areas. These values, in all instances, were obtained by concentrating the plankton in one or two liters of sea water and extracting the pigments with 5.0 cc of 90% acetone (Creitz and Richards 1955). In order to read accurately on these scales, it was necessary to fold one or two of the scales to meet the restrictions of paper size. The range given to chlorophyll *b* is quite arbitrary, since this pigment was seldom found in large amounts in

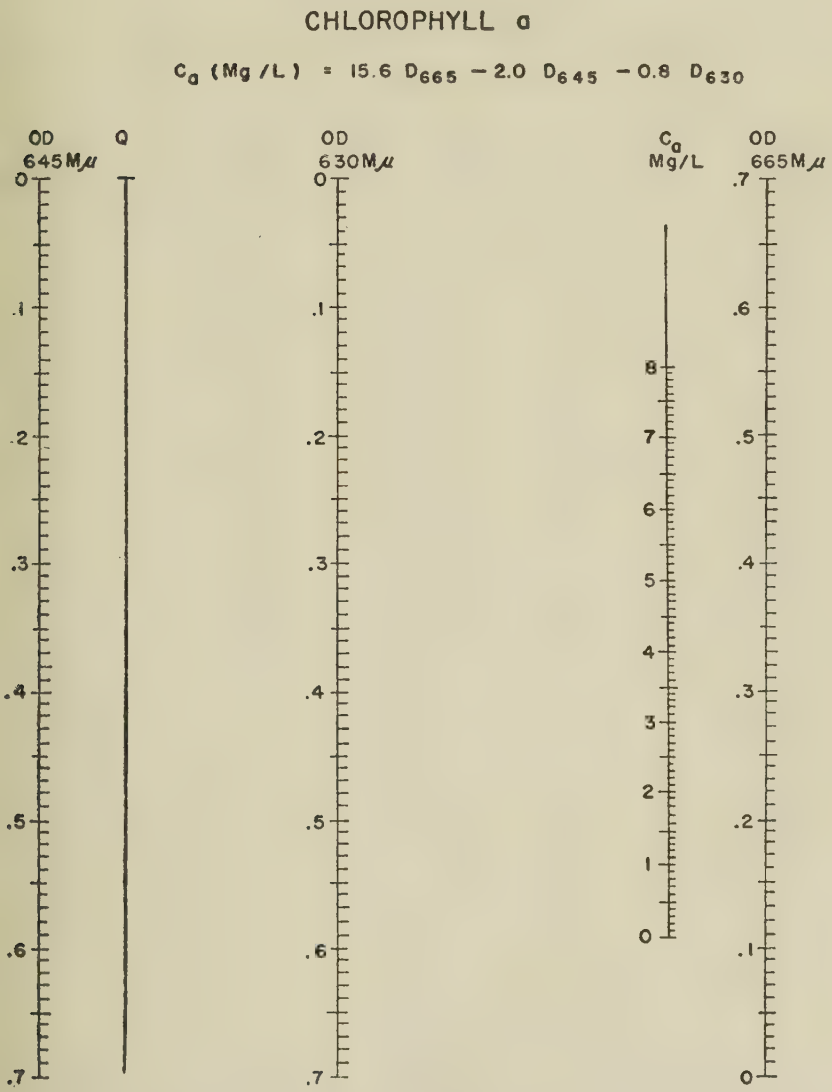
CHLOROPHYLL a
C_a (Mg/L) = 15.6 D_{665} − 2.0 D_{645} − 0.8 D_{630}
OD 645Mμ
Q
OD 630Mμ
C_a Mg/L
OD 665Mμ
0
.1
.2
.3
.4
.5
.6
.7
8
7
6
5
4
3
2
1
0

Figure 3

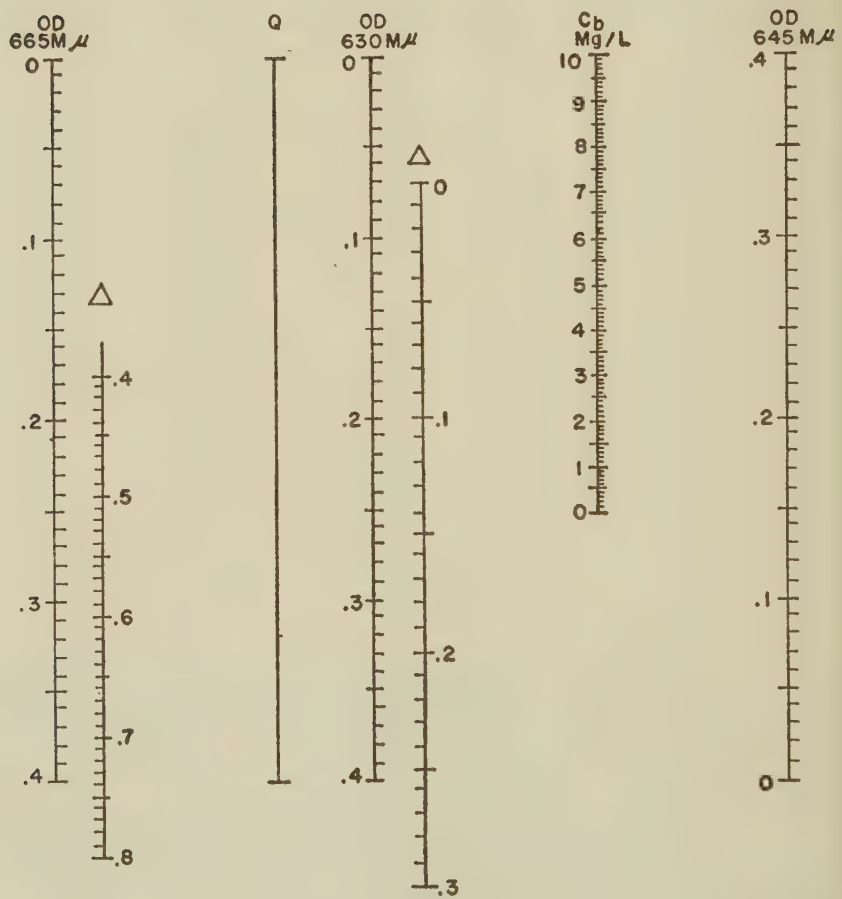

Figure 4

marine plankton. The range of values shown for the animal (astacian) carotenoids may too low, since some zooplankters are not caught in standard hydrographic sampling bottles. No optical density values are extended farther than 1.0, since an extract with a concentration giving an optical density reading higher than 0.90 will not follow

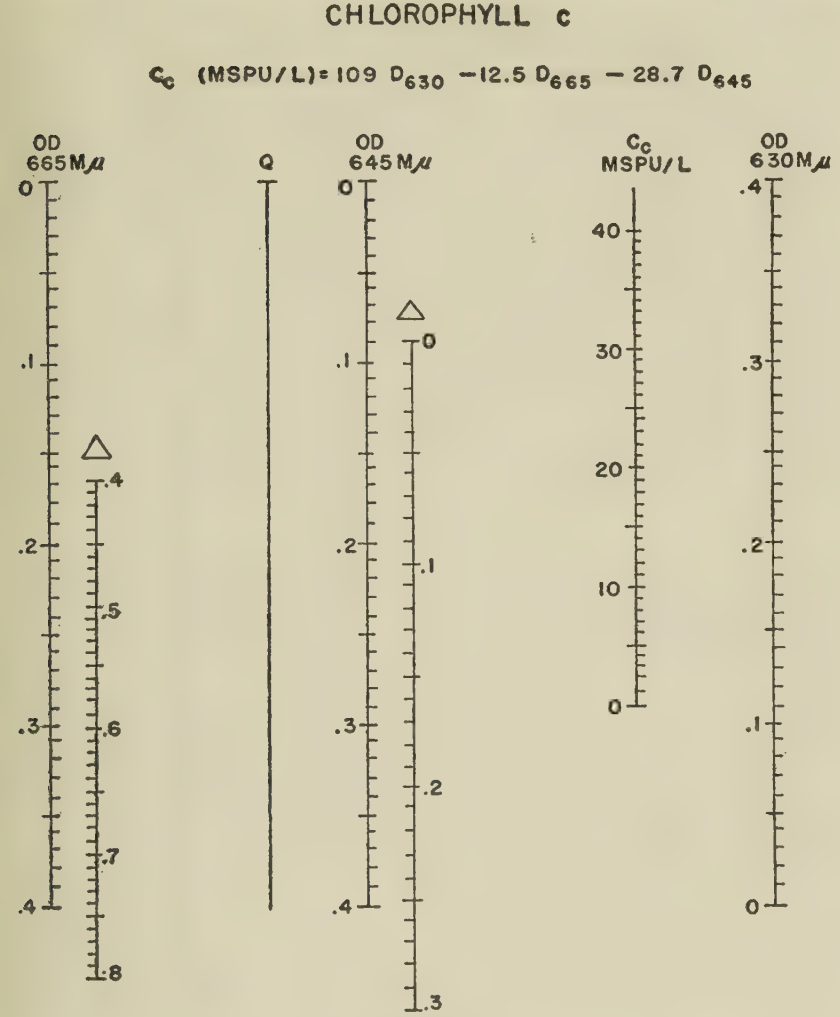

Figure 5

Beer's Law and therefore the extract must be diluted (Richards with Thompson, 1952). Greater color sensitivity may be obtained by using longer light paths. The plankton pigment nomographs, following the original equations, are based on optical density values using a 1 cm light path. When longer light paths are employed, either the optical density readings or the pigment values may be corrected accordingly.

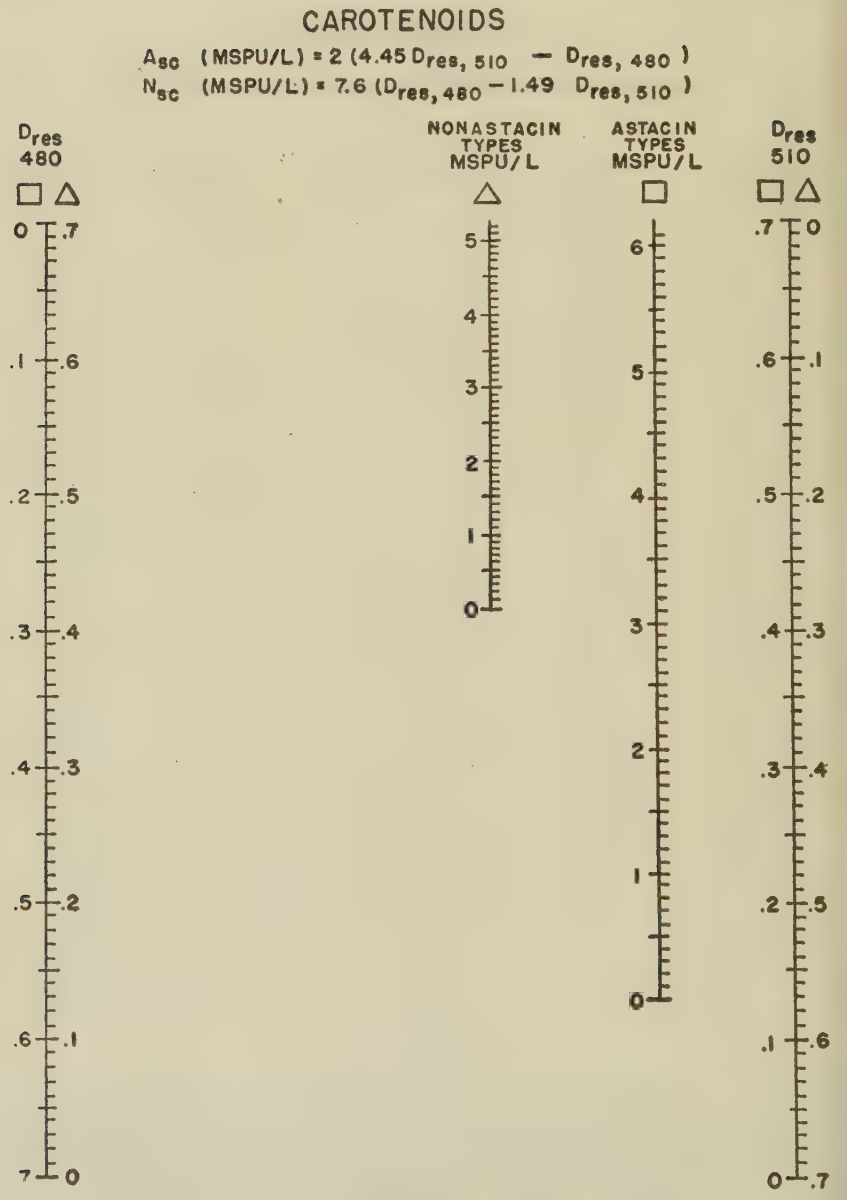
CAROTENOIDS
A_{sc} (MSPU/L) = 2 (4.45 $D_{res, 510}$ − $D_{res, 480}$)
N_{sc} (MSPU/L) = 7.6 ($D_{res, 480}$ − 1.49 $D_{res, 510}$)
D_{res} 480
NONASTACIN TYPES MSPU/L
ASTACIN TYPES MSPU/L
D_{res} 510
0 .7
.1 .6
.2 .5
.3 .4
.4 .3
.5 .2
.6 .1
7 0
5 4 3 2 1 0
6 5 4 3 2 1 0
.7 0
.6 .1
.5 .2
.4 .3
.3 .4
.2 .5
.1 .6
0 .7

Figure 6

Directions for the Use of the Nomographs. To obtain chlorophyll values from the nomographs, optical density readings on scales adjacent of line Q are aligned and the intersection on the Q line is determined. This point is then aligned with the reading for the third optical density scale. The intersection of this line with the chlorophyll scale gives the value of the chlorophyll in question. For the carotenoid nomographs, residual absorbencies 510 and 480 mμ must be considered together with values for the chlorophyll observed in the same sample. Chlorophyll *a* and *b* values are aligned to determine the intersection of the Q_{510} scale. This intersection is aligned with the chlorophyll *c* value and the intersection on W_{510} is determined. The final step consists of aligning the intersection of W_{510} with the correct value of D_{510} and reading the value of D_{res510} directly at the intersection. The same procedure is followed for obtaining D_{res480} values. The amounts of astacian and nonastacian carotenoids are obtained by aligning residual absorbencies 510 and 480 mμ and reading the amounts of either pigment at the intersection of the respective scales.

References

Creitz, G. I. and F. A. Richards

1955. The estimation and characterization of plankton populations by pigment analysis. III. A note on the use of "millipore" membrane filters in the estimation of plankton pigments. J. Mar. Res., *14* (3): 211–216.

Kulmann, A. C.

1954. Nomographic Charts. McGraw-Hill Book Co. Inc., New York. 244 pp.

Levens, A. S.

1948. Nomography. John Wiley and Sons, New York. 175 pp.

Richards, F. A. with T. G. Thompson

1952. The estimation and characterization of plankton populations by pigment analysis. II. A spectrophotometric method for the estimation of plankton pigments. J. Mar. Res., *11* (2): 156–172.